Progressive Slowing of the Cerebrovascular Response in the Temporal and Parietal Cortex of Patients with Alzheimer's Disease and Mild Cognitive Impairment

by

Kenneth Royce Holmes

A thesis submitted in conformity with the requirements
for the degree of Master of Science

Institute of Medical Science
University of Toronto

Progressive Slowing of the Cerebrovascular Response in the Temporal and Parietal Cortex of Patients with Alzheimer's Disease and Mild Cognitive Impairment

Kenneth Royce Holmes

Master of Science

Institute of Medical Science
University of Toronto

2017

Abstract

There is accumulating evidence that neurovascular dysfunction plays a major role in Alzheimer's disease (AD). Recent investigations now suggest that cerebrovascular reactivity (CVR) is impaired in AD and may underpin part of the neurovascular contribution. However, our understanding of the relationship between the magnitude of CVR, the speed of cerebrovascular response, and the progression of AD is still limited. This is especially true in patients with mild cognitive impairment (MCI), which is recognized as the prodromal stage of AD.

The purpose of this thesis was to investigate AD and MCI patients using new repeatable and accurate measures of cerebrovascular function, namely the magnitude and speed of vascular response to a vasoactive stimulus. The findings of this thesis demonstrate that AD is associated with a progressive slowing of the cerebrovascular response in proportion to the progression of the disease.

Acknowledgments

Completion of my graduate studies at the University of Toronto would not have been possible without the support and encouragement of numerous individuals that I have had the pleasure of working with.

First and foremost, I would like to thank my supervisor, Dr. David Mikulis, for providing me with this opportunity. You entrusted me with this incredible study and I will be forever grateful for that. Moreover, you have been my role-model and have help me build a blue-print for my own career. I would also like to thank the members of my Progress Advisory Committee, Dr. Joseph Fisher, Dr. Adrian Crawley, and Dr. Sandra Black for their guidance throughout my project and time spent reviewing my thesis. Dr. Fisher, I can only describe your approach to science as feverous. Your passion is wholly inspiring, and I hope to carry that quality into my future as a researcher. Adrian, you have been an incredible teacher and invaluable resource. Your teachings have provided me with a foundational understanding of medical imaging that I will build on for the rest of my life. Dr. Black, your insightful comments have been key in guiding my experimental design and helping my project realize its potential.

I must thank Julien Poublanc for the countless hours he has spent teaching me the methods I have used to analyze data. Kevin, your support has been instrumental these past two years, and I am proud to call you my good friend. I am thankful for the hard work of Abby Skanda in coordinating our study. I also thank Dr. David Tang-Wai in helping recruit subjects, Dr. Melanie Cohn for running our neuropsychological testing, and Eugen Hlasny and Keith Ta for their patience and accommodation in scanning subjects for this study. I am appreciative of my time with Dr. James Duffin, who played a key role in my learning. I thank Olivia Sobczyk for her help, and for exercising discipline during our meetings when the rest could not. Larissa, we have just met, but I already know that the study could not be in better hands.

I still feel the same excitement and sense of wonder about our work as I did four years ago when I was a new summer student. My path is taking me somewhere new, but I know I will find my way back to the group again one day. With all that said, I feel greatly indebted to everyone at the Mikulis Lab and those who we collaborate with. As they say, if I have seen further, it is by standing on the shoulders of giants.

Contributions

Kenneth Royce Holmes (author): Project lead; study design, subject recruitment, data acquisition, image analysis, interpretation of results, and thesis write up.

Dr. David Mikulis (supervisor): Study design and conceptualization, guidance and oversight to project lead, results interpretation, and review of thesis.

Dr. Adrian Crawley: Study design and conceptualization, guidance and oversight to project lead, results interpretation, and review of thesis.

Dr. Joseph Fisher: Study design and conceptualization, guidance and oversight to project lead, results interpretation, and review of thesis.

Dr. Sandra Black: Guidance and oversight to project lead, results interpretation, and review of thesis.

Dr. Melanie Cohn: Neuropsychological testing, guidance to project lead

Dr. Tang-Wai: Provided assistance in subject recruitment

Julien Poublanc: Provided expertise and support in data processing and analysis

Dr. Kevin Sam: Provided support in data acquisition and processing

Abby Skanda: Research coordinator; managed project recruitment and bookings

Olivia Sobczyk: Provided support in data acquisition

Table of Contents

List of Abbreviations

20-HETE	20-Hydroxyeicosatetraenoic acid
AA	Arachidonic Acid
ACA	Anterior Cerebral Artery
ACZ	Acetazolamide
AD	Alzheimer's Disease
AMPAR	α-Amino-3-Hydroxy-5-Methyl-4-Isoxazolepropionic Acid Receptor
ANCOVA	Analysis of Covariance
APP	Amyloid Precursor Protein
ASL	Arterial Spin Labeling
BBB	Blood Brain Barrier
BNA-R	Behavioural Neurology Assessment-Revised
BOLD	Blood Oxygen Level-Dependent
Ca^{2+}_{v}	Voltage-gated Calcium Channel
CAA	Cerebral Amyloid Angiopathy
CBV	Cerebral Blood Volume
CDR	Clinical Dementia Rating
CERAD	Consortium to Establish a Registry for Alzheimer's Disease
cGMP	Cyclic Guanosine Monophosphate
$CMRO_2$	Cerebral Metabolic Rate of O_2
CNS	Central Nervous System
COX-1	Cyclooxygenase-1
CPP	Cerebral Perfusion Pressure
CSF	Cerebrospinal Fluid
CT	Computed Tomography
CVD	Cerebrovascular Disease
CVR	Cerebrovascular Reactivity
dHb	Deoxyhemoglobin
DSC	Dynamic Susceptibility Contrast
EET	Epoxyeicosatrienoic Acid
eNOS	Endothelial Nitric Oxide Synthase
EOAD	Early Onset Alzheimer's Disease
EPI	Echoplanar Imaging
ERK	Extracellular Signal-Regulated Kinase
FDG-PET	Fluorodeoxyglucose-Posititron Emission Tomography
FLAIR	Fluid-Attenuated Inversion Recovery
fMRI	Functional Magnetic Resonance Imaging
GABA	γ-Aminobutyric Acid
gCPP	Global Perfusion Pressure

GM	Grey Matter
GRE	Gradient Echo
H^+	Hydrogen
HC	Healthy Control
HIF-1α	Hypoxia-Inducible Factor-1α
HIPDM	N,N,N′-Trimethyl-N′-(2-Hydroxy-3-Methyl-5-Iodobenzyl)-1,3-Propane-Diamine
HMPAO	^{99m}Tc-Hexamethylpropyleneaminoxime
HRF	Hemodynamic Response Function
ICA	Internal Carotid Artery
ICP	Intracranial Pressure
IEL	Internal Elastic Lamina
K^+	Potassium
LOAD	Late Onset Alzheimer's Disease
LRP1	Low-Density Lipoprotein Receptor-Related Protein 1
LTD	Long-Term Depression
LTP	Long-Term Potentiation
MAP	Mean Arterial Pressure
MCA	Middle Cerebral Artery
MCI	Mild Cognitive Impairment
MFV	Mean Flow Velocity
mGluR	Metabotropic Glutamate Receptors
MLCK	Myosin Light Chain Kinase
MMSE	Mini-Mental State Examination
MRI	Magnetic Resonance Imaging
NFT	Neurofibrillary Tangles
NMDA	N-Methyl-D-Aspartate
NMDAR	N-Methyl-D-Aspartate Receptor
nNOS	Neuronal Nitric Oxide Synthase
NO	Nitric Oxide
NP	Neuritic Plaques
NVC	Neurovascular Coupling
NVU	Neurovascular Unit
OEF	Oxygen Extraction Fraction
$PaCO_2$	Arterial Pressure of CO2
PaO_2	Arterial Pressure of Oxygen
PCA	Posterior Cerebral Artery
PET	Positron Emission Tomography
PGE_2	Prostaglandin E_2
PLA_2	Phospholipase A_2
RAGE	Receptor for Advanced Glycation of End Products

rCPP	Regional Cerebral Perfusion Pressure
RF	Radiofrequency
rOEF	Regional Oxygen Extraction Fraction
SNR	Signal-To-Noise Ratio
SPECT	Single Photon Emission Computed Tomography
SPGR	Spoiled Gradient Echo
SVD	Small Vessel Disease
TCD	Transcranial Doppler
TFA	Transfer Function Analysis
TIA	Transient Ischemic Attack
TR	Repetition Time
VaD	Vascular Dementia
VR	Virchow-Robins
VSMC	Vascular Smooth Muscle Cell
WM	White Matter

List of Tables

List of Figures

List of Appendices

Chapter 1
Introduction

1 Introduction

1.1 Gross Neuroanatomy

A general understanding of structural neuroanatomy will be helpful in interpreting subsequent chapters. The adult brain consists of four macrostructures, the cerebrum, diencephalon, brainstem and cerebellum. This thesis will focus on Alzheimer's disease (AD) pathology as it relates to the cerebrum, which will be the main focus of this section. The cerebrum, which comprises a majority of the brain, possesses a left and a right hemisphere, though its anatomy can be further subdivided into paired frontal, parietal, occipital and temporal lobes, each involved in a specific, though often overlapping, subset of brain functions (Jacobson & Marcus, 2008).

The cerebrum contains a highly convoluted surface layer of grey matter (GM) termed the cerebral cortex, which is composed of neuronal cell bodies, dendrites and unmyelinated axons. Containing approximately 16 billion neurons, the cerebral cortex is organized into a laminar arrangement, supported by a scaffolding of support cells known as glial cells (Jacobson & Marcus, 2008). There are three different types of glial cells that need to be considered. Astrocytes physically interact with cerebral blood vessels and ventricles, playing an important homeostatic function maintaining the chemical environment for neurons, mediating neurovascular signaling, and supporting repair processes. Oligodendrocytes produce myelin sheaths to insulate axons, improving conduction. Finally, microglial cells occupy a role in the central nervous system similar to that of macrophages peripherally (Jacobson & Marcus, 2008; Brodal, 2010).

Beneath the cerebral cortex lies an internal network of myelinated axonal projections, known as white matter (WM), which comprises approximately 60% of total brain tissue. The cerebrum also contains a number of subcortical GM structures including the basal ganglia, hippocampus and amygdala. Lastly, the cerebrum possesses an interconnected system of anatomical spaces, called ventricles, occupied by a clear, colourless fluid known as cerebrospinal fluid (CSF).

Functionally, the cerebrum includes regions responsible for sensory, motor, auditory, and visual function, in addition to limbic regions that integrate emotional processing with other functions to evaluate external stimuli and determine a response. The term limbic generally refers to the cerebral structures involved with emotional processing, but these brain areas are also involved in many other higher order cognitive functions, such as learning and memory formation. These structures occupy much of the temporal and frontal lobes, and include the cingulate gyrus, hippocampal formation and parahippocampal gyrus (Jacobson & Marcus, 2008).

1.2 Anatomy of the Cerebral Circulation

1.2.1 Macrovascular supply of the brain

The brain's arterial supply originates from two sources, (i) the internal carotid arteries (ICA) and (ii) the vertebral arteries. The internal carotid arteries primarily supply blood to the anterior regions of the brain, while the vertebral arteries are largely responsible for perfusing posterior structures. The organization of the brain's vascular tree reflects this function. The ICAs enter the skull via the carotid canals located anterior to the foramen magnum. The ICAs then proceed to bifurcate at the basal surface of the cerebral hemispheres to form the anterior cerebral arteries (ACA) and middle cerebral arteries (MCA), with each bearing responsibility for a separate vascular zone. Conversely, the vertebral arteries enter the skull by way of the foramen magnum, then merge at the pontomedullary junction to form the basilar artery along the midline. As the basilar artery ascends the intracranial compartment, it gives rise several smaller branches that

supply the cerebellum and brainstem structures before bifurcating into the left and right posterior cerebral arteries (PCA). Two posterior communicating arteries connect the PCA to the ICA just proximal to the level of the bifurcation of the ICA into the MCA and ACA, and a single anterior communicating artery connects the right and left ACA. These pathways merge the ICA blood supply with the vertebral blood supply and form a structure known as the circle of Willis, the importance of which will be covered in later sections (Cipolla, 2009).

While the posterior circulation is the sole blood supply to the brainstem and cerebellum, the cerebrum receives flow from both the ICAs and vertebral arteries (Cipolla, 2009). The MCAs comprise approximately 80% of the total cerebral blood flow (CBF), supplying most of the lateral surface of the temporal and parietal lobes, as well as a portion of subcortical structures including the internal capsule, basal ganglia, and choroid plexuses. The ACA supplies the frontal lobes, anterior limb of the internal capsule, part of the basal ganglia and the superior medial aspect of the parietal lobes. The PCA, which completes the blood supply of the cerebral hemispheres, provides blood to the occipital lobes, the inferomedial portion of the temporal lobes and the thalami.

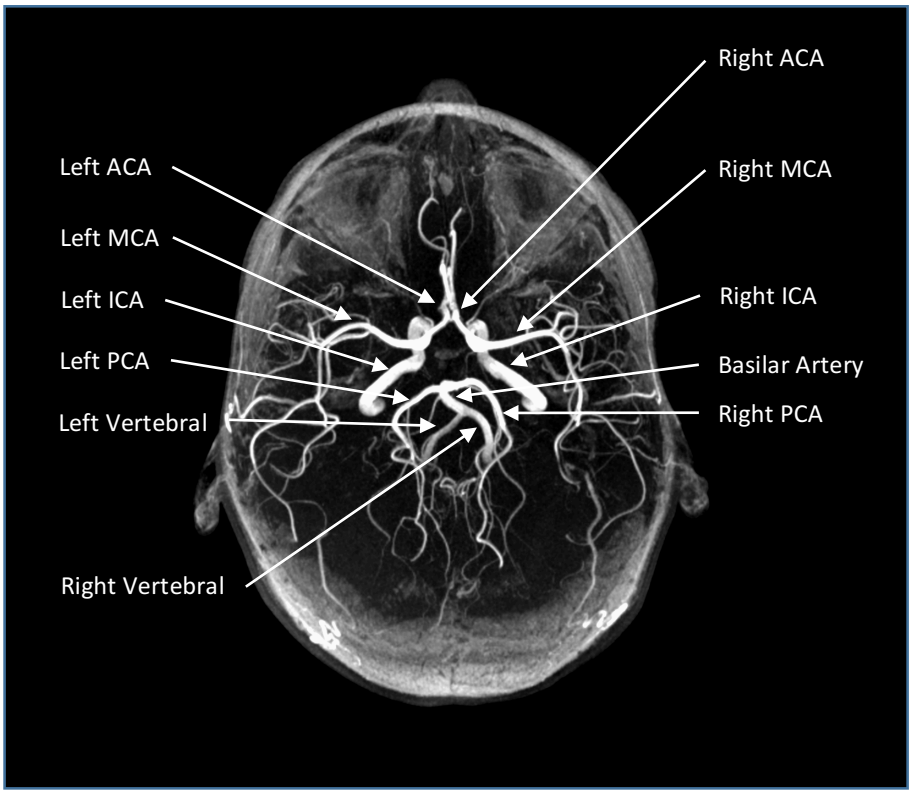

Figure 1.1 MR angiography of author, demonstrating major vessels of interest

The major cerebral arteries proceed to project outwards from the circle of Willis to reach the surface of the cerebrum, where they become the pial arteries. The pial arteries traverse the surface of the brain surrounded by CSF, usually within the subarachnoid space (Jones, 1970). Eventually, the pial arteries give rise to penetrating arterioles, which re-enter the brain tissue through invaginations in the subarachnoid space, termed Virchow-Robin (VR) spaces, to become parenchymal arterioles (Iadecola, 2004). During this process, the glia limitans surrounds the parenchymal arterioles to form the *tunica adventitia* of the vessel, which then comes into direct contact with astrocytic end-feet (Figure 1.2) (Rennels & Nelson, 1975). At the terminal end of the parenchymal arterioles lie the vascular beds composed of capillaries responsible for the exchange of oxygen, nutrients, waste products and other solutes (Cipolla, 2009).

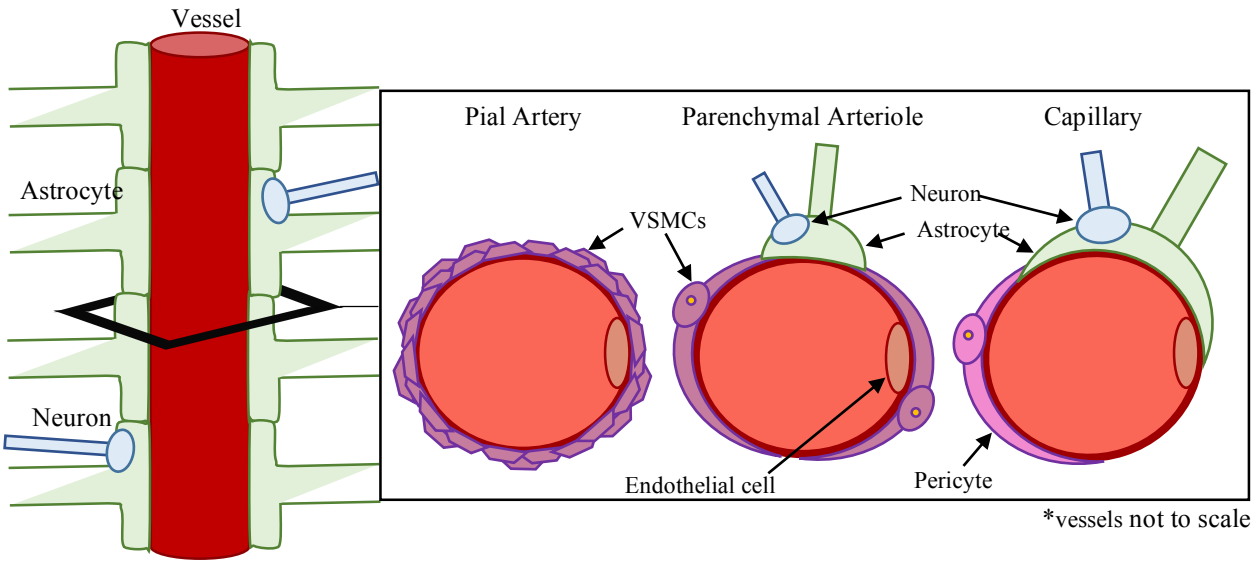

Figure 1.2. Cerebral vessel enclosed by astrocytic end-feet and vessel cross-sections. The pial arteries give rise to penetrating arterioles, which enter the brain tissue via VR spaces to become parenchymal arterioles. During this process, the glia limitans surrounds the parenchymal arterioles to form the *tunica adventitia*, bringing the vessel into direct contact with astrocytic end-feet. Pial arteries possess two or three layers of smooth muscle cells, while parenchymal arterioles are reduced to a single layer of smooth muscle. Capillaries have no *tunica media* or *adventitia*, instead relying on the contractile properties of associated pericytes to regulate tone.

Venous outflow is accomplished by a system of interconnected valveless cerebral veins and dural sinuses. The organization of the cerebral veins can be subdivided into superficial veins and deep veins (Cipolla, 2009; Kiliç & Akakin, 2008). The superficial cortical veins, including the superficial middle cerebral vein, vein of Labbé and vein of Trolard, are responsible for draining

the cerebral cortex and the adjacent subcortical white matter. After exiting the cerebral hemispheres, these veins run within the subarachnoid space, eventually piercing the meninges to drain into the dural venous sinuses. The deep veins consist of the medullary veins, subependymal veins, internal cerebral veins, basal veins and the great vein of Galen, which drain the deep white matter and grey matter structures into the straight sinus. Blood from the sinuses then empties into the jugular veins by way of the confluence of sinuses, then transverse sinuses and sigmoid sinuses (Cipolla, 2009; Kiliç & Akakin, 2008).

1.2.2 Structure of cerebral vessels

The wall of cerebral arteries is comprised of three layers: (i) The outer *tunica adventitia*, constructed of collagen, elastin, fibroblasts, and perivascular nerves in the case of pial vessels, (ii) the muscular centre layer, the *tunica media*, consisting of vascular smooth muscle cells (VSMC), elastin, and collagen, and (iii) the inner *tunic intima*, consisting of the internal elastic lamina (IEL) lined by the vascular endothelium. Unlike systemic arteries, cerebral arteries do not possess an external elastic lamina, and thus rely solely on the IEL (Cipolla, 2009).

Large arteries can have up to 20 layers of smooth muscle cells, while smaller pial arteries possess two to four layers of VSMC and parenchymal arterioles are reduced to a single layer of smooth muscle (Cipolla, 2009). Capillaries have no *tunica media* or *adventitia*, instead relying on the contractile properties of associated pericytes for regulation of vascular tone (Figure 1.2). Also, cerebral vessels possess unique endothelial cells that are not fenestrated and are interconnected by adhesions known as tight junctions. This feature constitutes the blood-brain barrier (BBB), and allows for the fine control of solute and water exchange between the blood supply and the tissue (Iadecola, 2004).

1.2.3 Vascular collateralization in the brain

The cerebrovascular system possesses a high level of redundancy, designed to prevent reductions in CBF in the event of a vascular occlusion (Jackman & Iadecola, 2014). A primary structure of vascular redundancy is the circle of Willis. This structure is formed by the unification of the vessels arising from the vertebral arteries with those arising from the ICAs. As previously mentioned, this is achieved by a pair of posterior communicating arteries connecting the PCAs to the ICAs and a singular anterior communicating artery connecting the right and left ACA. By leveraging communicating pathways within the cerebral circulation, any vascular territory can derive flow from multiple sources. When faced with an occlusion within, or proximal to, the circle of Willis, the resulting pressure gradient distal to the occlusion will produce a redistribution of blood flow from intact arteries to feed affected vessels. It should be noted that the level of compensation achieved will be influenced by the vessel diameter of the communicating arteries in a given individual (Dickey et al., 1996). Also, only 20-25% of the population have a complete circle of Willis, in which no communicating arteries are absent or hypoplastic.

The other major structure of redundancy is the network of pial arteries that traverses the cerebral cortex. The pial arteries originate from the arteries leaving the circle of Willis, projecting across the surface of the brain and anastomosing greatly to form a vascular mesh. This high degree of collateralization prevents a loss of blood supply to the penetrating arterioles in the event of an occlusion in any one region of the pial network (Jackman & Iadecola, 2014). This assertion is supported by reports that the occlusion of a single pial vessel results in a robust redistribution of blood flow to re-establish blood supply distal to the occlusion, while occlusions of penetrating arterioles cause severe decreases in CBF because no collateral pathways are present at that level (Nishimura et al., 2010; Schaffer et al., 2006).

1.2.4 The neurovascular unit

The concept of neurovascular coupling (NVC) will be discussed later in this chapter, thus it is important to introduce the structural elements that mediate this process, which together are known as the neurovascular unit (NVU). The NVU is comprised of both vascular and neural cells, including neurons, astrocytes, myocytes, pericytes, and vascular endothelial cells (Iadecola, 2004; Muoio et al., 2014). Each of these components plays a distinct role in NVC, though the term "neurovascular unit" is used to reflect their tight functional coordination in linking CBF with neuronal activity. The mechanisms of NVC will be discussed more extensively in subsequent sections, however, briefly, the structural elements of the NVU are as follows:

1. Neurons - The neuron is the primary driver of the NVU as blood flow is intimately linked to the synaptic activity generated by nearby neurons. As the primary excitatory neurotransmitter, glutamate is thought to be the main synaptic messenger in NVC.

2. Astrocytes - Astrocytes were once thought to play a indirect support role in NVC, but it is now recognized that astrocytes are sensitive to glutamatergic and GABAergic (γ-aminobutyric acid) signaling and are an important conduit for neuronal signals to be transmitted to adjacent blood vessels (Muoio et al., 2014; Zonta et al., 2003).

3. Vascular Smooth Muscle Cells (VSMC) and Pericytes - VSMCs and pericytes encompass the primary vasomotor effectors involved in NVC. VSMCs are found in larger calibre resistance vessels such as the pial arteries and parenchymal arterioles, while pericytes are directly associated with capillaries. Both cells demonstrate contractile properties and can dilate or constrict the lumen of their respective vessels in response to vasoactive stimuli. Recent work by Hall and colleagues interrogating the contribution of pericytes and capillaries to the regulation of CBF has suggested that capillary dilation accounts for approximately 84% of the total vascular response during NVC, and that regulation of vasomotor tone in capillaries is mediated through the same signal pathways as those that regulate vascular VSMCs (Hall et al., 2014). However, the dominance of capillaries in NVC has since been disputed by Hill et al., who insist that CBF in

controlled by arteriolar VSMCs (Hill et al., 2015). The true contribution of each component remains controversial.

4. Endothelial Cells - The endothelial cells of the BBB were long considered to be uninvolved in NVC, however it is understood that these cells release vasoactive factors that regulate vascular tone and current evidence suggests that this may also modulate the activity of the NVU. The interaction of endothelial-derived vascular signals and those coming from the neurons has yet to be fully understood (Duchemin et al., 2012; Muoio et al., 2014).

1.2.5 Glymphatic flow

Efficient clearance of excess fluid and wastes is a key process in metabolically active tissues. While the central nervous system (CNS) lacks traditional lymphatic vessels, the glymphatic system is an emerging waste clearance system in the CNS that leverages the perivascular space formed by cerebral vessels and the astrocytic end-plate to clear fluid and metabolic waste from the parenchyma (Iliff et al., 2012). The prevailing understanding of the structure of the glymphatic system has three main elements: (i) the periarterial CSF inflow route, (ii) the interstitial fluid (ISF) compartment, and (iii) the perivenous ISF outflow route (Iliff et al., 2012; Nedergaard, 2013).

The pial surface arteries lie in the subarachnoid space surrounded by CSF. When the pial arteries give rise to penetrating arterioles, VR spaces are formed around the penetrating arterioles that are continuous with the subarachnoid space, and thus are also filled with CSF. As penetrating arterioles dive deeper into the brain parenchyma, the VR spaces narrow and eventually terminate, however the perivascular space continues as the basal lamina in parenchymal arterioles and capillaries. The porous structure of the basal lamina gives way to flow, allowing CSF to travel from the subarachnoid space down to the capillary beds. Indeed, recent work has demonstrated that CSF does travel down the perivascular space and readily exchanges with the ISF through aquaporin-4 water channels concentrated in the end-feet of the astrocytes that

envelop the parenchymal blood vessels (Iliff et al., 2012; Iliff & Nedergaard, 2013; Nagelhus et al., 2004). The driving force of glymphatic transport is not entirely elucidated, but recent work has demonstrated that arterial smooth muscle pulsation along the length of the pial and parenchymal vessels generates pulse waves that may drive CSF into the interstitial compartment (Iliff et al., 2013; Iliff et al., 2012). In fact, mouse studies have found that administering a drug that increases arterial pulsatility results in greater CSF penetration into the brain parenchyma (Iliff et al., 2013). The resultant penetration of CSF into the parenchyma then drives bulk flow of ISF towards the perivenous space surrounding central veins, carrying with it any dissolved wastes or other solutes. Finally, ISF that enters the perivenous space drains out of the brain, possibly to the cervical lymphatic system (Johnston et al., 2004).

Though research investigating the glymphatic system is still in its infancy, findings already indicate that impairment of glymphatic flow is associated with a number of neurological diseases including Alzheimer's disease (de Leon et al., 2017; Peng et al., 2016). A radiolabel tracer study has reported that between 40% and 80% of large peptides, including amyloid-β, are removed from the brain through glymphatic system (Iliff et al., 2012). New findings by de Leon and colleagues demonstrate that CSF clearance is impaired in AD and CSF clearance reductions are associated with increased brain amyloid-β deposition (de Leon et al., 2017).

1.3 Control of Cerebral Blood Flow

1.3.1 Overview

The human brain is a highly metabolically active organ, comprising just 2% of total body mass while consuming 20% of the body's energy output (Attwell et al., 2010). A majority of this energy is used to reverse ion currents that underpin synaptic activity (Attwell & Laughlin, 2001). Neuronal tissue has little capacity to store energy molecules to support this metabolic demand, thus proper brain function is highly dependent on the sufficient and consistent delivery of oxygen and glucose via the cerebral blood supply. If CBF is disturbed, normal brain function ceases

within seconds and irreparable damage will occur within minutes (Hossmann, 1994). As a result, the brain has developed a number of integrated pathways that regulate CBF to guard tissues against fluctuations in blood pressure and align local perfusion to the needs of surrounding tissue (Cipolla, 2009). In general, mechanisms of this nature fall into one of two general categories: (i) cerebral autoregulation, which aims to maintain constant CBF in the face of fluctuating blood pressure, and (ii) NVC, which augments CBF to accommodate local increases in metabolic activity. Both mechanisms achieve their desired effect on CBF by modulating the diameter of cerebral vessels to change vascular resistance. This strategy is ideal for a couple of reasons. Firstly, according to Poiseuille's law,

$$\boldsymbol{CBF = \frac{\pi P r^4}{8 \eta l}}$$

CBF is determined by perfusion pressure (*P*), vessel length (*l*) and radius (r), and blood viscosity (η). Of the parameters that could be feasibly adjusted, it is apparent the radius of the vessel is likely the most potent modulator of CBF. Flow through a vessel is proportional to the vessel radius to the fourth power, meaning that small adjustments to vessel calibre elicit large changes in CBF. Moreover, leveraging vessel diameter also enables a faster and more fine-tuned control of regional blood flow than could be achieved by altering other relevant parameters such as cardiac output to change cerebral perfusion pressure (CPP). Also of note, to effectively increase flow in a given region using this strategy, vessels upstream of that location must also vasodilate to prevent a drop in downstream microvascular pressure. Thus, flow regulation requires the conduction of vasoactive signaling upstream to proximal arterial segments (Iadecola et al., 1997).

Blood flow control may become compromised due to vascular injury resulting from the presence of vascular risk factors or as a result of a specific disease pathology. In either event, the ischemic burden created by poor coordination of CBF and metabolic demand increases the susceptibility of the brain to further cellular dysfunction and injury (Jackman & Iadecola, 2014). This thesis aims to examine the role of CBF dysregulation in the context of AD. To date, limited research has evaluated the nature of Alzheimer's-related vascular alterations with respect to blood flow control. By better understanding the regulatory mechanisms that underpin control of blood flow, we may better understand the hemodynamic consequences we can expect to see in AD. To that

end, an adequate discussion of the primary methods by which CBF is regulated, namely cerebral autoregulation and NVC, as well as the cerebrovascular response to CO_2, will be discussed as a prerequisite for subsequent sections.

1.3.2 Cerebral autoregulation

Global CPP (gCPP) is related to mean arterial pressure (MAP) and intracranial pressure (ICP):

$$\boldsymbol{gCPP = MAP - ICP}$$

Under normal physiological conditions, gCPP is dictated largely by MAP, which can fluctuate dramatically depending on several factors such as blood volume and autonomic input (Cipolla, 2009). On a regional basis, increases in vascular resistance will also reduce regional CPP (rCPP) downstream of the affected vessel. In the event of static vascular resistance, changes in CPP will directly and profoundly influence CBF. However, to mitigate the risk of ischemic brain damage, CBF must be maintained within a narrow range of 45-50 ml/100g/min. The ability of the brain to achieve this tight control of blood flow can largely be attributed to a homeostatic mechanism known as cerebral autoregulation. Cerebral autoregulation is a compensatory response that vasodilates or vasoconstricts cerebral resistance vessels in response to changes in intravascular pressure to ensure a constant flow of blood to downstream vascular beds. Cerebral autoregulation has an operational pressure range, known as the autoregulatory range, that spans from approximately 60-150 mmHg (Paulson et al., 1990). Beyond this range, the cerebrovasculature is unable to effectively compensate for changes in blood pressure and CBF will then change in relation to the change in CPP (as shown in Figure 1.3).

For the purposes of this research, it should also be noted that the autoregulatory range can be altered both as a long term compensation to vascular changes such as hypertension, but also by other non-pressure-related CBF-modifying processes, namely CO_2 (Meng & Gelb, 2015). Intuitively, cerebral autoregulation and other control mechanisms must integrate at the level of vascular tone regulation. Therefore, when applying a CO_2 stimulus to interrogate vascular reactivity, alterations to the autoregulatory range must be considered. A recent model of the CO_2

effect on cerebral autoregulation posits that hypercapnia causes an increase in the lower boundary of the autoregulatory range because of the additive vasodilatory effects of hypercapnia and hypotension, and a decrease in the upper limit of the autoregulatory range due to the antagonistic effect of hypercapnia overpowering the pro-constrictive effect of hypertension, though this has been disputed (Meng & Gelb, 2015). This equates to a reduction in the autoregulatory range when under hypercapnic conditions, increasing susceptibility to pressure-related changes in CBF. However, the body of work that spawned this model was largely in animals and used markedly stronger hypercapnic stimuli than that used in this research. Among the limited findings in humans, McCulloch et al. reported that under anesthesia, the arterial pressure of CO_2 (P_{aCO_2}) at which cerebral autoregulation started to become impaired ranged was approximately 60 mmHg depending on the anesthetic used (McCulloch et al., 2000).

Recent work using more advanced regression models has also provided new insights into the temporal dynamics of cerebral autoregulation. Within the autoregulatory range, the capacity of the vasculature to counteract fluctuations in CPP depends on the frequency of fluctuations. Higher frequency pressure fluctuations demonstrate greater coherence and gain between intravascular pressure and CBF than those of lower frequency (Hamner et al., 2004; Tan & Taylor, 2014). Simply put, faster fluctuations more readily produce changes in CBF because the cerebral vessels are unable to respond quickly enough (Tan, 2012) (Figure 1.3). Conversely, slower CPP fluctuations can be more effectively addressed by the autoregulatory response. With that, it is important to recognize that impairment to the speed of vascular response may result in poorer autoregulatory control.

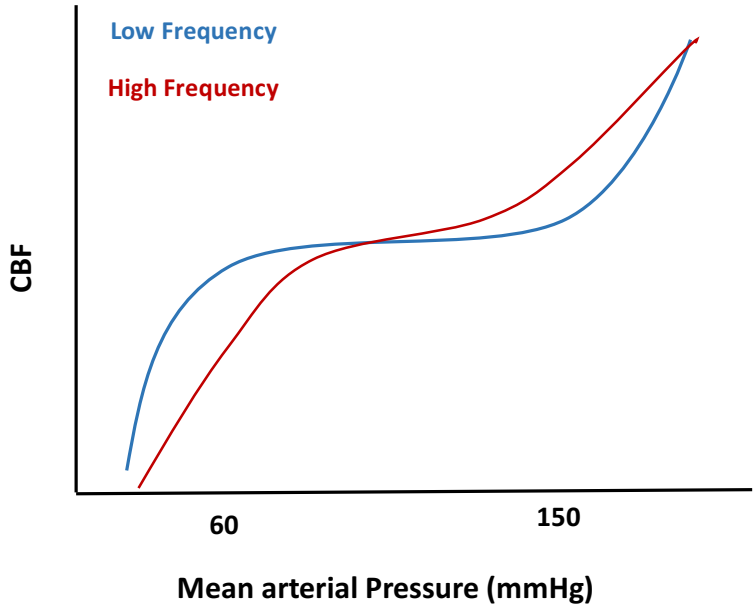

Figure 1.3. Influence of frequency of intravascular pressure fluctuation on cerebral autoregulation. Changes in MAP are more effectively counteracted within the autoregulatory range in the face of lower frequency fluctuations of MAP compared to higher frequency fluctuations. Content of figure adapted and altered from (Tan, 2012; Tzeng & Ainslie, 2014).

The physiological basis for cerebral autoregulation is centred around the intrinsic ability of the VSMCs to directly detect changes in transmural pressure and readily alter vascular tone in response. This feature is present in arterial vessels of varied caliber, from large arteries to small resistance arterioles, and has been termed the myogenic response. Originally described by Bayliss over 100 years ago, the entire mechanism of the myogenic response has yet to be fully understood, though evidence suggests that it is driven primarily by Ca^{2+} currents in cerebrovascular smooth muscle (Bayliss, 1902; Cipolla, 2009). Though the initiating events in the myogenic response are also not definitively elucidated, it is believed that stretch-sensitive cation channels cause membrane depolarization that activates voltage-gated $Ca^{2+}{}_{v}$ channels, leading to Ca^{2+} influx which activates myosin light chain kinase (MLCK), a key pro-constrictive enzyme (Knot & Nelson, 1998). Membrane-bound mechano-sensitive enzymes are also thought to play a substantial role in the myogenic response, eliciting an intracellular cascade that may activate numerous intracellular targets including cytochrome P450, which produces 20-Hydroxyeicosatetraenoic acid (20-HETE), a potent vasoconstrictor (Lange et al., 1997; Cipolla, 2009). Finally, Ca^{2+}-dependent potassium (K^{+}) channels have also been proposed as a key negative feedback mechanism in cerebral autoregulation. Abolishing the activity of Ca^{2+}-

dependent K^+ channels has been found to enhance myogenic responsiveness, supporting the belief that this channel provides negative feedback to the myogenic response to prevent aberrant contractile activity (Brayden & Nelson, 1992; Cipolla, 2009; Schubert et al., 2008).

1.3.3 Neurovascular coupling

Due to the energetically dynamic nature of neuronal tissue, metabolic demand can fluctuate dramatically over short periods of time. This poses a unique challenge to the brain as neural tissue has a limited capacity to store energy molecules in appreciable quantities. Fortunately, the brain has evolved a system, termed neurovascular coupling (NVC), to accommodate the constantly changing metabolic needs of individual brain regions. While cerebral autoregulation attempts to maintain a constant CBF throughout the brain, NVC follows an entirely different mandate, aiming to adjust regional CBF to better reflect functional activity. The term "neurovascular coupling" is used to reflect the tight functional coordination of neurons and nearby blood vessels. Simply put, neurons generate the signals initiating vasodilation, astrocytes act as conduits to transmit those signals to VSMCs, pericytes, and endothelial cells, which then generate a highly coordinated vasomotor response to adjust CBF. This resultant increase in CBF during neuronal activity has since been coined functional hyperemia (Iadecola & Nedergaard, 2007). Interestingly, functional MRI (fMRI) experiments that have measured the increase in CBF in response to neural activation have found flow to increase 45%, while oxygen consumption increases only 16% (Davis et al, 1998). This apparent oversupply of CBF is a normal observation in healthy individuals, and while there is no definitive explanation for its purpose, some compelling hypotheses have been generated. This seemingly excessive increase in blood flow may be a built-in safeguard against diseases that impair blood flow or it may be necessary to accommodate increased neural activity in ways that are not yet fully understood, such as for the dissipation of metabolic heat (Mikulis, 2013; Yablonskiy et al., 2000).

The mechanism underlying NVC has been another topic of intense discussion. A number of molecules have been suggested as messengers in NVC used to communicate the local energetic needs to cerebral vessels (Attwell et al., 2010). Early work suggested that NVC may be mediated

by a negative-feedback mechanism involving the consumption of either O_2 or glucose, or the production of CO_2. However, subsequent studies that modulated blood O_2 partial pressure and glucose concentrations have since concluded that neither molecule regulates CBF in this manner (Attwell et al., 2010; Mintun et al., 2001; Powers, Hirsch, & Cryer, 1996). These findings are consistent with the notion that it is unlikely that a negative feedback mechanism would be capable of causing extended functional hyperemia, as the signal generated by the local depletion of O_2 or glucose would be almost immediately reversed by the ensuing rise in CBF. A similar concept can be used to refute the idea that CO_2 is the primary mediator of NVC, as any vasodilatory signal generated by CO_2 would quickly deteriorate because the subsequent increase in CBF elicited by neuronal activity would clear CO_2 from the area. Therefore, the presence of a prolonged vasodilatory response to neural activation also precludes CO_2 as the primary mediator, and this is supported by observations of the alkalization of neural tissue during activation as a result of CO_2 washout (Chesler, 2003; Makani & Chesler, 2010).

Feedback mechanisms of NVC have largely been superseded by a neurotransmitter-mediated feed-forward mechanism following the discovery that neurotransmitter signaling, most notably glutamatergic, plays a leading role in CBF regulation and that astrocytes are key mediators in this mechanism (Attwell et al., 2010). Glutamatergic signaling activates metabotropic glutamate receptors (mGluR) on nearby astrocytes leading to an increase in intracellular Ca^{2+} concentration that activates phospholipase A_2 (PLA_2). This enzyme reacts with cellular lipid membranes to liberate arachidonic acid (AA), a fatty acid used in several enzymatic pathways to produce vasoactive products, including prostaglandin E_2 (PGE_2) and epoxyeicosatrienoic acid (EET). Both molecules relax vascular smooth muscle by binding to EP_4 smooth muscle prostaglandin receptors or opening smooth muscle Ca^{2+}-activated K^+ channels, respectively (Fleming, 2014; Metea, 2006). Takano and colleagues found that prostaglandin synthesis by cyclooxygenase-1 (COX-1) in astrocytes mediated approximately 71% of the neurovascular response (Takano et al., 2006). The remainder of the vascular response to neuronal activity may be explained by EET or direct neuronal signaling to blood vessels. Paradoxically, astrocytic AA has also been found to be metabolized by cytochrome P450 into 20-hydroxyeicosatetraenoic acid (20-HETE), a potent vasoconstrictor, and thus increases in astrocytic Ca^{2+} concentration can actually lead to constriction of nearby blood vessels (Amruthesh et al., 1993; Attwell et al., 2010; Kroetz & Xu, 2005; Metea, 2006; Mulligan & MacVicar, 2004). This phenomenon may be explained by the

discovery that the metabolic state of local neural tissue directly regulates the polarity of astrocytic control of CBF. When O_2 availability is reduced during astrocyte activation, glycolysis inside the astrocyte outpaces oxidative metabolism resulting in an accumulation of lactate. Increased lactate levels change the dominant AA metabolite to PGE_2 by blocking PGE_2 reuptake from the perivascular space, resulting in a stronger vasodilatory signal (Gordon et al., 2008). Essentially, astrocytes also act as local O_2 sensors and adjust the neurovascular response accordingly (Attwell et al., 2010).

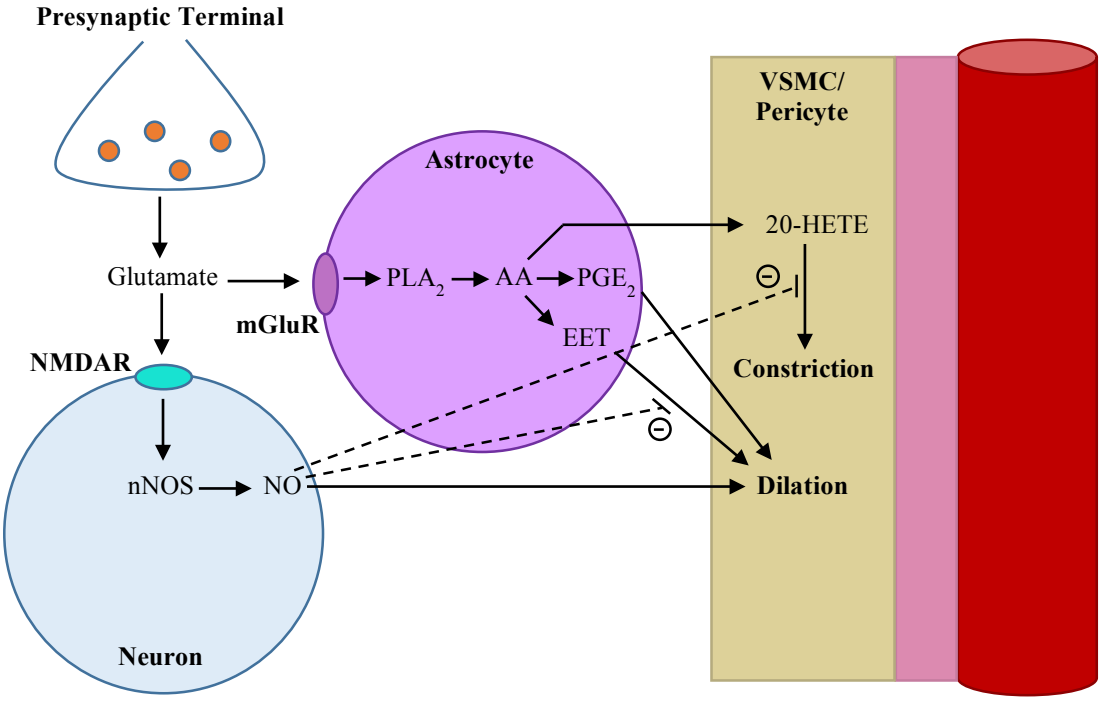

Figure 1.4. Diagram of proposed mechanisms of NVC. In astrocytes, glutamate release activates mGluR causing an influx of Ca^{2+} which activates PLA_2. PLA_2 liberates AA that is metabolized into PGE_2, EET, and 20-HETE, which regulate nearby VSMCs. Neuronally, glutamate activates NMDA receptors causing Ca^{2+} influx which activates nNOS, increasing NO release. NO may also inhibit the activities of EET and 20-HETE, promoting the activity of PGE_2 produced by astrocytes. Content of figure adapted and altered from (Attwell et al., 2010).

Presynaptic release of glutamate also activates neuronal N-methyl-D-aspartate (NMDA) receptors, causing Ca^{2+} influx and the activation of neuronal nitric oxide synthase (nNOS). Nitric oxide (NO) produced in the neuron can freely diffuse to nearby blood vessels, where it activates soluble guanylyl cyclase (Attwell et al., 2010). This generates cyclic guanosine monophosphate (cGMP), an important secondary messenger that signals smooth muscle relaxation through

multiple pathways (Garthwaite & Boulton, 1995; Ignarro et al., 1999). Firstly, increased cGMP in smooth muscle inhibits Ca^{2+} entry into the cell, reducing intracellular calcium concentrations, which normally binds calmodulin to activate MLCK. Secondly, cGMP activates K^+ channels, leading to hyperpolarization and relaxation in VSMCs. Lastly, cGMP stimulates a cGMP-dependent protein kinase that activates myosin light chain phosphatase, which antagonizes the activity of MLCK, resulting in greater smooth muscle relaxation.

The activities of these parallel glutamate-dependent NVC pathways are further complicated by a number of modulatory interactions between them. Neuronal NO non-selectively inhibits both the EET and 20-HETE synthesis pathways, but upregulates COX-1 activity, which is responsible for producing PGE_2 (Alonso-Galicia et al., 1997; Attwell et al., 2010; Fujimoto et al., 2004; Sun et al., 1998). This may be important in magnifying the vasodilatory signal relayed by astrocytes, with some research concluding that this role comprises a majority of NO's role in NVC (Attwell et al., 2010; Sun et al., 1998). Additionally, secondary to glutamate, GABAergic signaling has also been found to mediate neurovascular coupling, however the extent of mediation and precise pathway through with this is achieved is not yet clear (Duchemin et al., 2012; Kocharyan et al., 2008).

Dysfunction of the neurovascular unit has been reported in a number of neurological conditions including stroke (Ruhrberg & Bautch, 2013) and AD (Zlokovic, 2010, 2011). Disruption of the neurovascular unit associated with AD will be discussed in a later section of this thesis.

1.3.4 CO_2 vasoreactivity

Cerebral blood vessels are sensitive to changes in the partial pressure of arterial CO_2 (P_{aCO_2}). In healthy vascular tissues, elevations in P_{aCO_2} lead to vasodilation of cerebral blood vessels resulting in an increase in CBF, while reductions in P_{aCO_2} result in cerebral vasoconstriction and a subsequent decrease in CBF (Kety & Schmidt, 1948). As well, reactivity to CO_2 is a key homeostatic function that regulates respiratory drive and helps maintain tissue pH within a set physiological range (Ainslie & Duffin, 2009; Chesler, 2003). Of note, the cerebrovascular response to changes in CO_2 is not uniform throughout the vascular tree as smaller caliber blood

vessels have been found to be more responsive to hypercapnia (Wei et al., 1980). This feature may be explained by the fact that resistance to flow is encountered mostly in the cerebral arterioles and capillaries, thus adequate control of small vessel tone is imperative to eliciting meaningful changes in CBF (Cipolla, 2009).

The mechanisms underlying the activity of CO_2 have proven to be highly complicated and remain to be fully elucidated. Some findings suggest that during hypercapnia, the resultant decrease in pH opens K^+ channels on vascular endothelial cells or VSMCs, leading to hyperpolarization that mediates the vasodilatory response (Ainslie & Duffin, 2009). The BBB has low permeability to H^+ and HCO_3^- ions, however CO_2 can freely diffuse across the vascular endothelium. Therefore, an increase in arterial CO_2 will increase the perivascular concentration of H^+ ions by driving the carbonic anhydrase reaction. On vascular endothelium, both voltage-gated K^+ channels and ATP-sensitive K^+ channels can open in response to changes in pH (Ainslie & Duffin, 2009; Berger, 1998; Xu et al., 2001). Opening endothelial K^+ channels results in an efflux in K^+ that hyperpolarizes the cell, however the pathway that translates this change into a vasomotor response is not as clear. Hyperpolarizing K^+ currents may be directly transmitted to associated VSMCs through myoendothelial junctions, closing voltage-gated Ca^{2+} channels on VSMC, thus reducing intracellular Ca^{2+} and dilating the vessel (Ainslie & Duffin, 2009; Golding et al., 2002; Jackson, 2005). Similarly, these hyperpolarizing currents could also be transferred to adjacent endothelial cells via endothelial gap junctions, allowing vasodilatory signals to be conducted to nearby vessel segments, enabling coordinated vascular responses (Ainslie & Duffin, 2009; Jackson, 2005).

Additionally, the release of vasodilatory factors such as NO and prostaglandins is another plausible pathway through which CO_2 may regulate vascular tone. While growing evidence indicates that NO plays an important mediator role in CO_2 vasoreactivity, there is still ongoing debate over the origin of the NO stimulus (Ainslie & Duffin, 2009; Leffler et al., 1994). Some argue that neuronal NOS (nNOS) produces the NO relevant to CO_2 vasoreactivity, while others suggest that endothelial NOS (eNOS) is resonsible (Brian, 1998; Lavi et al., 2006). Evidence also exists for contributions by other vasoactive molecules, including C-natriuretic peptide and adrenomedullin, possibly initiated by shear stress on the vascular endothelium during hypercapnic vasodilation (Ainslie & Duffin, 2009; Chun et al., 1997).

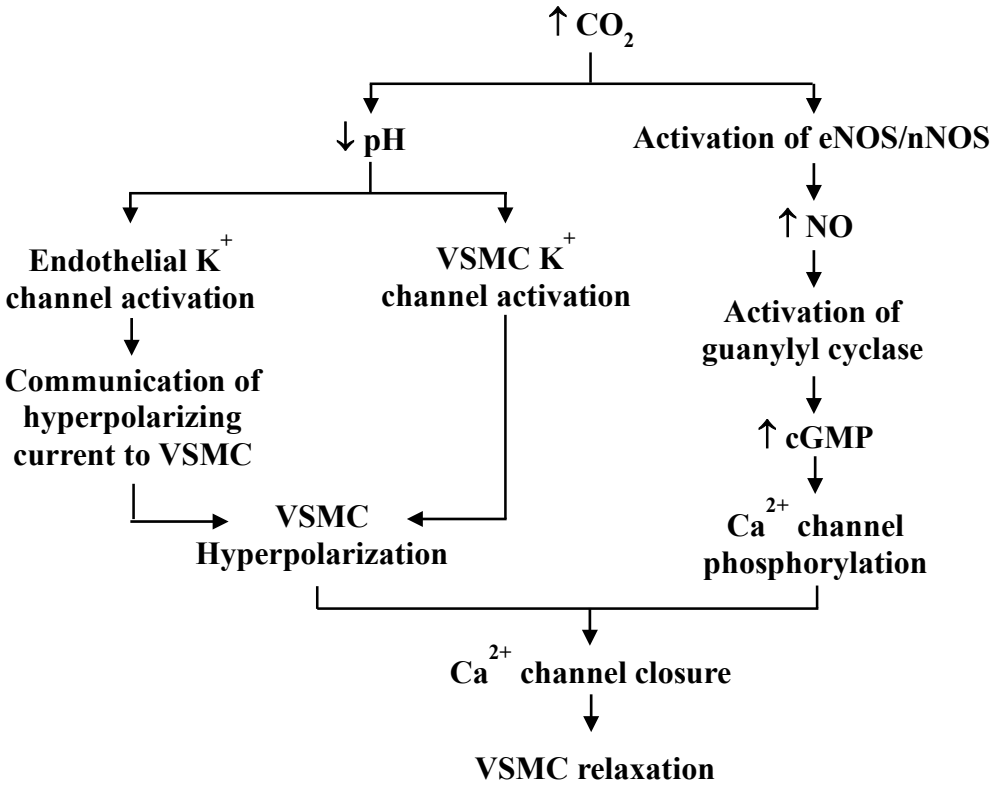

Figure 1.5. Summary flow chart of proposed mechanisms of CO_2 vasoreactivity. Increased CO_2 will decrease perivascular pH and potentially activate NOS (endothelial or neuronal). Decreased pH has been found to open K^+ channels on the endothelium and VSMCs leading to hyperpolarization. NOS activation increases NO production, which promotes phosphorylation of Ca^{2+} channels. Together, these two pathways reduce conductivity of Ca^{2+} channels, causing VCMC relaxation.

Interestingly, the findings from a number of *in vitro* studies appear to refute the possibility of some of the mechanisms proposed above. Interrogation of isolated cerebral arterioles has revealed that hypercapnia does cause vasodilation in the absence of extravascular cells (Dietrich & Dacey Jr, 1994). Also, cerebral vessels with a damaged or denuded endothelium have also been shown to retain reactivity to CO_2 (Wang et al., 1994; You et al., 1994). These reports suggest that VSMCs and pericytes are solely responsible for hypercapnic vasodilation; however it is possible that there exist several overlapping pathways that mediate the vascular response and that blocking a single pathway is not sufficient to dramatically impair reactivity. In fact, considering all the findings presented in this section, these reports may provide stronger evidence for the existence of multiple complementary pathways involving either endothelial and extravascular cells, rather than for the total non-participation of these cells in the vascular response to CO_2.

1.4 Cerebrovascular Reactivity

1.4.1 What is cerebrovascular reactivity

The brain's ability to dictate CBF is reliant on the capacity of arterial vessels and capillaries to readily change diameter. For this reason, the integrity of this function has been of particular interest to researchers examining blood flow dysregulation as a potential contributor to disease. This introduces the concept known as cerebrovascular reactivity (CVR). CVR, broadly defined, is the change in CBF per unit change in a given vasoactive stimulus. This metric provides a quantitative measure of the brain's capacity to augment CBF in the face of a vasoactive stimulus. The CVR response can be resolved into two main components: (i) a magnitude component defining the magnitude of reactivity of the cerebral vasculature, which assesses cerebrovascular reserve, or the extent to which vessels are able to accommodate increases in CBF demand (Goode et al., 2009), and (ii) a temporal component that describes the speed of the cerebrovascular response to vasoactive stimuli, which may also be of clinical interest as it is an indicator of vascular compliance (Poublanc et al., 2015). For simplicity, from this point on, the magnitude component will simply be referred to as CVR, while the temporal component will be specifically referred to as the speed of cerebrovascular response or the time constant used to define it "τ" (explained later).

In diseases that impinge on normal CBF, the brain will attempt to maintain adequate CBF mainly through cerebral autoregulation, dilating cerebral resistance vessels and consuming cerebrovascular reserve (Derdeyn et al., 1999; Yonas & Pindzola, 1994). This compensatory vasodilation may sustain normal function and prevent acute injury, however damage may still be incurred by the introduction of a hemodynamic deficit, where increases in metabolic demand will fail to elicit an adequate response in blood flow. Or in other words, cerebral autoregulation has exhausted cerebrovascular reserve. Also, once the resistance vessels in the affected area have maximally vasodilated, any subsequent reductions in perfusion pressure will result in a linear reduction in CBF, a phenomenon that has been termed vascular "steal".

As a direct physiological test of vascular reserve, CVR can be a useful metric in evaluating both the susceptibility of tissues to hypotension-induced ischemia and the integrity of NVC throughout the brain. It should be noted that CO_2-mediated flow regulation and NVC likely integrate at the level of the smooth muscle, thus CVR imaging techniques may only detect neurovascular uncoupling related to vascular injury and may not be able to identify disruption to NVC mechanisms upstream of the blood vessel. Reduced CVR is associated with increased stroke risk in patients with carotid artery occlusion and stenosis (Markus & Cullinane, 2001; Silvestrini et al., 2000), as well as deleterious structural changes such as cortical thinning and age-related ischemic white matter disease (Conklin et al., 2011; Fierstra et al., 2010; Sam et al., 2016c). Reduced CVR has actually been found to precede the development of white matter hyperintensities in age-related ischemic white matter disease, suggesting a causal role of CVR impairment in ischemic injury (Mandell et al., 2008; Sam et al., 2016b). Additionally, neuropsychological evaluation of steno-occlusive patients with impaired cerebral hemodynamics shows measurable cognitive deficits (Balucani et al., 2012). Interestingly, surgical revascularization has been found to at least partially reverse cortical thinning and slow cognitive decline in these patients (Baracchini et al., 2012; Fierstra et al., 2011). Hemodynamic impairment has also been observed in a number of neurological diseases including depression and AD (Lemke et al., 2010; Silvestrini et al., 2012), however the characterization of the hemodynamic components of many of these diseases is far less robust. The specific hemodynamic findings in AD will be covered in a later section of this thesis.

Disease-related alterations to the speed of cerebrovascular response have been examined far less frequently, possibly due to methodological challenges in accurately measuring this metric. Methodological considerations towards assessing the cerebrovascular response will be covered in later sections, but in brief, the difficulty lies in achieving an abrupt step change in P_{aCO_2}, as gradual increases in P_{aCO_2} may make it difficult to resolve vascular responses with a time course shorter than that of the stimulus. Poublanc and colleagues reported prolongation of the vascular response in patients with unilateral steno-occlusive disease, ipsilateral to their stenosis (Poublanc et al., 2015). New findings have also demonstrated a link between the speed of cerebrovascular response to vasodilatory stimuli and age-related ischemic white matter disease (Sam et al., 2016a), indicating that delayed vascular reactivity may contribute to the vascular burden

associated with impaired vasoreactivity. Current findings on speed of the cerebrovascular response in AD will be discussed later in this chapter.

All together, these findings suggest that localizing impaired CVR and/or speed of cerebrovascular response and quantifying the extent of impairment may complement traditional neurologic assessment in a number of conditions. In fact, CVR maps have already been used to evaluate clinical outcomes in patients following cerebral revascularization surgery (Han et al., 2011; Mikulis, 2013; Mikulis et al., 2005).

1.4.2 Methodological considerations for measuring CVR

Unfortunately, the methodology for assessing CVR has yet to be standardized. Thus, when faced with measuring CVR there are two main technical considerations: (i) the application of the vasoactive stimulus to elicit a vascular response, and (ii) measuring the resultant change in CBF. Numerous options are available to fulfill both requirements, with each carrying distinct advantages and drawbacks.

1.4.2.1 Vasoactive stimulus

"It is this inability to standardize the vasoactive stimulus, or alternatively, precisely and accurately measure the stimulus at the active site, that has most impeded comparison of CVR between various studies, and between individuals in the same study."

- Fierstra et al., 2013

Most CVR studies rely on inhaled CO_2 or acetazolamide administration, however other strategies such as breath-holding and induced hypotension have also been employed. This thesis takes particular interest in measuring both CVR and the speed of the vascular response to vasodilatory

stimuli in AD, therefore this section will examine the applicability of each vasoactive stimuli towards accomplishing this.

Hypotension

While superficially, induced hypotension looks to be an ideal method for evaluating CVR, difficulties constructing a consistent and repeatable hypotensive stimulus (Mahoney et al., 2000) and concerns about the risk of hypotension-induced ischemia have made this technique unattractive to most researchers (Fierstra et al., 2013).

Acetazolamide

Acetazolamide (ACZ) is a commonly used drug in CVR imaging as a vasodilatory stimulus. ACZ achieves its effect by inhibiting carbonic anhydrase to produce cerebral acidosis, resulting in the relaxation of VSMCs. ACZ's popularity likely stems from its ease of implementation, lack of subject involvement, and its strong safety index (Fierstra et al., 2013; Okazawa et al., 2001). However, achieving a standardized stimulus with ACZ is still a considerable challenge. The effect of ACZ is highly variable because of individual differences in both pharmacokinetics and responsiveness to ACZ at a given concentration. To control for this variability, it is generally recommended that one uses a supramaximal dose to ensure maximal vasodilation in all subjects. Unfortunately, this strategy is still not without notable drawbacks. ACZ doses in the supramaximal range are associated with high incidence of adverse effects, which may lead to poor compliance, and the variable temporal dynamics of the stimulus still make comparing the speed of vascular response between subjects infeasible (Fierstra et al., 2013).

Hypercapnia

Breath holding

Hypercapnia is a potent vasodilatory stimulus and is both well tolerated and safe, even in severely ill patients (Spano et al., 2013). With that, CO_2 has proven to be an ideal stimulus for CVR investigations, however the implementation of a CO_2 challenge is complicated by the numerous ways that this can be accomplished. Respiratory maneuvers, such as breath-holding, are perhaps the easiest way to induce changes in P_{aCO_2}, being non-invasive and requiring little to no equipment. Some studies have utilized breath-holding with moderate success (Silvestrini et

al., 1999; Vernieri et al., 1999), however the major problem with this technique is that the length of the breath-holding period often does not reflect the resultant change in P_{aCO_2} (Fierstra et al., 2013). The relationship between breath-holding time and P_{aCO_2} is not linear, and an individual's rate of CO_2 production, respiratory physiology and technique in executing the breath-hold (ex. inspiration immediately before breath-hold) can all dramatically alter the final change in P_{aCO_2} (Fierstra et al., 2013). Additionally, the dynamics of the stimulus cannot be measured during the breath holding period, making the true stimulus applied to each subject unknowable. This is a particularly troublesome issue given the profound influence patient cooperation has on the achieved stimulus. Lastly, it should be noted that breath-holding can elicit a meaningful change in arterial pressure of oxygen (P_{aO_2}) and CBF, which may confound the CO_2 stimulus (Prisman et al., 2008; Sasse et al., 1996).

Fixed inspired CO_2 Challenge

A fixed inspired CO_2 challenge is another common means of altering $PaCO_2$. Exposing patients to gas with a fixed percentage of CO_2 appears to be a standard stimulus, however individual physiological parameters such as rate of CO_2 production and minute ventilation alter the P_{aCO_2} each subject achieves (Fierstra et al., 2013). For instance, an inspired CO_2 challenge may increase ventilation rate, and by extension, increase elimination of CO_2, such that $PaCO_2$ is not substantially changed by the stimulus. Nonetheless, fixed inspired CO_2 is still widely used as a means of interrogating hemodynamic impairment in numerous diseases including AD (Cantin et al., 2011; Richiardi et al., 2015; Yezhuvath et al., 2012). This method of stimulus delivery has been especially limiting on the ability of these studies to confidently remark on the speed of vascular response. The ideal stimulus for measuring the speed of the vascular response is an abrupt step change in P_{aCO_2}, however, this cannot be achieved using fixed inspired CO_2 (Poublanc et al., 2015). In fact, fixed inspired CO_2 challenges result in an biexponential rise in P_{aCO_2} due to "wash in" effects caused by the lung (Fisher, 2016; Mark et al., 2010; Poublanc et al., 2015). As well, measurements of P_{ETCO_2} do not accurately reflect P_{aCO_2} when using a fixed inspired CO_2 stimuli, making it infeasible to quantify the achieved stimulus non-invasively (Poublanc et al., 2015; St Croix et al., 1995). Additionally, fixed inspired CO_2 suffers from the same potential confound as breath-holding by failing to prevent fluctuations in P_{aO_2} during acquisition (Prisman et al., 2008).

Prospective end-tidal gas targeting

In contrast, using a computer-driven prospective end-tidal targeting system with a sequential gas delivery breathing circuit addresses the limitations of breath-holding and fixed inspired CO_2, enabling the precise application and maintenance of an abrupt, quantifiable step change in P_{aCO_2} while remaining normoxic, irrespective of minute ventilation (Banzett et al., 2000; Slessarev et al., 2007). A sequential gas delivery breathing circuit enables precise user control of the alveolar ventilation, enabling the accurate targeting of individual end-tidal gas tensions, regardless of changes in the subject's minute ventilation or breathing pattern (Slessarev et al., 2007). Perhaps most importantly, by leveraging rebreathing of expired gas that has been equilibrated with the subject's P_{aCO_2}, the gradient between P_{ETCO_2} and P_{aCO_2} is minimized, allowing P_{ETCO_2} to be used as a surrogate measure of P_{aCO_2} (Fierstra et al., 2013; Ito et al., 2008). Using the other described stimuli, the input signals are at best crudely estimated, generally onvolving 'on/off' waveforms as models of the breathing state (free-breathing vs. breath-holding or presence/absence of inspired CO_2) (Poublanc et al., 2015). Conversely, prospective end-tidal targeting enables noninvasive breath-to-breath measurement of the real P_{aCO_2} stimulus.

1.4.2.2 Imaging CBF changes

A number of different tools are also available for measuring CBF in humans including transcranial Doppler (TCD), single photon emission computed tomography (SPECT), Xenon-enhanced computed tomography (CT), positron emission tomography (PET), Dynamic susceptibility contrast (DSC) MRI, arterial spin labeling (ASL) MRI and Blood oxygen level-dependent (BOLD) MRI (Wintermark et al., 2005). Some important consideration for each technology in the context of CVR will be discussed below.

Transcranial Doppler

Utilizing ultrasound, TCD is a simple, non-invasive method for measuring CBF in the brain. However, this technique has very limited spatial coverage and cannot measure flow changes beyond the level of major cerebral arteries, limiting its utility in assessments of CVR.

SPECT, Xenon CT, PET and DSC MRI

These imaging options generally have limited appeal because they require the administration of an exogenous contrast, and all except DSC MRI expose patients to ionizing radiation. SPECT can produce a quantitative measure of CBF, however when applying a vasoactive stimulus two imaging sessions are required with a delay between them for contrast washout. Xenon CT requires the inhalation of xenon which may complicate the administration of an inhaled CO_2 stimulus. PET imaging would be an ideal modality for quantitatively measuring changes in CBF in CVR studies, however it requires oxygen-15 as a tracer, necessitating access to a cyclotron. Lastly, DSC MR perfusion imaging utilizes gadolinium-based paramagnetic contrast agents to measure CBF. This technique can yield a semi-quantitative measure of CBF, however it requires a well-calibrated arterial input function, or else calculations of CBF will be inaccurate (Wintermark et al., 2005). Furthermore, DSC imaging is unable to provide temporal assessment of the cerebrovascular response due to delays between contrast injections.

ASL MRI

ASL MRI non-invasively quantifies CBF by magnetically labelling water protons of blood entering the brain and uses them as an endogenous contrast. Labelled protons contribute less to the MR signal, thus by subtracting the signal acquired after tagging from a control image, CBF can be computed in standard units. An important strength of ASL is that it does not require an arterial input function, however inappropriate selection of a post-labelling delay can affect accuracy of CBF measurements. Also of note, the signal-to-noise ratio (SNR) is particularly low in ASL MRI, requiring one to average multiple “tagged” and “control” images to produce a reliable measure of CBF. This inevitably lengthens scan time, limiting the temporal resolution of your measurements and making ASL MRI unsuitable for the purposes of examining CVR dynamics. Nonetheless, ASL MRI remains a popular tool for the measurement of resting CBF.

BOLD MRI

BOLD MRI leverages the paramagnetic property of deoxyhemoglobin (dHb) to detect changes in CBF (Ogawa et al., 1990). The primary limitation of BOLD for CVR imaging lies in the fact that it does not directly detect CBF, rather this modality measures the washout of dHb as a surrogate measure of CBF. There are several drawbacks of this in the context of CVR. Firstly, BOLD CVR

relies on the assumption that the cerebral metabolic rate of O_2 ($CMRO_2$) is constant throughout the acquisition, as fluctuating $CMRO_2$ would directly change dHb concentration, confounding the measured change in CBF. Secondly, the relationship between concentration of dHb and CBF is not linear across all values of CBF, though it is believed that change in dHb concentration is proportional to the change in CBF in the CBF range relevant to this study (ie. during 15 mmHg above resting P_{aCO_2} stimulus). Thirdly, BOLD signal cannot be converted into standard units, thus measurements are limited to percent change. Moreover, the maximum achievable percent change in BOLD signal is determined by the amount of dHb in a given voxel at rest, and thus is influenced by other factors, namely cerebral blood volume (CBV) and oxygen extraction fraction (OEF). Lastly, BOLD is prone to low frequency signal drift, necessitating multiple baselines be captured during CVR imaging for drift correction in post-processing.

While the limitations of BOLD MRI are not trivial, the advantages of BOLD MRI for CVR investigation are numerous. BOLD CVR is non-invasive, requiring no exogenous contrast, and can be accomplished in a single, timely acquisition. BOLD imaging offers a relatively high spatial resolution, full coverage of the brain and a high enough temporal resolution to evaluate dynamics of the cerebrovascular response. Furthermore, BOLD CVR has been validated against ASL MRI (Mandell et al., 2008), and has found to be highly reproducible, demonstrating an intraclass correlation coefficient between 0.88 and 0.92 in sequential scans (Kassner et al., 2010). BOLD MRI and quantification of the BOLD signal will be revisited later in this thesis.

1.5 Alzheimer's Disease

1.5.1 What is Alzheimer's disease?

Alzheimer's disease (AD) was first described in 1906 by German physician Dr. Alois Alzheimer as an insidious neurodegenerative disorder of the CNS (Braak & Del Tredici, 2014; Stelzmann et al., 1995). Today, AD is known to be the most common cause of dementia in the world, accounting for 60-80% of the estimated 40 million cases worldwide (Barker et al., 2002; Ferri et

al., 2005; Mayeux & Stern, 2012; Prince et al., 2013). AD can be subdivided into two types, early-onset AD (EOAD) and sporadic or late-onset AD (LOAD), with sporadic AD making up over 95% of cases (Reitz & Mayeux, 2014). With increasing life expectancies and an aging global population, current projections estimate the global prevalence of dementia will reach 115 million by the year 2050 (Prince et al., 2013; Reitz & Mayeux, 2014). The socio-economic costs related to dementia are immense. In the United States alone, approximately 5.4 million people are suffering from clinical AD. The direct healthcare costs associated with dementia in the US in 2015 were estimated at US$236 billion, plus an additional US$221 billion in indirect costs for family and other unpaid caregivers (Alzheimer's Association, 2016).

The first clinical manifestation of AD is usually a mild decline in memory with otherwise unaffected cognition. As the diseases progresses, more domains become affected, practical skills deteriorate and personality changes often manifest. In later stages of AD, patients will experience a decline in language, executive function, and visuospatial capacities, and finally, severe dysfunction of their autonomic and motor systems (Albert et al., 2011; Braak & Del Tredici, 2014; Dubois et al., 2014; McKhann et al., 2011). To date, clinicians are limited to "provisional" diagnoses of AD during end stages of the disease. Despite continued efforts in developing new diagnostic and prognostic tools, clinical diagnosis still requires a *post mortem* examination to pathologically confirm the presence of AD (Beach et al., 2012; Braak & Del Tredici, 2014; Montine et al., 2012).

The pathological effects of Alzheimer's disease reach all corners of the brain, however not all regions are affected equally. Rather, AD demonstrates a progressive, systematic targeting of specific brain regions that is well-conserved chronologically across patients, and generally reflects the progression of clinical symptoms. Though the rate of progression is known to vary widely between cases, once initiated, the pathology associated with AD is not known to improve or go into remission (Braak & Del Tredici, 2014). The pathological process occurs over decades, only visible during the later stages of the disease. The key pathological features that define AD, and the mechanisms underlying them, will be discussed below.

1.5.2 Proteopathy in Alzheimer's disease

Above all, AD is a proteopathy. The cardinal feature of AD pathology is the presence of abnormal proteinaceous aggregates, of which there are two main types: (i) intraneuronal filamentous inclusions consisting of aggregated tau protein, followed by (ii) extracellular plaques composed of amyloid-β protein (Braak & Del Tredici, 2014). These deposits appear at markedly different time points in the disease and are observed in distinctly different regions of the brain, commencing with the aggregation of tau protein to form intraneuronal inclusions, followed by the formation of amyloid-β plaques in the extracellular space about a decade later (Braak & Braak, 1997; Braak & Del Tredici, 2014; Duyckaerts & Hauw, 1997). Once introduced, both proteopathies then spread to previously unaffected structures in a deterministic manner. It is believed that essentially all the pathophysiological consequences of AD are, to some extent, related to these two proteins.

Tau Protein

Found mainly in neurons, tau protein functions to support self-assembly and stability of axonal microtubules, one of the major cytoskeletal networks responsible for a number of key cellular functions including intracellular transport. Tau protein is also found in lower concentrations in dendrites and glia, but in these structures different proteins are believed to be responsible for microtubule stability (Braak & Del Tredici, 2014; Mandelkow & Mandelkow, 1998; Mandelkow et al., 2007). While normal tau species associate strongly with microtubules to confer stability, increased phosphorylation of tau can cause it to dissociate from microtubules and dissolve into the cytoplasm. Tau protein's phosphorylation state is constantly changing and the intended purpose behind tau phosphorylation is not entirely clear, but it appears to be involved in supporting axonal remodeling for the purposes of neural development or synapse formation (Braak & Del Tredici, 2014). This is supported by observations that phosphorylation increases during mitosis, as well as that fetal tau, the only tau isoform present in early neural development, generally experiences the highest phosphorylation state of any tau variant (Braak & Del Tredici, 2014; Goedert et al., 1993). In any case, an equilibrium is eventually reached between low phosphorylation state tau bound to microtubules and dissolved high phosphorylation state tau

according to the net activity of regulatory kinases and phosphatases (Ballatore et al., 2007). In AD, this equilibrium is perturbed by an increase in tau phosphorylation, leading to a substantial increase in the unbound tau fraction (Ballatore et al., 2007; Braak & Del Tredici, 2014; Grundke-Iqbal et al., 1986). Unlike microtubule-bound tau, soluble tau monomers can form aggregates, though even in subjects afflicted with AD, though the exact conditions that need to exist for aggregation to commence are still not fully understood, however it is generally accepted that higher concentrations of monomeric hyperphosphorylated tau in the axoplasm likely increases the probability of tau aggregation, or the probability of a pathogenic conformational change that may initiate aggregation (Alonso et al., 2001; Ballatore et al., 2007; Braak & Del Tredici, 2014). These aggregates possess dramatically different properties from monomeric tau, most notably a resistance to regulation of phosphorylation state and to cellular removal mechanisms (Braak & Del Tredici, 2014; Kovacech et al., 2010). As a result, hyperphosphorylated tau aggregates are irreversible and highly persistent. These tau aggregates continue to accumulate and assemble into larger paired helical filaments, which then cluster to form insoluble neurofibrillary tangles (NFT) (Friedhoff et al., 2000).

As mentioned earlier, tau pathology in AD does not affect neurons indiscriminately. The progression of tau pathology is highly stereotypic, commencing in a specific location and then progressing through the brain is a deterministic manner, with little inter-patient variability. This has led to the development of an AD pathological staging based on tau pathology (Braak & Braak, 1991; Braak & Del Tredici, 2014). Tau lesions first present in the locus coeruleus, a noradrenergic nucleus in the pons, then spread to other brainstem nuclei with diffuse cortical projections (stages a-c). From there, tau pathology migrates to the cerebral cortex, namely the transentorhinal cortex (stage I), before progressing into the nearby entorhinal cortex and hippocampus (stage II). In stage III, tau pathology spreads to the inferior temporal cortex. This stage is particularly noteworthy as it generally marks the onset of symptoms, with stages III-IV corresponding to mild cognitive impairment (MCI) and stage V-VI corresponding to dementia due to AD. Progressing into the later pathological stages, tau lesions spreads to include most of the temporal cortex and begins to encroach on adjacent structures including the insular cortex, inferior frontal structures, and the anterior cingulate (stage IV). Stage V is significant in that we see widespread involvement of the cerebral cortex, including prefrontal and high order sensory areas, leaving only primary sensory and motor cortices mostly unscathed. Finally, in stage VI

essentially all cortical regions demonstrate noticeable NFTs, including the primary sensory and motor cortices (Braak & Del Tredici, 2014). Interestingly, the spatiotemporal progression of tau lesions mirrors the process of myelination in the cortex, only in the reverse order. This may be explained by the fact that areas that begin myelination earlier in development also tend to end up being the most heavily myelinated. This implies that myelination plays a significant role in preventing the development of AD pathology (Braak & Del Tredici, 2014). This is indirectly supported by observations that the cognitive alterations associated with in AD are also similar to the maturation process, though again in reverse order, a phenomenon termed retrogenesis (Ashford & Bayley, 2013; Rubial-Álvarez et al., 2013). Additionally, nearly all the neurons that are susceptible to AD-related tau pathology are projection neurons with long axons (Braak & Del Tredici, 2014). Almost invariably, neurons that are predisposed to developing intraneuronal tau inclusions are also poorly myelinated. Active projection neurons with long, sparsely myelinated axons will expend more energy than their myelinated counterparts and are subject to greater oxidative stress due to increased mitochondrial activity (Pohanka, 2014). Moreover, increased myelination may enable oligodendrocytes to provide greater levels of axonal support (Braak & Del Tredici, 2014; Nave, 2010). Better understanding the benefits derived from these characteristics may provide some insight into the mechanism of action of tauopathies.

Mechanistically, tau-related toxicity has largely been attributed to the disruption of neuronal transport and other cytoskeletal functions due to the loss of tau's normal MT-stabilizing activity in axons (Ballatore et al., 2007; Braak & Del Tredici, 2014; Roy et al., 2005). Given the unique morphological structure and high metabolic demands of neurons, it is unsurprising that these cells are heavily reliant on the efficient transport of resources and organelles for normal cellular function (Roy et al., 2005; Saxton & Hollenbeck, 2012). Indeed, the contribution of loss of tau function towards AD was demonstrated convincingly when it was shown that MT-stabilizing drug paclitaxel was effective at preventing the neurodegenerative phenotype of tau/amyloid transgenic mouse models (Zhang et al., 2005). Additionally, large aggregates of tau, such as NFTs, have also been argued to directly impede axonal transport by occupying excessive amounts of space, physically blocking the movement of intact motor proteins and cargo (Braak & Del Tredici, 2014).

While it was long believed that NFTs were the primary cause of tau-related neuronal injury and death, new findings are beginning to refute this notion. Instead, evidence now suggests that these

smaller soluble aggregates of hyperphosphorylated tau exert cause significant injury and may underlie, or at least contribute to, a number of pathophysiological features of AD (Kopeikina et al., 2012). This includes the disruption of microtubule-based neuronal transport, deficits in mitochondrial transport, Ca^{2+} dyshomeostasis, synaptic dysfunction and loss, and caspase activation (Braak & Del Tredici, 2014; Kopeikina et al., 2012; Li et al., 2007). It is possible that to mitigate such effects, neurons affected by tau pathology actually seek to convert small tau aggregates into larger, insoluble tau accumulations to minimize tau burden, thus the formation of NFTs may ultimately be an intentional measure that is protective in nature (Braak & Del Tredici, 2014).

Amyloid-β Protein

Aberrant production and accumulation of amyloid-β protein is another fundamental abnormality in AD. This neurotoxic peptide is the result of abnormal cleavage of amyloid precursor protein (APP), a normally occuring membrane-bound protein in neurons (Mattson, 2004). APP consists of a large extracellular N-terminus, a single membrane-spanning domain, and a shorter cytoplasmic C-terminus. The primary function of APP is not definitively known, though it likely possesses some functionality as a cell surface receptor. In addition, APP has also been suggested to have neurotrophic and cell adhesion functions (Muller & Zheng, 2012). Normally, APP is enzymatically processed and degraded through a pathway that precludes the formation of neurotoxic amyloid-β protein (Figure 1.6a). In this pathway, APP is cleaved by α-secretase, releasing the N-terminus fragment (APPsα) into the extracellular space. The remaining portion of APP bound to the membrane is then cleaved by γ-secretase, producing another extracellular fragment known as p3, which is essentially a truncated version of amyloid-β, and a single intracellular fragment consisting of the C-terminal domain of APP (Braak & Del Tredici, 2014; Haass et al., 2012). All of these products are relatively innocuous, readily degraded, and not prone to aggregation. Conversely, in AD, amyloid-β protein is produced by an alternative enzymatic pathway (Figure 1.6b), whereby the activity of α-secretase is replaced by β-secretase, which cleaves APP at a different location, producing a different N-terminus fragment (APPsβ) and a different membrane-bound fragment (Vassar et al., 1999). As a result, when the membrane-bound portion is subject to γ-secretase cleavage, a different peptide is released, amyloid-β, instead of p3 (Haass et al., 1992, 2012; Mattson, 2004; Shoji et al., 1992).

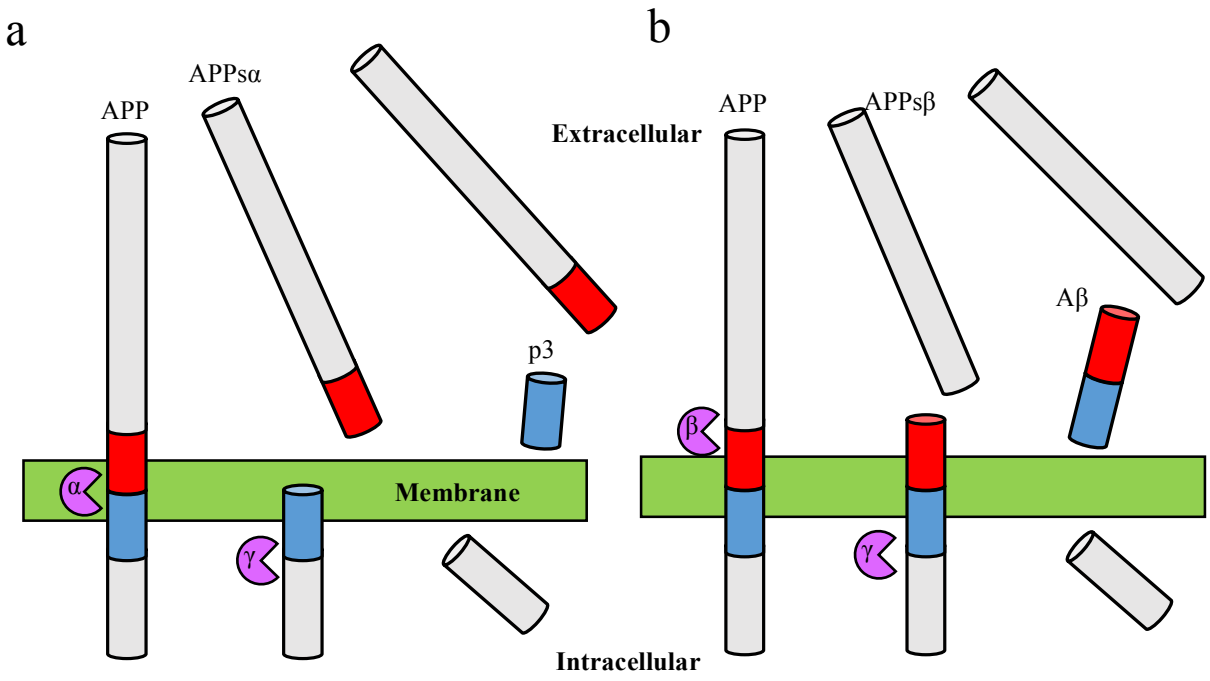

Figure 1.6. Diagram of APP Processing Pathways. (a) non-amyloidogenic pathway: APP is cleaved sequentially by α- and γ-secretase to produce APPsα, p3, and an intracellular protein fragment. (b) amyloidogenic pathway: APP is cleaved sequentially by β- and γ-secretase to yield APPsβ, toxic amyloid-β, and an intracellular protein fragment. Content of figure adapted and altered from (Haass et al., 2012).

Specifically, the amyloid-β species implicated in AD degeneration is the 42-amino acid variant (amyloid-β_{42}), however the 40-subunit variant (amyloid-β_{40}) is also produced and may play some role, especially in vascular amyloidosis (Selkoe, 2008; Serrano-Pozo et al., 2011). The extracellular plaques observed in AD are formed from these amyloid-β monomers through a multi-step polymerization mechanism. Either through spontaneous nucleation of amyloid-β or in the presence of amyloid-β seeds, peptide monomers will begin to aggregate into multimers (dimers and oligomers), which then cluster together to form amyloid fibrils. Amyloid-β fibrils will also continue to clump together to form large insoluble amyloid-β plaques in the extracellular space (Haass et al., 2012). APP is most heavily expressed on neurons near synapses, and evidence seems to suggest that amyloid-β is not produced in appreciable quantities by any of the glial cells in the brain (Beyreuther & Masters, 1991; Fiala, 2007). Due to these findings, it is believed that neurons are the primary producer of neurotoxic amyloid-β in AD. However, studies of amyloid-β transport into the brain by the receptor for advanced glycation of end products (RAGE) has begun to challenge this notion, suggesting that influx of systemic amyloid-β into the

brain may be considerable. Recent findings suggest that EOAD patients carrying presenilin mutations show increased amyloid-β production, though sporadic AD patients do not (Mawuenyega et al., 2010; Potter et al., 2013). Conversely, both the early-onset and late-onset form of AD suffer from impaired clearance of amyloid-β. It should be mentioned that non-secretase APP processing pathways also exist, including a caspase pathway (Lu et al., 2003), however the influence these alternative pathways have on amyloid-β pathology is currently not well understood (Haass et al., 2012).

Amyloid-β plaques in AD are not found uniformly within the CNS, occurring with dramatically different frequency and severity depending on the region in the brain. The cerebral WM is largely spared of amyloid-β deposits, as they mainly develop in GM structures. Overall, the spatial progression of amyloid-β plaques is somewhat less predictable than that of the intraneuronal tau inclusions, however amyloid-β deposition still occurs at specific sites and advances throughout the brain in a largely stereotypic manner, which has been described by a five phase scheme (Thal et al., 2002). Firstly, amyloid-β deposits are found exclusively in the cortex, mainly depositing in sparsely myelinated regions of the basal temporal and frontal cortices (phase 1). The second phase (phase 2) is characterized by the new involvement of allocortical brain regions, specifically the entorhinal cortex and hippocampus proper. There may also be some involvement of the amygdala, insula or cingulate cortex. In phase 3, plaque formation expands to include the dentate gyrus begins, as well as several subcortical structures including the thalamus, hypothalamus, and striatum. Phase 4 is marked by amyloid-β deposition in all areas of the neocortex, as well as a number of new brainstem nuclei. During the final stage of amyloid-β pathology, stage 5, deposition of amyloid-β is observed in the cerebellar cortex (Braak & Del Tredici, 2014; Thal et al., 2002). Also, in the later phases of AD, amyloid-β plaques can combine with dystrophic neurites, abnormal astrocytes and microglial cells, and abnormal cellular processes that contain aggregated tau to form neuritic plaques (NP) (Braak & Braak, 1997; Braak & Del Tredici, 2014).

For decades, amyloid-β protein has been thought to be the primary neuropathological substrate in the development and progression of AD, and accordingly, has been the most widely investigated. With that, the amyloid cascade hypothesis of AD, first developed by Glenner and Wong, has largely been the dominant theory of AD pathogenesis and progression (Glenner & Wong, 1984). This hypothesis postulates that the accumulation of amyloid-β protein causes a cascade of

biochemical events leading to synaptic dysfunction, neuroinflammation, and cell death (Hardy & Selkoe, 2002; Selkoe, 1991). The most convincing evidence in support of the amyloid cascade hypothesis has come from genetic studies in patients with familial AD. In essentially every case of autosomal dominant EOAD where the genetic mutation has been elucidated, the affected gene has been shown to cause an increase in the production of amyloid-β_{42} (Scheuner et al., 1996). This includes known mutations of the APP gene, enhancing β-secretase activity, as well as mutations of the genes encoding presenilin 1 and 2, which produce components of the γ-secretase complex responsible for cleaving APPsβ into amyloid-β (Goate et al., 1991; Haass et al., 1995; Scheuner et al., 1996). Despite the immense efforts expended interrogating the nature of amyloid-β pathology, our understanding of the mechanism by which amyloid-β achieves its deleterious effects is still limited. However, that is not to say that progress has not be made in the intervening years. While a number of concepts have been retained from the original amyloid cascade hypothesis, our understanding of the role of amyloid-β has undergone considerable refinement in the last three decades. For example, early iterations of the amyloid cascade hypothesis of AD often held that large amyloid plaques exerted the major neurotoxic effect of amyloid-β on nearby cellular processes and glial cells (Selkoe, 1991). However, the multiplicity of observations of active soluble amyloid-β oligomers in the brains of AD patients (Gong et al., 2003; McLean et al., 1999; A E Roher et al., 1996; Shankar et al., 2008) spawned the belief that larger insoluble amyloid-β plaques may act more as reservoirs for smaller, soluble, and potentially more toxic amyloid-β oligomers (Mucke & Selkoe, 2012). This concept is consistent with the findings in mouse models of AD that indicate that major functional and anatomical alterations occur long before the arrival of large amyloid-β plaques (Hsia et al., 1999; Mucke et al., 2000; Mucke & Selkoe, 2012). Similar to tau pathology, there is evidence that the formation of amyloid-β plaques may even confer a protective benefit by sequestering toxic amyloid-β oligomers (Nunomura et al., 2001). Indeed, the oligomeric form of amyloid-β has become central to our current understanding on amyloid-β toxicity (Mucke & Selkoe, 2012).

As mentioned earlier, the main pathophysiological consequences of amyloid-β accumulation are synaptic dysfunction and neuroinflammation, which in turn contribute to cell death and neurodegeneration. Numerous studies have repeatedly demonstrated that increased concentrations of oligomeric amyloid-β directly impair glutamatergic function and eventually lead to synapse loss (Hsia et al., 1999; Li et al., 2009; Mucke & Selkoe, 2012; Shankar et al.,

2007). Excitatory glutamatergic signaling is heavily regulated by N-methyl-D-aspartate receptor (NMDAR) and α-amino-3-hydroxy-5-methyl-4-isoxazolepropionic acid receptor (AMPAR) activity on postsynaptic dendrites. NMDAR activity is particularly important as the extent of NMDA-mediated Ca^{2+} currents determines whether glutamatergic activity induces long-term potentiation (LTP) or long-term depression (LTD) (Mucke & Selkoe, 2012). LTP is the generally accepted mechanism underlying memory formation and is known have trophic effects on dendrites and increase the recruitment of AMPARs into the postsynaptic density. Conversely, LTD is known to promote dendritic atrophy and synaptic loss (Kullmann & Lamsa, 2007). Amyloid-β oligomers have been shown to interact with NMDARs and other glutamate receptors causing inhibition of LTP, enhancement of LTD, and a loss of dendritic spine density in normal rodent hippocampus (Li et al., 2009; Mucke & Selkoe, 2012; Shankar et al., 2007, 2008). The exact mechanism underpinning oligomeric amyloid-β-mediated synaptic depression is still debated, although it appears to be mediated by an increase in internalization of glutamate receptors, or paradoxically, by a blockade of neuronal reuptake of glutamate from the synaptic cleft (Hsieh et al., 2006; Li et al., 2009; Snyder et al., 2005). Increased glutamate concentrations in the synaptic cleft would initially cause increased NMDAR activity, however a prolonged elevation would eventually cause receptor desensitization, resulting in increased LTD. Additionally, impaired glutamate reuptake may also increase activation of extrasynaptic glutamate receptors, which may inhibit LTP (Li et al., 2011). In essence, amyloid-β-mediated synaptic depression may be the consequence of a spike in postsynaptic glutamate receptor activity, leading to NMDAR desensitization and internalization, and a concurrent stimulation of extrasynaptic glutamate receptors promoting LTD (Mucke & Selkoe, 2012). The current consensus also does not definitively rule out an additional amyloid-β plaque component to the synaptic dysfunction in AD, with some evidence indicating that amyloid-β plaques cause significant injury to dendritic spine, leading to a significant reduction in density of dendritic contacts (Spires-Jones et al., 2007). Amyloid-β-mediated glutamatergic alterations are also thought to be an important factor in causing calcium dysregulation in AD. Excess glutamate receptor activation, due to impaired synaptic clearance, could lead to a massive Ca^{2+} influx that cannot be accommodated by homeostatic mechanisms. Such a disturbance could activate one of several intracellular degradation pathways, eventually leading to cell death (Berliocchi et al., 2005).

More recently, increasing attention has been given to determining whether amyloid-β exerts toxicity through an interaction with tau pathology. This is a reasonable hypothesis given that tau protein and NFTs are more closely linked to cognitive deterioration than amyloid-β pathology (Nelson et al., 2012). While this area is still under investigation, current data suggests that amyloid-β pathology precedes tau hyperphosphorylation and aggregation (Bloom, 2014; Stancu et al., 2014). Crucially, in this context, amyloid-β pathology refers to the aberrant production of amyloid-β, not plaque formation, which occurs far later. One notable issue with concluding a direct causal relationship between amyloid-β and tau protein is that these disease processes are not well co-localized throughout the earlier stages of AD. Postmortem examination of young subjects demonstrating AD pathology has shown that tau aggregates form in the locus coeruleus despite the lack of any noticeable deposition of amyloid-β (Braak & Del Tredici, 2011). In response, some have proposed that amyloid-β and tau pathology may initiate independently, but the presence of amyloid-β could may still accelerate the progression of tau pathology (Jack et al., 2013). Furthermore, the relationship between tau pathology and amyloid-β pathology appears to be far more complicated than simply the former being the result of the latter. Rather, evidence suggests that tau pathology is a key prerequisite for amyloid-β toxicity. Roberson and colleagues reported that lowering tau levels prevented neuronal dysfunction and behavioral deficits in transgenic mouse models of AD (Roberson et al., 2007). A second mouse study corroborated this finding, but also added that mice that lacked tau had significantly lower plaque development when compared to transgenic mice that expressed tau (Leroy et al., 2012). Other studies have since found a number of tau-dependent effects of amyloid-β oligomers including MT disassembly, impaired LTP and ectopic cell cycle re-entry (Bloom, 2014). This is further supported by PET radiotracer studies that have identified elderly individuals with noticeable amyloidosis who remain cognitively intact (Aizenstein et al., 2008). Overall, this evidence suggests that amyloid-β may exist upstream of tau, but ultimately, they may interact in a more complex manner (Bloom, 2014).

1.5.3 Alzheimer's disease as a prion disease

Another interesting facet of AD is the similarity of amyloid-β and tau pathology to that of human prion diseases; a comparison that has been drawn numerous times in the research arena. Originally, the mechanisms underpinning the development AD pathology were described as "cell-autonomous", meaning that the mechanism underlying the formation of NFTs in each cell was not initiated or influenced by surrounding cells (Goedert, 2015). The deterministic spread of AD was presumed to be the result of variable regional vulnerability to the disease. New findings are beginning to suggest that cell-to-cell transmission may actually drive the spread of AD-related proteopathy, with some hypothesizing that tau inclusions form in only a small number of cells and spread predictably to adjacent brain regions (Goedert, 2015). Multiple studies have demonstrated that an introduction of pathological tau protein or tau protein aggregates into the brains of unaffected animals can cause the development and spread of new tau inclusions (Ahmed et al., 2014; Clavaguera et al., 2009). Amyloid-β appears to behave in a similar manner, as the introduction of even small amounts of amyloid-β-containing brain extracts into unaffected animals can induce cerebral β-amyloidosis in primates and human wild-type APP mice (Baker et al., 1993; Eisele et al., 2009; Morales et al., 2012; Stöhr et al., 2012). This is highly reminiscent of a human prion disease, though there is still major reluctance to explicitly classify AD as a type of prion disease as transmission of AD between humans has not yet been demonstrated (Goedert, 2015).

1.5.4 Brain atrophy in Alzheimer's disease

Considerable attention has been given to analyses of structural MRI in defining the anatomical changes occurring in the AD brain, namely cerebral atrophy as a result of neuronal loss. MRI estimates of regional volumes in AD cohorts show that the anatomical distribution of brain atrophy follows a pattern that is at least partially reflected by the pattern of "cortical destruction" from neurofibrillary changes reported by Braak and colleagues (Braak et al., 1993). The most

pronounced regional atrophy in AD is found in the medial-temporal lobe, precuneus, and tempo-parietal cortex, although AD patients have been shown to have widespread cortical atrophy especially later in the disease (Cohen and Sweet, 2011; Montagne et al., 2016). In particular, numerous studies have reported that AD patients suffer from lower hippocampal and amygdalar volumes (Jack et al. 1992, 1997; Lehericy et al., 1994) and marked atrophy of the entorhinal cortex (Bobinski et al., 1999), in addition to noticeable expansion of the cerebral ventricles (Carmichael et al., 2007). A recent review of imaging studies of the hippocampal subfields in AD patients concluded that atrophy occurs mainly in the CA1 subregion (de Flores et al., 2015). The extent of atrophy in the CA1 subregion has also been shown to be correlated with cognitive decline in AD and *APOE* ϵ4 carrier status (Apostolova et al., 2010; Kerchner et al., 2014). MCI patients also have reduced volumetric estimates in these same regions, which generally lie in between those of AD patients and older controls, supporting the notion that MCI is an early stage of AD (Du et al., 2001; Pennanen et al., 2004). Conversely, the occipital lobe and the primary sensory and motor cortices are largely spared from atrophy until later stages of AD (Cohen and Sweet, 2011).

Longitudinal studies have observed increased rates of atrophy in both MCI and AD patients. On average, AD patients exhibit an annual rate of hippocampal atrophy of approximately 4.7%, whereas older controls average just under 1.5% hippocampal atrophy per year (Barnes et al., 2009). Once again, MCI patients are intermediary between AD and controls, exhibiting an annual hippocampal atrophy rate of about 3% (Cohen and Sweet, 2011). Similarly, structural MRI studies have found that across the brain rates of cortical atrophy are significantly higher in MCI and AD patients when compared to cognitively normal elderly individuals (Cohen and Sweet, 2011; Scahill et al., 2002; Thompson et al., 2004a, 2004b).

The white matter is not spared of injury in AD. A number of WM abnormalities are observed in AD, including loss of oligodendrocytes, Wallerian degeneration, and demyelination, particularly in the corpus callosum and periventricular WM (Montagne et al., 2016). A meta-analysis by Li and colleagues found that prominent WM atrophy was observed bilaterally near memory-related structures such as the hippocampus, amygdala, and entorhinal cortex (Li et al., 2012).

1.5.5 Cerebrovascular pathology in Alzheimer's disease

The relationship between cerebrovascular disease (CVD) and AD has received considerable attention. The presence of CVD was once used as the demarcation of AD and vascular dementia (VaD), however converging evidence supports a major vascular component in the pathogenesis and progression of AD. Epidemiological studies have shown that AD and CVD share numerous risk factors including hypertension and obesity during midlife, hypercholesterolemia, hyperhomocysteinemia, diabetes mellitus, and smoking (Gorelick et al., 2011; Meng et al., 2014; Tolppanen et al., 2014). Moreover, multiple cardiovascular conditions, such as atrial fibrillation and congestive heart failure, have also been linked to AD (Mielke et al., 2007; Toledo et al., 2012). Other studies have reported that the presence of vascular risk factors in patients with MCI predicts conversion to clinical AD (Li et al., 2011; Luchsinger et al., 2005).

Cerebral infarcts have been found to frequently coexist with AD pathology. At autopsy, almost half of patients diagnosed with probable AD demonstrate mixed pathologies, most commonly AD and infarcts (Schneider et al., 2009). As well, studies have confidently shown that in subjects suffering from AD, infarcts have major deleterious effects on cognition. One such study, known as the Nun Study, demonstrated that brain infarction and cerebrovascular pathology increased the severity of the clinical symptoms of AD (Snowdon et al., 1997). Remarkably, they found that in autopsy confirmed cases of AD pathology, only individuals with infarcts developed dementia. This link between cerebrovascular disease and AD was later validated in a cohort of Japanese-American men in the Honolulu-Asia Aging study, with the authors reporting that the incidence of dementia was greatest in the presence of both AD proteopathy and CVD (Petrovitch et al., 2005). Although the full extent of the interaction between CVD, infarcts, and AD pathology has yet to be elucidated, further studies have convincingly argued that vascular injury is additive with AD pathology in reducing cognitive function (Schneider et al., 2004) and lowering the threshold for dementia due to AD (Chui et al., 2006; Esiri et al., 1999; Toledo et al., 2013). Wardlaw and colleagues estimated that up to 45% of all dementia cases worldwide are at least partly due to age-related cerebral small vessel disease (Wardlaw et al., 2013).

Despite these findings, the question remains whether AD pathology and cerebrovascular pathology are simply parallel disease processes that only integrate at the level of causing injury

to the brain, leading to cognitive impairment and dementia, or if there is some causal relationship between the two pathologies and if so, in what direction. In the last two decades, it has become increasingly clear that vascular disease does not only coexist with the neurodegenerative process of AD, as we now know that CVD directly contributes to the progression of AD (Farkas & Luiten, 2001; Iadecola, 2004), and may also play a key role in initiating the disease (Zlokovic, 2011). Reciprocally, it is also apparent that AD pathology may in turn have deleterious effects on cerebral blood vessels. As a result, a "vicious circle" may ensue, accelerating AD progression.

Some particularly compelling evidence supporting a possible causal interaction between CVD and AD came by way of post-mortem examinations of AD brains that reported an association between AD an atherosclerotic disease (Attems & Jellinger, 2014). In a study of 921 AD patients and 133 normal controls, Honig and colleagues found that the presence of intracranial atherosclerosis in AD patients was strongly associated with an increased frequency of neuritic plaques (Honig et al., 2005). Beach et al. reproduced these results in a sample of 215 AD patients and 92 older controls, adding that increasing atherosclerotic grade was also significantly associated with higher Braak neurofibrillary tangle stage (Beach et al., 2007). A third autopsy study by Yarchoan and colleagues built on these findings, reporting that atherosclerosis ratings were significantly correlated with neuritic plaque, neurofibrillary tangle and cerebral amyloid angiopathy ratings in AD patients (Yarchoan et al., 2012). Ultimately, the authors concluded that the current body of work examining atherosclerosis in AD provides convincing evidence that CVD and AD are highly interrelated and suggest the existence of reciprocally synergistic mechanisms that potentiate both vascular pathology and AD proteopathy.

The neurovascular hypothesis of AD

Neurovascular dysfunction is increasingly recognized as a major contributor to AD (de la Torre, 2010; Marchesi, 2011; Zlokovic, 2005, 2010, 2011). As reviewed earlier, the neurovascular unit (NVU) comprises neurons, glial cells, VSMCs and pericytes, and vascular endothelial cells. The parts of the NVU work together in concert to regulate CBF such that it is spatially and temporally coupled with neuronal activity, and hence metabolic demand. Functional imaging studies have also demonstrated neurovascular uncoupling and diminished functional hyperemia in patients with AD and even those at risk for developing AD before the appearance of any appreciable neurodegenerative changes or cognitive symptoms (Bookheimer et al., 2000; Sheline

et al., 2010; Smith et al., 1999). Accumulating evidence now indicates that deterioration of the neurovascular unit directly contributes to the progression of AD, and suggests that vascular injury may even initiate the disease. According to the popular two-hit vascular hypothesis of AD developed by the Zlokovic group, damage to the cerebral microcirculation accrues due of vascular risk factors, genetic risk factors, lifestyle and/or environmental influences (hit one), initiating a pathological cascade that eventually leads to AD-related dementia (Zlokovic, 2011). The primary vascular alterations associated with this hypothesis include BBB disruption leading to dysfunction and increased BBB permeability, cerebral hypoperfusion, and neurovascular uncoupling. Simply put, breakdown of the BBB allows neurotoxic molecules to pass from the blood into the parenchyma, injuring neurons mainly by causing inflammation and edema. BBB dysfunction also reduces amyloid-β clearance across the BBB and is thought to increase production of amyloid-β from APP, together resulting in an accelerated accumulation of toxic amyloid-β peptide. Moreover, vascular injury causes hypoperfusion and neurovascular uncoupling, which impart a significant ischemic burden on the brain and may even promote increased production of amyloid-β independently of (Zlokovic, 2011). Altogether, vascular injury directly contributes to the second “hit”, where aberrant accumulation of amyloid-β exerts substantial neurotoxic effects on the brain, eventually leading to neurodegeneration. While the vascular contribution to AD is still far from consensus, the main components of the two-hit vascular hypothesis appear to be well supported by the literature.

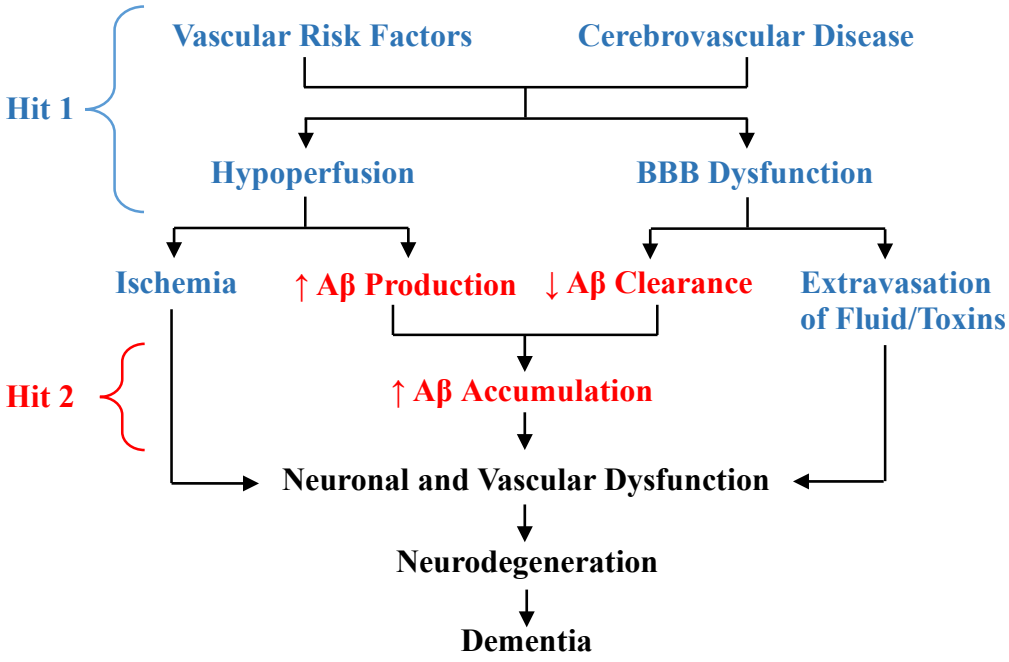

Figure 1.7. Flow chart of neurovascular hypothesis of Alzheimer's disease. According to the popular two-hit vascular hypothesis of AD developed by the Zlokovic group, damage to the cerebral microcirculation accrues due of vascular risk factors, CVD, genetic risk factors, lifestyle and/or environmental influences (hit one), causing hypoperfusion and BBB dysfunction which initiates a pathological cascade that eventually leads to AD-related dementia (hit two) (Zlokovic, 2011). Hypoperfusion puts an ischemic burden on the brain and potentially increases amyloid-β (Aβ) production. BBB dysfunction impairs Aβ clearance and causes extravasation of toxic molecules into the parenchyma. Together, these insults can cause neuronal dysfunction, neurodegeneration, and eventually, dementia. Content of figure adapted and altered from (Zlokovic, 2011).

BBB disruption

The BBB is comprised of vascular endothelial cells and mural perivascular pericytes (Zlokovic, 2008). Together with the glial cells, the BBB is responsible for maintaining the composition of extracellular environment, which is exceedingly important for normal synaptic transmission, neuronal remodeling, and neurovascular coupling. There is growing evidence of significant BBB dysfunction in AD. Specifically, in AD we see significant disruption of tight junctions, an increase in extravasation of fluids and proteins across the BBB, and enzymatic breakdown of the capillary basement membrane, which together constitute a disruption of the BBB (Zlokovic, 2011). This is supported by observations that the abundance of tight junction proteins and their adaptor molecules is significantly reduced in AD (Zlokovic, 2008), which is likely the result of increased matrix metalloproteinase activity which is also associated with the disease (Rosenberg,

2009; Zlokovic, 2011). Burgmans and colleagues reviewed the literature examining BBB disruption in the context of AD (Burgmans et al., 2013). Given the current body of work, they concluded that there is significant interplay between amyloid-β and the BBB, forming a toxic feedback loop between BBB degradation and cerebral amyloidosis. The authors gathered that amyloid-β is toxic to vascular endothelium, increasing the permeability of the BBB and promoting monocyte adhesion. In return, BBB disruption likely impairs the clearance of amyloid-β and causes extravasation of fluid and proteins such as immunoglobulins and albumin into brain tissues, leading to chronic oedema and inflammation (Farrall & Wardlaw, 2009). A recent study by Montagne et al. used dynamic contrast-enhanced MRI to assess BBB integrity in the aged hippocampus (Montagne et al., 2015). The authors reported noticeable age-dependent BBB disruption in the hippocampus, which worsened in MCI patients. Their findings suggest that BBB disruption is an age-related event that occurs at a very early stage in those destined to develop clinical AD. A review by Erickson and Banks also concluded amyloid-β accumulation can only partially explain the disruption of the BBB in AD (Erickson & Banks, 2013), lending further credence to the concept that neurovascular dysfunction exists upstream of AD pathology.

Cerebral hypoperfusion

Cerebral hypoperfusion has been repeatedly observed in AD patients, with the temporal and parietal cortices found to be the most consistently affected (Eberling et al., 1992; Farkas & Luiten, 2001; Imran et al., 1999; Johnson et al., 2005; Roher et al., 2012; Verclytte et al., 2016). Moreover, reduced CBF is demonstrable several years before the diagnosis of clinical AD. ASL perfusion imaging studies of MCI patients have revealed that hypoperfusion develops early in the disease and spreads in a predictable manner that is at least partially reflective of the accumulation of amyloid-β within the brain parenchyma (Binnewijzend et al., 2013; Dai et al., 2009). However, one important difference between staging of amyloid-β deposition and functional markers of AD, such as hypoperfusion and hypometabolism, is that amyloid-β accelerates dramatically early in the disease then plateaus soon after cognitive symptoms manifest, whereas functional metrics show a more gradual evolution that better correlates with clinical progression and may serve as better prognosticators. Commencing in the precuneus, hypoperfusion spreads stereotypically to the remaining parietal cortex and the cingulate gyrus, then to the frontal and temporal cortices, sparing the occipital lobe until the late stages of AD (Love & Miners, 2016). This is of particular interest when considering the neuropathological

substrate of cerebral hypoperfusion in AD. Many have proposed cerebral amyloid angiopathy (CAA) as the cause of the hypoperfusion. However, in AD, the occipital lobe can be severely affected by CAA. While this does not preclude the possibility that perfusion abnormalities in AD patients are due to structural injury to cerebral blood vessels, it does suggest that cerebral hypoperfusion in AD cannot be fully explained by structural pathology related to CAA. Interestingly, the pattern of hypoperfusion correlates well with the regional reduction of glucose uptake in AD, as measured using fluorodeoxyglucose (FDG)-PET imaging (Jagust et al., 2010; Landau et al., 2011). However, the reduction in perfusion is likely not solely the result of reduced metabolic demand. PET imaging studies have found that regional oxygen extraction fraction (rOEF) is significantly increased in AD patients, particularly in the temporal and parietal cortices (Nagata et al., 2000; Tohgi et al., 1998). When considered in combination with a report from Tarumi and colleagues that the tissue oxygenation index of MCI patients was reduced compared to controls, these findings suggest that at least in earlier stages of AD the reduction in CBF is associated with an inadequacy in the blood supply (Tarumi et al., 2014).

Ischemia is the inevitable consequence of any pronounced reduction in CBF, thus prolonged cerebral hypoperfusion carries significant consequences for neurons. Low-grade hypoperfusion can impair peptide synthesis, a necessity for synaptic remodeling and, by extension, memory formation (Zlokovic, 2011). More marked reductions in CBF impair ATP synthesis, leading to energy deficits that will affect the maintenance of ionic gradients and synaptic transmission. Similarly, hypoperfusion can also perturb pH and water balance, which can cause edema, further compromising the blood supply and promoting the accumulation amyloid-β and hyperphosphorylated tau (Moskowitz et al., 2010; Zlokovic, 2011). In animal models of AD, hypoperfusion has been shown to cause spatial memory impairment, synaptic dysfunction, and amyloid-β aggregation (Wang et al., 2010). A second study by Sun and colleagues found that hypoxia also increases amyloid-β levels by upregulating the expression of β-secretase (Sun et al., 2006). Zhang et al. confirmed these findings, adding that the increase in β-secretase expression is mediated by an increase in hypoxia-inducible factor-1α (HIF-1α) (Zhang et al., 2007). Acute hypoxia also increases tau phosphorylation via the extracellular signal-regulated kinase (ERK) pathway (Fang et al., 2010), downregulates the activity of amyloid-β-metabolizing enzyme neprilysin (Wang et al., 2011), and promotes the overexpression of serum response factor and myocardin in cerebral VSMCs which inhibit amyloid-β clearance by downregulating the low-

density lipoprotein receptor-related protein 1 (LRP1) clearance pathway (Bell et al., 2009; Zlokovic, 2011). Koike et al. added to these findings, reporting that in AD models, even mild and transient hypoperfusion insults enhance β-secretase expression and tau phosphorylation, which persists for several weeks post-injury (Koike et al., 2010). In addition, hypoperfusion and hypoxia elicit changes in mitochondrial function (Zlokovic, 2011). A review by Carvalho et al. noted that ROS production by complex III of the electron transport chain increases under hypoxic conditions, causing damage to neurons and blood vessles (Carvalho et al., 2009). Additionally, Chandel et al. found that ROS production during hypoxia also stabilizes HIF-1α, enhancing its activity on β-secretase expression (Chandel et al., 2000).

Amyloid-β and the cerebrovasculature

Several lines of evidence also support that amyloid-β pathology has a profound effect on the cerebrovasculature itself. The most obvious example of this interaction is the infiltration of amyloid-β into the walls of cerebral vessels, a pathology termed cerebral amyloid angiopathy (CAA) (Vinters, 1987). In CAA, amyloid usually accumulates between the tunica adventitia or media of arterioles and capillaries, but may also penetrate into VSMCs themselves (Pezzini et al., 2009; Viswanathan & Greenberg, 2011). In a majority of cases of AD, post-mortem autopsy reveals some degree of both CAA and small vessel disease (SVD). In fact, Kalaria and Ballard found that after examining 300 neuropathologically confirmed AD cases, over 95% possessed CAA, all cases showed microvascular degeneration and over 30% had infarcts (Kalaria & Ballard, 1999). Similar findings were reported by Jellinger and Attems in a sample of 173 AD cases and 130 age-matched controls (Jellinger & Attems, 2003). CAA was present in 97% of AD brains and cerebrovascular lesions were significantly more frequent in AD patients than in controls (56.4% vs. 42.4%, respectively). In CAA, vascular amyloid deposits are mainly found in the vessels of the cerebral cortex and leptomeninges, but the cerebellum and brainstem may be affected by CAA as well (Gilbert & Vinters, 1983; Masuda et al., 1988). The disease is more common and tends to be more severe in AD patients compared to controls, especially in AD patients carrying the *APOE* ϵ4 genotype (Chalmers et al., 2003; Schmechel et al., 1993). The exact origin of the vascular amyloid causing CAA in the context of AD has not been fully elucidated, though it is believed to be mostly produced by neurons, the same as parenchymal deposits, however systemic amyloid-β may contribute (Herzig et al., 2006; Zlokovic, 2011). Amyloid deposition can cause a number of adverse structural changes to cerebral blood vessels.

Pathological examinations of blood vessels afflicted with CAA show a loss of VSM cells, thickening of the vessel wall, narrowing of the lumen, and microhemorrhage (Vinters, 1987; Viswanathan & Greenberg, 2011; Zekry et al., 2003). A study by Scheibel et al. also observed swelling and distortion of capillaries and cavities in the walls of larger vessels produced by amyloid nodules (Scheibel et al., 1989).

Functionally, amyloid-β has been shown to directly impair resting perfusion of cerebral tissues and disrupt neurovascular regulation of blood flow (Farkas & Luiten, 2001; Iadecola, 2004; Zlokovic, 2011). This is likely in part because amyloid-β has been shown to be a potent vasoactive molecule, inducing vasoconstriction in cerebral vessels (Crawford et al., 1997; Suo et al., 1998). Thomas et al. demonstrated that amyloid-β increased vasoconstriction in rat aorta pretreated with the phenylepinephrine (Thomas et al., 1996). A second study by Crawford and colleagues added that amyloid-β potentiated the activity of endothelin-1, a highly potent endogenous vasoconstrictor (Crawford et al., 1997). Importantly, Niwa and colleagues later demonstrated comparable vasoconstrictive effects of amyloid-β in cerebral vessels, without the need for any pharmacological pre-treatment (Niwa et al., 2001). Unsurprisingly, in AD, the consequences of amyloid-β on the cerebrovasculature are not trivial. Gurol et al. reported that plasma amyloid-β concentration is independently associated with extent of WMHs in subjects with AD and MCI (Gurol et al., 2006). This finding is consistent with a second study that observed a significant relationship between reduced CSF amyloid-β_{42}, a marker for increased amyloid burden (Fagan et al., 2006), and WMH load in AD patients (van Westen et al., 2016). Studies have also suggested that CAA in AD patients is associated with a greater frequency of WMHs when compared to AD patients without CAA (Viswanathan & Greenberg, 2011). Interestingly, Grimmer and colleagues found that WMH load was significantly associated with higher amyloid-β deposition over a 28-month follow-up period (Grimmer et al., 2012), providing further evidence of the reciprocity between cerebrovascular pathology and amyloid pathology, even in the earliest stages of the AD. Cognitively, a review by Greenberg and colleagues concluded that vascular amyloid has notable deleterious effects on cognition even after controlling for age and other AD pathology (Greenberg et al., 2004). Furthermore, Viswanathan et al. found that the vascular injury caused by CAA was directly associated with impaired cognition, supporting that the notion that the cognitive effects of vascular amyloid are mediated by direct impairment of cerebral vessels (Viswanathan et al., 2008).

Glymphatic system

An emerging concept in vascular research in AD is the potential role of perivascular CSF clearance pathways in the progression of the disease. As previously mentioned, work in mouse models has demonstrated that CSF enters the brain through the periarterial spaces and drains via the perivenous space, a pathway termed the glymphatic system (Iliff et al., 2012). Iliff and colleagues also demonstrated that large proteinaceous molecules, such as amyloid-β, are cleared through this pathway. A recent study by Peng et al. found that in a mouse model of AD, glymphatic transport was significantly reduced compared to wild-type, and the impairment appeared to be due to the toxicity of amyloid-β itself (Peng et al., 2016). Importantly, failure of the glymphatic system preceded any appreciable deposition of amyloid-β, suggesting a role in the pathogenesis of the disease. These findings are consistent with a previous mouse study of the glymphatic system that reported an age-related loss of glymphatic function in wild-type mice, and also found evidence that compromised cerebral vessel wall pulsatility may be the cause of glymphatic impairment (Kress et al., 2014). Loss of glymphatic transport has yet to demonstrated in AD patients. However, a PET imaging study in humans reported a 23% reduction in ventricular CSF clearance in AD patients, and found impaired CSF clearance was associated with increased amyloid-β deposition (de Leon et al., 2017), suggesting that impaired glymphatic flow could also contribute to AD. Interestingly, impaired vessel pulsatility, manifesting as increased arterial stiffness, may be particularly telling of the important relationship between cerebrovascular function and amyloid-β pathology. In a study of cognitively-intact elderly participants, Hughes and colleagues found that arterial stiffness was significantly higher in individuals who were amyloid-β positive (Hughes et al., 2013). A second study by Hughes et al. examined the relationship between arterial wall stiffness and cerebral accumulation of amyloid-β in 82 non-demented elderly subjects (Hughes et al., 2014). The authors found that even a modest elevation in pulse wave velocity at baseline (a measure of arterial stiffness) was associated with subsequent doubling in the rate of amyloid-β deposition over two-year follow-up.

1.5.6 CVR in Alzheimer's disease

There is now a growing body of evidence that CVR in response to CO_2 is impaired in AD (Glodzik, 2013). Early studies reported mixed findings when assessing CVR in AD patients. One of the early studies evaluating CVR was published by Kuwabara and colleagues, who applied fixed inhalation of 5% CO_2 as a vasodilatory stimulus and used ^{15}O PET imaging to measure CBF among 5 AD patients, 5 subjects with Binswanger's disease, and 5 elderly controls (Kuwabara et al., 1992). Although the AD group showed a widespread reduction in resting blood flow, the CVR response to CO_2 was not significantly when compared with the control group. A second imaging study by Jagust et al. reported similar findings (Jagust et al., 1997). They used PET with the perfusion tracer N,N,N′-trimethyl-N′-(2-hydroxy-3-methyl-5-iodobenzyl)-1,3-propane-diamine (HIPDM) and examined CVR in response to fixed inspired CO_2 stimulus. Conversely, Stoppe and colleagues observed a significant reduction in CVR in AD patients in a sample of 12 AD patients and 9 older healthy controls (Stoppe et al., 1995). The authors used an intravenous injection of 1g acetazolamide as a vasodilatory stimulus during ^{99m}Tc-hexamethylpropyleneaminoxime (HMPAO) SPECT imaging. They found a widespread reduction in CVR among AD patients, including the frontal, temporal and parietal cortices. These findings were later corroborated by Oishi and colleagues, who employed Xenon CT to measure the change in CBF in response to acetazolamide administration in 10 AD cases and 10 elderly healthy controls (Oishi et al., 1999).

TCD studies have more reliably shown CVR impairment in AD patients, perhaps due to larger sample sizes afforded to these experiments (Glodzik et al., 2013). Vicenzini and colleagues examined a sample of 60 AD patients, 58 VaD patients and 62 older healthy controls using CO_2 inhalation and TCD (Vicenzini et al., 2007). The authors found that CVR was depressed in both AD and VaD patients when compared to healthy controls. These findings were confirmed by a second experiment of 17 AD patients, 17 VaD patients and 20 healthy controls (Bär et al., 2007). Again, CVR was significantly reduced in both AD and VaD when compared to the control group, and CVR in the dementia groups did not differ. A meta-analysis of TCD studies of cerebral hemodynamics in AD and VaD concluded that patients with AD have pronounced

cerebrovascular disturbances (Sabayan et al., 2012). However, they also found the severity of the disturbances in cerebral hemodynamics is lower in AD patients than in VaD patients.

More recent studies investigating CVR have favoured the use of MRI techniques over those mentioned above (Glodzik et al., 2013). CVR was examined in 17 AD patients and 17 age-matched controls using BOLD MRI as a surrogate measure of CBF (Yezhuvath et al., 2012). Like many previous studies, the vasodilatory challenge was achieved using a fixed inspired CO_2 stimulus. AD patients demonstrated diminished CVR compared to controls, however the spatial distribution of impairment differed from previous findings. Despite reporting a resting CBF reduction in posterior cortical structures, the authors found that the observed CVR impairment was restricted to frontal structures, namely the prefrontal, anterior cingulate, and insular cortices. Moreover, CVR in frontal regions was significantly correlated with Boston Naming Test scores, but not with general measure of cognition such as Mini–Mental State Examination (MMSE). Cantin et al. employed a similar methodology to examine CVR in 9 AD patients, 7 MCI patients and 11 age-matched controls (Cantin et al., 2011). Utilizing BOLD MRI and fixed inspired CO_2, the authors reported that CVR was significantly reduced in both the AD and MCI group compared to controls, though found no difference between patient groups. CVR impairments were diffuse, but seemed predominant in posterior areas. These findings suggest that CVR deficits may occur early in the disease and could contribute to progression, though the spatial location of CVR deficits remains to be fully elucidated.

Interestingly, new evidence suggests that the *APOE* ε4 allele may be partially responsible for impaired CVR in AD. A study of 18 young carriers of the *APOE* ε4 allele revealed significantly reduced CVR compared to non-carriers (Suri et al., 2015). The authors posited that a lifelong vascular deficit related to the *APOE* ε4 allele could cause significant hypoperfusion and microvascular damage leading to impairments such as endothelial dysfunction and impaired amyloid-β clearance, and may reflect a vascular contribution to the vulnerability of ε4-carriers to AD later in life. Conversely, elevated CVR in ε2-carriers may contribute to their protection to the disease.

Beyond changes in CVR magnitude, very few studies have assessed the speed of vasoreactivity to CO_2 in MCI or AD patients. Cantin and colleagues observed that MCI and AD groups produced a different slope of vascular response to a hypercapnic challenge when compared to

controls (Cantin et al., 2011), suggesting altered temporal dynamics. However, neither the extent nor the spatial distribution of temporal changes to vasoreactivity was thoroughly studied, and no relationship between cognition and speed of cerebrovascular response was established. A recent study by Richiardi and colleagues sought to measure the speed of the cerebrovascular response in 20 AD patients, 15 MCI patients, and 28 older healthy controls (Richiardi et al., 2015). MCI and AD patients showed significant widespread reduction in speed of cerebrovascular response to fixed inhalation of 7% CO_2, and speed of cerebrovascular response correlated with MMSE scoring. Furthermore, the observed changes in speed of cerebrovascular response could not be explained by GM atrophy, microangiopathy, or motion.

Overall, the evidence regarding CVR in AD is promising but still limited. Current knowledge suggests vasoreactivity is impaired in AD and MCI, however, there is little agreement on the spatial pattern of these deficits. Also, previous studies possess a few notable limitations. Almost all the studies listed fixed inhalation of CO_2 as a vasodilatory stimulus. The drawbacks associated with this strategy were covered in section 1.4.2., but in brief, a fixed inspired CO_2 challenge achieves a variable P_{aCO_2} stimulus depending on individual physiological parameters such as rate of CO_2 production and minute ventilation. Additionally, measuring P_{ETCO_2} does not reflect P_{aCO_2} during free-breathing (Jones et al., 1969; St Croix et al., 1995), therefore, the stimulus is largely unknowable. With respect to measuring speed of cerebrovascular response to hypercapnia, an abrupt step stimulus is recommended, however, fixed inspired CO_2 challenges result in a biexponential rise in P_{aCO_2} due to the "wash in" effect caused by the lung (Fisher, 2016; Mark et al., 2010). A supramaximal acetazolamide injection also fails on this front, as the variable temporal dynamics of the stimulus still make comparing the speed of vascular response between subjects impossible.

Proposed mechanisms of CVR reduction in AD are largely the same as those proposed to explain the marked hypoperfusion. Pre-existing CVD and vascular risk factors such as hypertension, hypercholesterolemia, and obesity are thought to contribute to vascular injury, diminishing dynamic range of cerebral vessels and leading to impairment of hemodynamic regulation (Glodzik et al., 2013). Another compelling mechanism for CVR impairment in AD is centred around the fact that amyloid-β is a potent vasoconstrictor of cerebral vessels (Crawford et al., 1997; Suo et al., 1998). Vascular amyloidosis is a hallmark of AD, most commonly manifesting as CAA, thus the vasoactivity of amyloid-β could substantially alter hemodynamic function.

Studies in transgenic mouse models overexpressing APP have shown that vascular dysfunction can occur even before noticeable deposition of parenchymal or vessel amyloid-β deposition (Niwa et al., 2002), suggesting that elevated soluble amyloid-β may also contribute to an exaggerated contractile state in cerebral blood vessels. Furthermore, amyloid-β has been shown to upregulate endothelin-1 (Palmer et al., 2012), and AD patients experience elevated levels of myocardin and serum response factor in VSMCs, causing the overexpression of proteins that promote a hypercontractile phenotype and CBF dysregulation (Chow et al., 2007; Glodzik et al., 2013).

Lastly, a study by Kimbrough and colleagues examined how the neurovascular unit is altered in a mouse model of AD (Kimbrough et al., 2015). They found that vascular amyloid deposits in between the astrocyte end-plate and the vessel wall, forming rigid ring-like structures around the vessel circumference. In vessel segments affected by amyloid deposits, stimulation of astrocytes or VSM cells produced dampened vascular responses. Conversely, vessel segments that were unaffected by these deposits responded similarly to blood vessels from control mice. The authors concluded that while astrocytes signaling was still intact, amyloid deposits render blood vessels rigid and reduce the dynamic range of affected vessel segments. This conclusion is further supported by a recent study Hughes et al. that reported that arterial stiffness was significantly higher in individuals who were amyloid-β positive (Hughes et al., 2013). In addition, a second study by Hughes et al. investigated the influence of arterial stiffness on amyloid-β deposition (Hughes et al., 2014). The authors found that even a modest elevation in pulse wave velocity at baseline (a measure of arterial stiffness) was associated with subsequent doubling in the rate of amyloid-β deposition over two-year follow-up. These findings may reflect a reciprocal relationship between loss of hemodynamic function and progression of AD.

1.5.7 Cerebral autoregulation in Alzheimer's disease

Cerebral autoregulation is responsible for maintaining constant CBF in the face of fluctuating blood pressure. Compelling evidence in animal studies supports significant impairment of cerebral autoregulation in AD (Claassen & Zhang, 2011). In transgenic mouse models of AD that recapitulate amyloid-β pathology, Iadecola and colleagues observed marked hypoperfusion in concert with diminished vasodilatory response and amplified vasoconstriction (Iadecola et al., 1999). Accordingly, cerebral autoregulation was also demonstrated to be significantly impaired (Niwa et al., 2002).

Observations of cerebral autoregulation in humans have been conflicting. In a TCD study of cerebral hemodynamics in AD patients using stand-squat maneuvers, Claassen and colleagues reported that while AD patients had a higher index of cerebrovascular resistance, cerebral autoregulation was not impaired (Claassen et al., 2009). A second study by Zazulia et al. used ^{15}O-PET to monitor CBF in AD patients following administration of a Ca^{2+} channel blocker, causing hypotension (Zazulia et al., 2010). Similarly, the authors found no impairment in cerebral autoregulation, however some have argued that the use of a drug to induce hypotension may confound the experiment (Claassen & Zhang, 2011). Conversely, van Beek and colleagues found that moderate orthostatic hypotension caused a greater decline in cerebral cortical tissue perfusion in AD patients compared to controls, indicating poorer cerebral autoregulation (van Beek et al., 2010). These findings have since been confirmed using TCD by den Abeelen et al., who reported that CBF fluctuations were 5% greater in AD patients than health controls during sit-stand maneuvers (27% vs 22%) (den Abeelen et al., 2014). One potential explanation for the discrepancy in findings could lie in the fact that the PET study of cerebral autoregulation assessed static autoregulation using a drug, whereas van Beek and den Abeleen assessed dynamic autoregulation with abrupt changes in blood pressure (Tiecks et al., 1995). This may indicate that impaired temporal dynamics underlie diminished cerebral autoregulation in AD. Nonetheless, further study is required to fully elucidate the status of cerebral autoregulation in AD.

1.5.8 The neuropsychological profile of Alzheimer's disease

Neuropsychological testing has been central to the characterization of AD and identifying the trajectory of cognitive deficits for use in tracking the disease (Albert, 1996; Locascio et al., 1995; Morris et al., 1989; Weintraub et al., 2012; Welsh et al., 1991). Additionally, understanding of the evolution of neuropsychological deficits may provide valuable insights into the pathogenesis and progression of AD. Developments in our understanding of the neuropathological staging of AD have made it clear that the symptoms of AD reflect the selective targeting of structural networks by AD pathology (Seeley et al., 2009). In the typical presentation of AD, neuropathology is initially confined to limbic structures involved in learning and memory (Braak & Braak, 1991; Jack et al., 1997), determining the cognitive manifestations early in the disease (Weintraub et al., 2012). Only after AD pathology has advanced to other cortical structures are additional neuropsychological deficits apparent.

These findings directly contributed to the 2011 revision of the diagnostic criteria for AD. The new criteria moved beyond a singular diagnosis of AD, aiming to encompass a continuum from health brain aging to clinical AD (Weintraub et al., 2012). The revision formalized the diagnosis of mild cognitive impairment (MCI) as an prodromal stage in the AD process (Albert et al., 2011b), preceding the diagnosis of dementia due to AD (McKhann et al., 2011). MCI is of particular interest in the development of diagnostic and prognostic imaging tools because the diagnosis of MCI is believed to represent a transitional state between healthy aging and clinical AD. An even earlier "Preclinical AD" stage was also defined, characterized by the existence of positive AD biomarkers despite the absence of any cognitive symptoms (Sperling et al., 2011). The development and implementation of tools for diagnosis and management of AD is still in its infancy, therefore, neuropsychological assessment remains an important tool in clinical practice and key metric for comparison in the research arena (Weintraub et al., 2012). This section will discuss the neuropsychological profile of AD patients.

In AD, the first pathological changes in the cerebrum are found in the medial temporal lobe structures that responsible for episodic memory function (Weintraub et al., 2012). Therefore, in agreement with the structures involved in early pathology, AD patients have notable difficulties in encoding and storing new information (Peña-Casanova et al., 2012). In fact, Mistridis and

colleagues reported that deficits in verbal episodic memory are measurable up to 8 years before the initial diagnosis of MCI is made (Mistridis et al., 2015). Impaired episodic memory can been effectively detected using a number of cognitive tests including free recall and recognition (Weintraub et al., 2012). Studies characterizing the episodic memory deficit in AD generally showed patients are equally impaired on recognition and free recall tasks (Delis et al., 1991; Welsh et al., 1991). This finding suggests that the memory deficits associated with AD are the result of poor memory consolidation rather than impaired retrieval of newly formed memories, but it has been strongly argued that both functions are significantly impaired (Weintraub et al., 2012). Other important contributors to memory loss in AD include reduced inhibitory activity leading to increased intrusion errors (Delis et al., 1991; Jacobs, 1990) and faulty incorporation of contextual information to strengthen memory formation (ie. faulty semantic memory further impairing episodic memory) (Goldblum et al., 1998; Weintraub et al., 2012).

With disease-modifying therapies on the horizon, a critical step in the management of AD patients will be the early and accurate diagnosis their disease. With that, Welsh et al. observed that on the CERAD word list learning task, delayed recall performance to be the best overall discriminatory measure for the diagnosis of AD, with a diagnostic accuracy of approximately 92% (Welsh et al., 1991). This measure was superior to all other measures derived from this test, including immediate recall scores, recognition memory scores, and intrusion error rate. A second study by Knopman and Ryberg confirmed these findings, reporting that delayed word recall testing carried an overall predictive accuracy of 95.2%. (Knopman & Ryberg, 1989; Weintraub et al., 2012), supporting the notion that impaired delayed memory may be the best indicator of AD pathology.

When assessing the cognitive trajectory of pre-dementia patients, multiple studies reported that AD is characterized by a long preclinical period during which subtle episodic memory deficits are detectable with otherwise stable cognition for years before the emergence of obvious cognitive and behavioral deficits (Chen et al., 2001; Small et al., 2000). The authors of these studies also observed that eventual AD patients often experience an accelerated decline starting approximately 1.5-3 years before dementia diagnosis, concluding that a sudden deterioration of episodic memory function, potentially in concert with the emergence of other cognitive deficits, may best predict the transition to clinical dementia.

AD patients often also present with numerous other cognitive deficits, including language, visuospatial, executive dysfunction, and semantic memory dysfunction, in addition to a number of neuropsychiatric symptoms (Lyketsos et al., 2011), even in early stages of the disease. For instance, numerous studies have demonstrated that early AD patients show difficulties in verbal fluency (Monsch et al., 1992), object naming (Hodges et al., 1991), and semantic categorization (Aronoff et al., 2006), supporting a loss of semantic memory (Weintraub et al., 2012). Deficits in executive functions such as problem solving, attentional control, and working memory are also seen in testing and may even be detectable in MCI patients (Chen et al., 2001). AD patients also tend to exhibit diminished visuospatial function (Weintraub et al., 2012). An appreciation of a patient's visuospatial deficits may be particularly important in atypical presentations of AD, such as those with posterior cortical atrophy. Some reports indicate that a decline in visual detection is detectable in MCI patients and may be a useful prognosticator (Johnson et al., 2009), though this notion is not yet widely recognized.

1.6 Magnetic Resonance Imaging

1.6.1 The basis of MRI

Central to MRI is the concept that an externally applied static magnetic field causes the hydrogen protons contained within the water of a subject to align with the direction of the field, assuming one of two states regarding their magnetic moment: parallel or anti-parallel to the static field (Cohen and Sweet, 2011). Given that parallel alignment is a slightly lower energy state, there is a small excess of protons parallel to the applied field compared to anti-parallel. This creates a net magnetization of the tissue in the direction of the static field. The magnetic field also causes the protons in the subject to precess at a frequency known as the Larmor frequency, which is related to the magnetic field strength and the gyromagnetic ratio of the atom of interest (ie. hydrogen). The phases of the individual precessing protons, or spins, are random, therefore the magnetization in the plane perpendicular to the static field is zero. A radiofrequency (RF) coil

then applies a separate magnetic field, known as the RF pulse, which is also oscillating at the Larmor frequency. This field excites protons, causing some to jump to the high energy anti-parallel state, which reduces the net magnetization parallel to the static field. However, the increase in high energy protons is unstable and fleeting. Following termination of the RF pulse, protons quickly return to the low energy state to re-establish magnetization parallel to the main field. This process is termed T1 relaxation. The RF pulse also causes alignment of the precession of the spins, bringing the spins into phase and creating a net magnetization in the transverse plane. However, heterogeneity in the local magnetic field due to interactions between protons causes dephasing of the spins, decaying the net magnetization in the transverse plane. This process is referred to as T2 relaxation. Both T1 and T2 relaxation are exponential over time and are described by time constants T_1 and T_2, respectively (Cohen and Sweet, 2011). The concept of relaxation is further complicated by unavoidable inhomogeneities in the main magnetic field, which cause spins to dephase faster than expected given the T_2 constant. This accelerated rate of relaxation is referred to as T_2^*, which is composed of the real T_2 of the imaging sample and the added decay due to field inhomogeneities, termed T_2'. Importantly, the value of T_1, T_2, and T_2^* can vary depending on tissue type being imaged. Differences in rates of signal decay can be leveraged in MRI to produce tissue contrast.

1.6.2 BOLD fMRI

BOLD fMRI can provide a surrogate measure of brain activity or regional blood flow, depending on the context. Ogawa and colleagues first established the feasibility of BOLD MRI by demonstrating that fluctuations in brain blood oxygenation produce a MR signal that can be used in imaging (Ogawa et al., 1990). This technique is based on T2* relaxation, which is sensitive to local concentrations of deoxyhemoglobin (dHb). The paramagnetic property of dHb causes inhomogeneities in the local magnetic field. Thus, the BOLD signal decreases when the concentration of dHb increases. Conversely, the BOLD signal peaks when dHb concentration reaches zero (ie. blood oxygenation reaches 100%). The development of BOLD imaging relied on an observation made by Fox and Raichle that brain activation elicits a greater increase in CBF than was predicted given the concurrent increase in oxygen consumption ($CMRO_2$) (Fox &

Raichle, 1986). We now know that this relationship may be explained by the fact that O_2 delivery is driven by the concentration gradient between the blood and parenchyma, thus an apparent oversupply of blood can help O_2 delivery by altering OEF. However, this was a controversial idea at the time that revolutionized the existing understanding of neurovascular regulation, and incidentally, provided a means (ie. functional hyperemia) by which BOLD imaging could be used to assess brain activation. Consider the following relationship:

$$\boldsymbol{CMRO_2 \propto CBF\, x\, [dHb]}$$

therefore, the BOLD signal is determined by a combination of $CMRO_2$ and CBF. If neural activity-related increases in CBF exactly matched the increase in $CMRO_2$, the local concentration of dHb would be unchanged, and by extension, so would the BOLD signal. Instead, we now know that following regional activation, the BOLD signal almost always increases in healthy tissue. This standard positive BOLD response reflects the delivery of more O_2 than the simultaneous increase in $CMRO_2$ consumes, leading to an increase in local tissue oxygenation. In other words, the effect on the BOLD signal of NVC dominates the effect of increased oxygen demand because of the tissue being active. There are also other factors that contribute to the BOLD signal such as cerebral blood volume, which increases when CBF increases (Attwell et al., 2010). In addition, it is important to note that the BOLD signal is complex and the underpinnings of BOLD fMRI are still not fully understood (Attwell et al., 2010; Logothetis, 2003). Logothetis and colleagues carried out simultaneous intra-cortical recordings of neural signals and fMRI responses (Logothetis et al., 2001). They found that local field potentials were the only signals that correlated with the hemodynamic response. These findings suggest that in the context of fMRI, the BOLD signal reflects the neuronal input and intra-cortical processing rather than the resultant spiking activity. Still, a complete understanding of the BOLD response remains to be elucidated. Nevertheless, BOLD MRI is one of the most powerful methods for probing human brain function. In the context of this thesis, the BOLD response is being leveraged in a similar, yet distinct manner. No stimulus is administered for the purposes of neuronal activation. Instead, a vasoactive stimulus is applied to elicit a global change in CBF, independent of neuronal activity. This enables the specific examination of the cerebrovascular function, without the confound of being mediated by NVC.

1.6.3 Quantifying the BOLD signal

Traditionally, MRI is used to acquire high-resolution anatomical images to assess structural morphology or localize anatomical structures. On the other hand, fMRI is used to detect fluctuations in the BOLD signal over time as a measure of neural activation or change in blood flow. BOLD fMRI consists of repeated multi-slice image acquisitions using T2*-weighted echoplanar imaging (EPI) sequences that leverage dHb as an endogenous contrast agent (Cohen and Sweet, 2011). This imaging technique yields a time series for each voxel that achieves both relatively high spatial and temporal resolution. A typical BOLD fMRI study generally involves the administration of a stimulus, followed by some form of measurable response. Concurrently, the MRI scanner samples the whole brain every 2-3 seconds using approximately 40-50 contiguous axial slices, each which a thickness of about 3mm and an in-plane resolution of $3mm^2$, producing 3mm isotropic imaging voxels (Cohen and Sweet, 2011). The resultant raw data must then undergo multiple preprocessing steps to achieve a final BOLD signal time course for each voxel. When this protocol is used in combination with a well-designed experimental challenge that changes the BOLD signal according to defined experimental states, one can assess brain activation associated with specific tasks, or in context of this thesis, assess regional vasoreactivity to a vasoactive stimulus.

The raw BOLD signal in each voxel is expressed in arbitrary units, thus it is usually converted to some standardized metric to allow for comparison across subjects (or time) (Cohen and Sweet, 2011). One such method involves dividing the BOLD time course by a subject's mean BOLD signal at rest then multiplying by 100 to produce percent change in BOLD signal. To determine if BOLD activations are significant, several statistical methods can be employed (Cohen and Sweet, 2011). For instance, the mean difference score calculated for each cycle can be compared against the null hypothesis in each voxel using a one-sample student's t-test. Other methods include using a multiple regression to assess the relationship between the acquired BOLD signal of a given voxel and the time course of the experimental stimulus (while also considering the contribution of other factors). In a multiple regression, each voxel is assigned a value for each input or predictor, also called a regressor. These values, termed parameter estimates or sample statistics, describe the proportion of the BOLD signal variance in that voxel that is explained by

each regressor. Significant activations are determined by assessing whether that value in a given voxel (ie. the strength of the relationship between the BOLD signal time series and the regressor) exceeds a significance threshold that accounts for multiple comparisons. Due to the large number of voxel being evaluated, thresholding often involves a combination of height and spatial extent thresholds, leveraging the non-random distribution of real activations to control false positive rate, while still achieving adequate statistical power.

1.7 Aims and Hypotheses

Several lines of evidence have demonstrated that neurovascular dysfunction plays a major role in AD. Recent investigations now suggest that hemodynamic function is impaired in AD and may underpin the neurovascular contribution to the disease. However, our understanding of the relationship between the magnitude of CVR, the speed of cerebrovascular response, and the progression of AD is still limited. This is especially true in patients with MCI, which is recognized as the prodromal stage of AD.

Primary Aim

The primary aim of this thesis is to determine whether patients with MCI and AD exhibit impaired magnitude and/or temporal dynamics of their cerebrovascular response to vasoactive stimuli as assessed by CVR imaging, specifically in cortical regions predominantly affected by AD.

The cerebrovascular response to vasoactive stimuli can be resolved into two components, (i) the magnitude of cerebrovascular response, which is also known as CVR, and (ii) the speed of cerebrovascular response. By administering an abrupt and robust hypercapnic vasodilatory challenge and imaging the resultant cerebrovascular response with BOLD MRI, both the CVR and speed of cerebrovascular response can be measured. In brief, CVR is broadly defined as the change in CBF in response to a vasodilatory stimulus, and therefore can be calculated as the slope of the regression of the BOLD signal by the P_{ETCO_2} time course. The speed of cerebrovascular response can be calculated from the same BOLD data by first convolving the

P_{ETCO_2} with a set of an exponential decay functions where the time constant (τ) is incrementally increased, then correlating the BOLD signal with each convolved curve. The time constant corresponding to convolved curve of highest correlation with the BOLD signal defines the speed of cerebrovascular response, expressed in seconds.

Secondary Aim

This thesis also has a secondary aim of evaluating the relationship of CVR and speed of cerebrovascular response with episodic memory impairment in a sample consisting of AD, MCI, and older healthy control subjects, representing the functional continuum between healthy aging and clinical AD.

Episodic memory loss is the earliest and most profound cognitive deficit associated with AD. Additionally, memory assessment has proven to be an early and relatively strong marker of disease severity, making it helpful for use in the development and testing of new diagnostic and prognostic tools. Each patient underwent the Consortium to Establish a Registry for Alzheimer's Disease (CERAD) Word List test to assess memory function. The immediate recall score and delayed recall score (percent retained) from the test were used as measures of immediate and delayed memory, and correlated with CVR and the speed of cerebrovascular response.

Rationale

The rationale behind studying CVR and the speed of the cerebrovascular response to CO_2 in AD and MCI patients is two-fold. Firstly, identifying hemodynamic impairment of any nature in MCI and/or AD patients will further the characterization of the vascular pathophysiology of AD, and may provide new insights into possible mediators of known neurovascular dysfunction, and by extension, ischemic injury in the disease. This is because any region exhibiting an impaired cerebrovascular response is experiencing a dissociation between the regulatory input on cerebral vessels and the resultant hemodynamic response, or in other words, neurovascular uncoupling. Therefore, the existence of a diminished or delayed vascular response may impose a substantial ischemic burden on tissues and contribute to the progression of AD in a meaningful way. Additionally, a number of important pathophysiological features associated with AD could potentially be explained by hemodynamic alterations detectable with CVR imaging. Diminished or slowed vasoreactivity may underpin findings of impaired cerebral autoregulation in AD

patients, increasing vulnerability of the cerebral microvasculature to fluctuations in perfusion pressure and potentially leading to ischemic injury or hypertensive barotrauma. Also, studies of the glymphatic system in animal models have indicated that arterial stiffness, manifesting as impaired vessel pulsatility may be a primary contributor to loss of glymphatic function, and may explain reports of impaired glymphatic clearance of amyloid-β in transgenic mouse models of AD. Again, this increase in arterial stiffness may be readily detected as an altered cerebrovascular response.

Secondly, investigating the cerebrovascular response to CO_2 in MCI and AD patients may yield new metrics of vascular contribution to the AD that could be feasibly implemented in a clinical setting and may benefit current neurologic assessment. The proposed methodology in this thesis is highly reliable and yields a direct physiological measure of cerebrovascular function, which may prove to be a more informative measure of vascular dysfunction than resting blood flow, which is thought to be tightly regulated at the expense of vascular reserve. Moreover, with studies in cognitively normal elderly subjects reporting that arterial stiffness confers a marked increase in risk of being amyloid pathology-positive at follow-up, a well-standardized measure of the dynamic vascular response to a vasoactive stimulus may also be a valuable to clinicians for assessing the pathophysiological substrate underlying impaired clearance of amyloid-β.

Hypotheses

Primary Hypotheses:

i. CVR will be reduced in AD compared to healthy controls, while MCI will exhibit CVR of intermediate value between AD and healthy controls, indicating a progressive loss of cerebrovascular reserve during disease progression.

ii. Speed of cerebrovascular response will be slower in AD compared to healthy controls, while MCI will exhibit an intermediate speed of response between that of AD and healthy controls, indicating a progressive slowing of the cerebrovascular response to vasoactive stimuli.

Secondary Hypotheses:

i. CVR across all subjects will show a positive correlation with episodic memory performance

ii. Speed of cerebrovascular response across all subjects will show a positive correlation with episodic memory performance

Chapter 2
Materials and Methods

2 Materials and Methods

2.1 Subject Recruitment

2.1.1 Participants

This study conforms to the standards outlined by the latest revision of the Declaration of Helsinki and was approved by the Research Ethics Board of the University Hospital Network. Subject recruitment was achieved through the memory clinic located at Toronto Western Hospital. Both male and female elderly adults were recruited for participation and provided both written and informed consent. Diagnosis of MCI and AD patients was performed by a neurologist in conformance with the 2011 guidelines set out by the National Institute on Aging and Alzheimer's Association consensus panels (Albert et al., 2011; McKhann et al., 2011). Older healthy controls (HC) were also recruited and screened according to the outlined inclusion and exclusion criteria. Subjects were asked to refrain from heavy exercise or caffeine intake on the day of the scan.

2.1.2 Inclusion and exclusion criteria

Inclusion criteria for this study:

1. A diagnosis of MCI (amnestic subtype) or early dementia due to AD

2. Over 50 years of age
3. Deemed fit for investigation by neurologist

Exclusion criteria for this study:

1. Medical contraindications to controlled hypercapnia
2. Incompatible with 3T MRI
3. Mixed AD and VaD
4. History of stroke or transient ischemic attack (TIA)
5. Uncontrolled hypertension, dyslipidemia or diabetes
6. History of unrelated neurological disease
7. Pulmonary disease
8. Medications known to interfere with CVR measurements

2.2 MRI Sequences with Acquisition Parameters

All studies were performed at Toronto Western Hospital on a 3-Tesla GE MRI system (Signa HDx platform, GE Healthcare, Milwaukee, Wisconsin) with an eight-channel phased array head coil. A 3rd generation RespirAct^{TM} gas blender was employed for control of P_{ETCO_2} during the BOLD CVR sequence. All patients underwent the following MRI protocol with whole-brain coverage:

1. Structural Imaging

- T1-weighted 3D spoiled gradient echo (FAST-SPGR) sequence [slice thickness = 1 mm; no interslice gap; field of view = 22 x 22 cm; matrix size = 256 x 256; flip angle = 12°; TE = 3.1 ms; TR = 7.8 ms; TI = 450 ms; 146 slices per volume]

2. Axial Single-Shot BOLD CVR Acquisition

- T2*-weighted echoplanar imaging gradient echo (EPI-GRE) sequence [slice thickness = 3.5 mm; field of view = 24 x 24 cm; matrix size = 64 x 64; flip angle = 70°; echo time = 30 ms; repetition time = 2400 ms; number of frames = 338]

3. 2D FLAIR Image

- Standard T2-weighted fluid-attenuated inversion recovery (FLAIR) image [slice thickness = 3 mm; 36 slices per volume; matrix size = 256 x 256; field of view = 22 x 22 cm; flip angle = 90°; TE = 138 ms; TR = 9002 ms; TI = 2250 ms]

4. Proton Density/T2-weighted Sequence

- Fast spin echo-XL [slice thickness = 3 mm; matrix size = 256 x 256; field of view = 24 x 24 cm; flip angle = 90^{o}; TE = 10.5/90 ms; TR = 3000 ms]

2.3 Vasodilatory Stimulus

As previously outlined, assessing CVR requires the delivery of a vasoactive stimulus. In this study, a hypercapnic breathing stimulus was delivered to each patient during BOLD MRI to fulfill this requirement. Control of P_{ETCO_2} was achieved using a respiratory apparatus called the RespirAct^{TM} (Thornhill Research Inc., Toronto, Canada) running the prospective gas-targeting algorithm of Slessarev et al. (Slessarev et al., 2007). This device is an automated gas blender that employs a prospective gas targeting method that allows it to independently manipulate end-tidal

gas tensions. Importantly, the RespirAct™ can achieve abrupt changes in P_{ETCO_2} (with 2-3 breaths) and sustain these changes for long periods of time to within ± 2 mmHg CO_2 of the target.

Before commencing the breathing stimulus, the O_2 and CO_2 sensors of the RespirAct™ must be calibrated. The O_2 sensor used in the RespirAct™ (Teledyne Analytical Instruments, City of Industry, California, USA) is accurate to within 1%, whereas the CO_2 sensor (Servomex Group Ltd., Sugar Land, Texas, USA) is accurate to within ± 0.1%. Subjects were then fitted with a facemask connected to a sequential gas-delivery breathing circuit (Figure 2.1). In brief, the sequential gas delivery circuit consists of inspiratory and expiratory arms separated by one-way valves. The two arms are connected via a bypass tube, which also contains a one-way valve whose opening pressure is greater than that of the other two valves. During exhalation, the exhaled gas flows through the expiratory arm into an expiratory reservoir (G_2). At the same time, gas delivered (G_1) to the circuit by the RespirAct™ collects in the inspiratory reservoir. At the beginning of inhalation, G_1 is drawn from the inspiratory reservoir, termed the G_1 bag. If the subject's minute ventilation exceeds the G_1 flow, the inspiratory reservoir will be depleted and the G_1 bag will collapse. Further inhalation will cause negative pressure in the inspiratory arm of the circuit, opening the bypass valve and allowing the expiratory reserve to supply the remainder of the breath. In fact, to achieve breath-to-breath control of P_{ETCO_2}, the subjects minute ventilation must stay above the G_1 flow. This is because the G_2 gas is already equilibrated with the blood in the pulmonary capillaries, meaning there is no CO_2 gradient between inhaled G_2 gas and the blood (Slessarev et al., 2007).

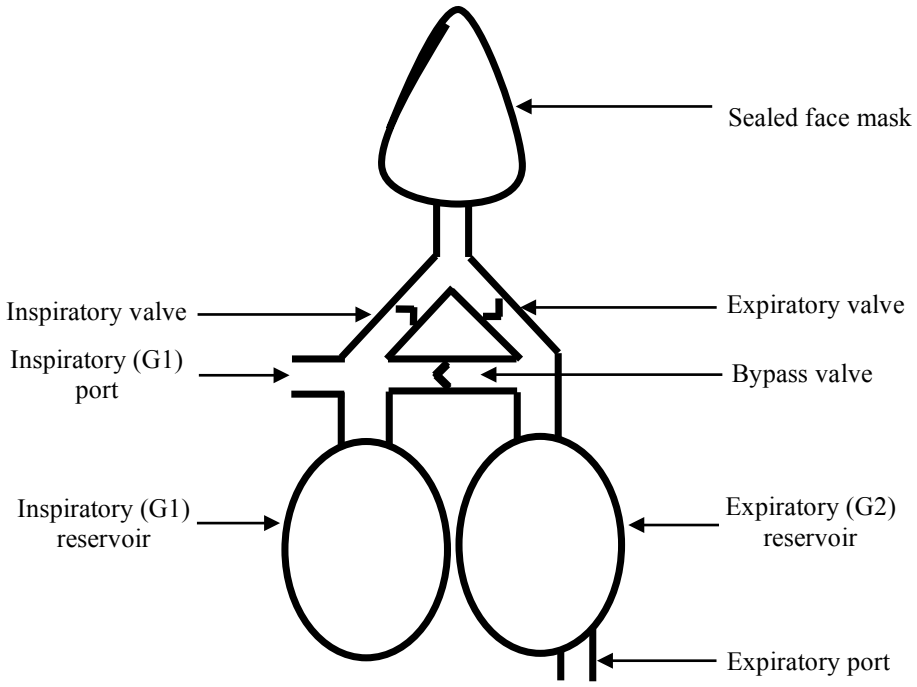

Figure 2.1. Diagram of sequential gas delivery circuit.

Under normal circumstances, an increase in minute ventilation would lead to an increase in alveolar ventilation, altering end-tidal gas tensions. However, with the sequential gas-delivery circuit, increases in minute ventilation will instead lead to greater inhalation of "neutral" G_2 gas, leaving alveolar ventilation unaffected. Therefore, when using the RespirAct™, alveolar ventilation is fixed to the G_1 flow, regardless of increases in ventilation.

The desired waveform for P_{ETCO_2} was programmed into the RespirAct™, which then calculates the gas delivery requirements for each subject using the algorithm of Slessarev and colleagues (Slessarev et al., 2007). These calculations require subject parameters including age, height, weight, and gender, which are used to estimate physiological parameters such as metabolic production of CO_2. For this study, a standardized CO_2 inspiratory stimulus was implemented, consisting of the following (Figure 2.2): baseline for 120 seconds at subject's resting P_{ETCO_2}, a hypercapnic step of 10 mmHg above resting for 120 seconds, baseline for 150 seconds, a hypocapnic step of 10 mmHg below resting followed immediately by a gradual ramp up to 15 mmHg above resting lasting 270 seconds, and a final baseline for 120 seconds, all during

normoxia. Throughout the duration of the scan, the RespirAct™ samples P_{ETCO_2} and P_{ETO_2}, recording the data into a time series for use in CVR calculations.

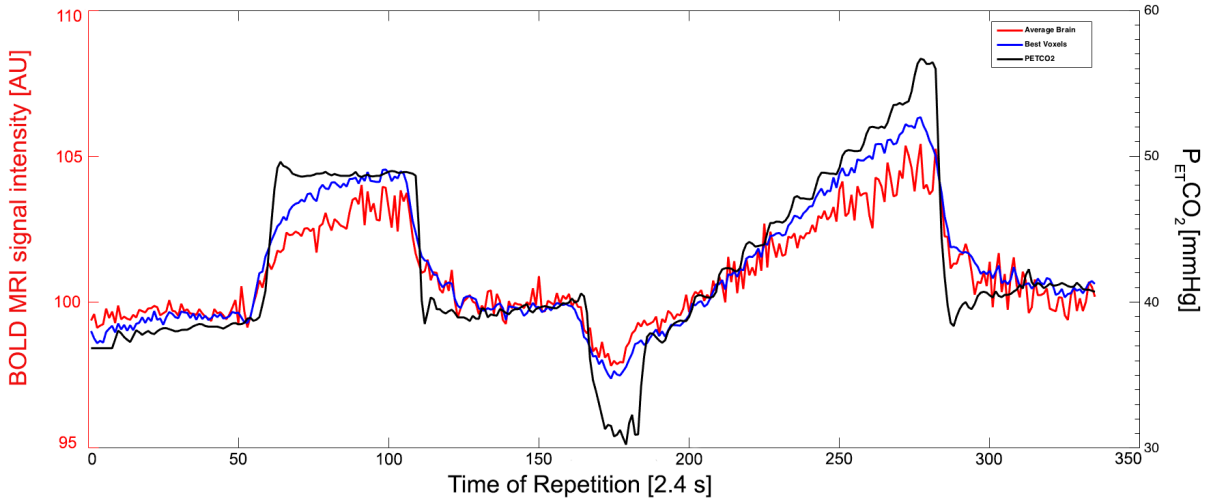

Figure 2.2. Actual P_{ETCO_2} time course and BOLD signal response from study subject. The black trace is the subject's P_{ETCO_2} over time. The red trace is the average brain BOLD signal over time, while the blue trace represents the average BOLD signal from a selection of the best response voxels.

2.4 Neuropsychological Testing

All subjects received a Behavioural Neurology Assessment-Revised (BNA-R). The BNA-R is an in-depth cognitive assessment tool that provides reliable measures of seven different cognitive domains: orientation, immediate recall, delayed recall, delayed recognition, visuospatial function, working memory/executive control, and language. When administering the BNA-R, it has been shown that patients with MCI score significantly lower in orientation, immediate recall, delayed recall, delayed recognition, and language but not on working memory/executive control or visuospatial function (Freedman et al., 2016). Also, the classification rate of the BNA-R for MCI vs. healthy control has been found to be superior to published data on the Montreal Cognitive Assessment. As reviewed earlier, AD demonstrates progressive, systematic targeting of cognitive domains. Episodic memory impairment is widely recognized as the earliest and most appreciable cognitive symptom in AD. For this reason, we sought to assess the relationship

between CVR and the speed of the cerebrovascular response across all subjects and episodic memory impairment. To achieve this, the scores from the immediate memory and delayed memory components of the BNA-R, consisting of the immediate recall score and delayed recall score (percent retained) from the Consortium to Establish a Registry for Alzheimer's Disease (CERAD) Word List test, were correlated with CVR and speed of cerebrovascular response. Additionally, a clinical dementia rating (CDR) assessment carried out on MCI subjects for validation of diagnosis, with all patients scoring a 0.5.

2.5 BOLD Processing

2.5.1 Preprocessing

The BOLD acquisitions were analyzed using AFNI software (Cox, 1996) and Matlab (2014b, The MathWorks, Inc., Natick, Massachusetts, US). Using AFNI, Raw BOLD data was first corrected for slice timing. This correction is used when all slices are not acquired simultaneously within each repetition (TR). Brain volumes were then volume re-registered to the first frame of the BOLD acquisition using a set of 3 translations and 3 rotations to address patient movement during the acquisition. In addition, scans were evaluated for extent of motion, and those with greater than 2mm of motion in any direction were discarded. Finally, the BOLD time series were scaled to percent change, which was achieved by dividing by the mean then multiplying by 100, then aligned to the T1-weighted anatomical images.

2.5.2 Calculating CVR

Each patient's P_{ETCO_2} time series was first time-shifted to the point of maximum correlation with the whole brain average BOLD signal using Matlab to align the onset time of stimulus with the

BOLD response, thus correcting for the time delay incurred due to the gas sampling delay and the transit time of blood from the pulmonary to cerebral circulation. CVR was then calculated as the regression coefficient of a linear, least-squares fit of the BOLD signal to the shifted P_{ETCO_2} time series on a per voxel basis (Figure 2.3). This operation was accomplished using:

$$\boldsymbol{S(t) = CVR \times PETCO_2(t) + B + \varepsilon(t)}$$

where S is the BOLD response, CVR is the slope of the regression between S and P_{ETCO_2}, B is the baseline BOLD signal, and ε(t) is the residual time series (ie. error). CVR is expressed as the percent change in BOLD signal per mmHg change in P_{ETCO_2}, providing a measure of the amplitude of the cerebrovascular response to a vasodilatory stimulus. For visualization purposes, the CVR value in each voxel can be assigned a colour and superimposed on the corresponding voxel of the anatomical images (using real-time linear interpolation) to produce a colour-coded CVR map (Figure 2.4).

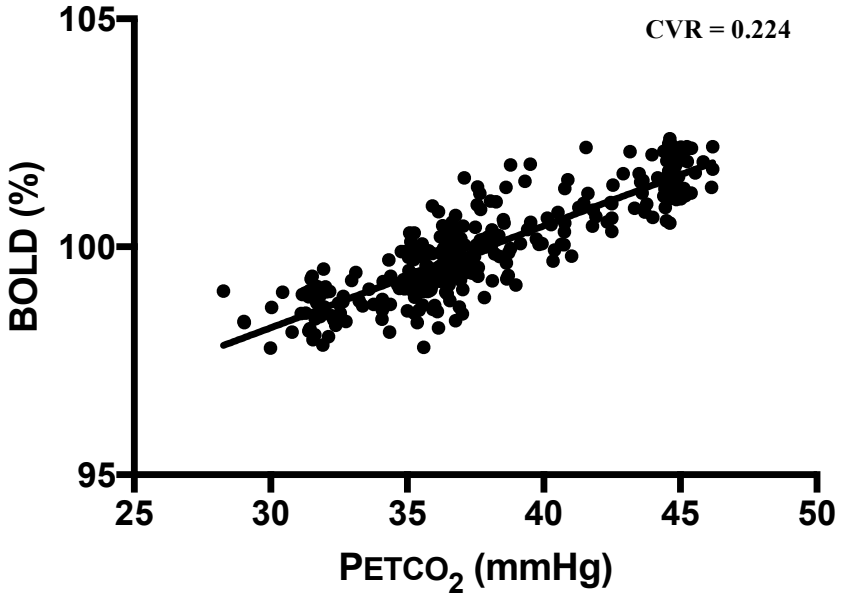

Figure 2.3. Sample plot of BOLD signal versus P_{ETCO_2} in a given voxel with line of best fit demonstrating regression coefficient (CVR). CVR is calculated as the regression coefficient of a linear, least-squares fit of the BOLD signal to the P_{ETCO_2} time series on a per voxel basis.

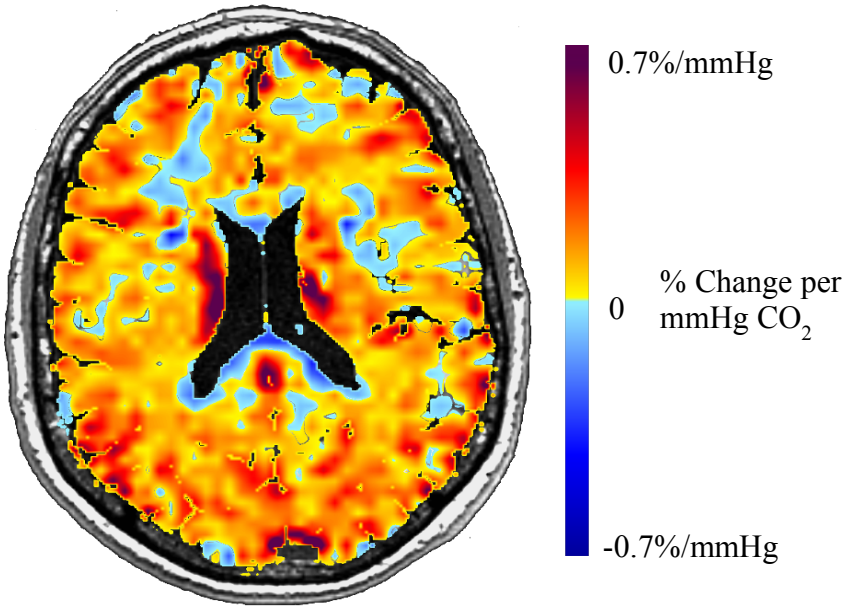

Figure 2.4. CVR map generated from the regression coefficient of BOLD and P_{ETCO_2} data. Colour-coded map of CVR superimposed on a T1-weighted anatomical map. Reds and purples indicate a strong positive CVR response, while blues indicate a drop in blood flow, known as steal physiology

2.5.3 Calculating speed of cerebrovascular response

The method to calculate the speed of cerebrovascular response has been previously described by Poublanc and colleagues (Poublanc et al., 2015). Using the time-shifted P_{ETCO_2} trace, the BOLD response to the hypercapnic stimulus was modeled by convolving the P_{ETCO_2} time series with a hemodynamic response function (HRF) in the form of an exponential decay functional, $\exp(-t/\tau)$, where t is time and τ is the time constant of the cerebrovascular response. Consider the following equation:

$$\boldsymbol{S(t) = A\,x\,\{PETCO_2(t)\ \otimes \mathbf{HRF}(t/\tau)\}\ +\ B\ +\ \varepsilon(t)}$$

which is similar to the previous equation, however $P_{ETCO_2}(t)$ has been replaced with $P_{ETCO_2}(t) \otimes \mathrm{HRF}(t,\tau)$, ie. is convolved with $\mathrm{HRF}(t,\tau) = e^{-t/\tau}/C(\tau)$, where $C(\tau)$ is a scaling factor equal to the area under the curve from $t=0$ to $t=5\tau$. Also, CVR has been replaced with A, which is a scaling

factor for the function. A set of 50 convolved P_{ETCO_2} curves is generated for τ values ranging from 2-100 seconds, in 2-second increments Figure 2.5. A Pearson correlation is then carried out between the BOLD response in each voxel and each convolved P_{ETCO_2} curve to determine the curve of best fit. The τ value associated with the curve of best fit defines the speed of cerebrovascular response to the vasodilatory stimulus, expressed in seconds. Therefore, smaller τ values reflect a faster vascular response, while larger τ values reflect a slower response.

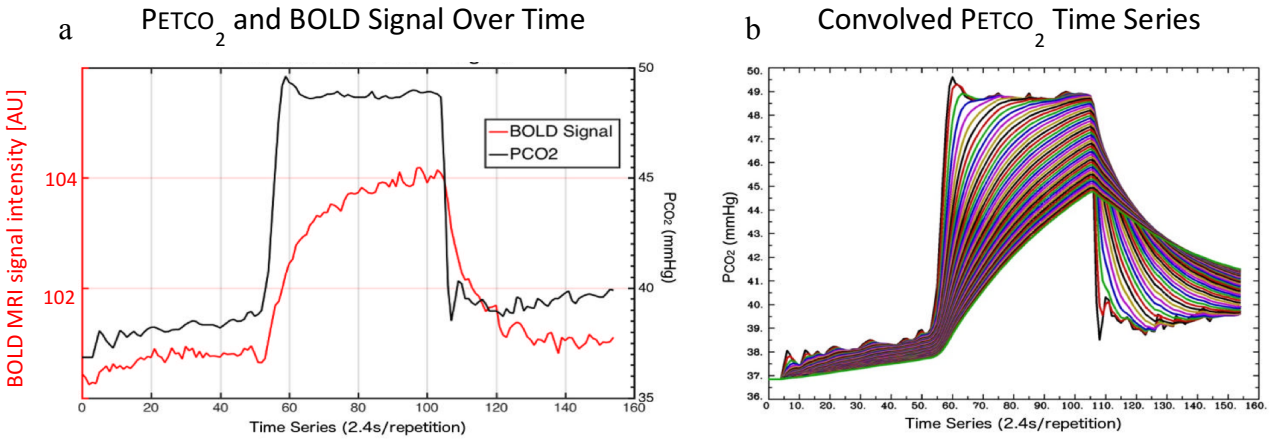

Figure 2.5. (a) Actual P_{ETCO_2} time course and BOLD signal response from study subject (b) P_{ETCO_2} time course and resultant set of convolution curves. A Pearson correlation is then carried out between the BOLD response (red trace) in each voxel and each convolved P_{ETCO_2} curve (coloured curves on right) to determine the curve of best fit. The τ value associated with the curve of best fit defines the speed of cerebrovascular response to the vasodilatory stimulus, expressed in seconds.

Again, the τ value in each voxel can be assigned a colour and superimposed on the corresponding voxel of the anatomical images (using real-time linear interpolation) to produce a colour-coded τ map (Figure 2.6).

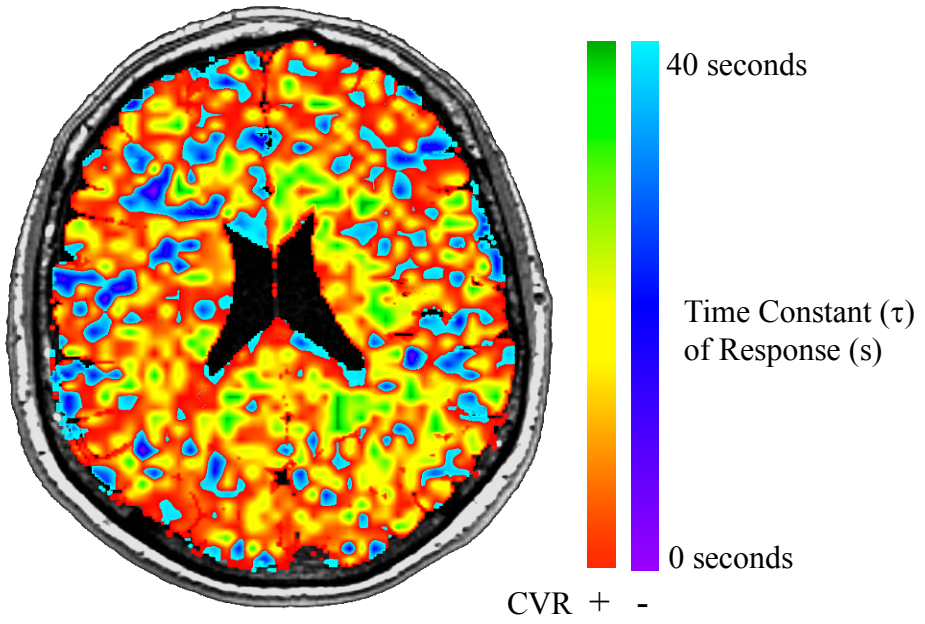

Figure 2.6. Map of time constant (τ) generated from best fit of BOLD and P_{ETCO_2} convolution. Colour-coded map of mean τ superimposed on a T1-weighted anatomical map. Reds and yellows indicate a fast speed of response, while greens indicate a slowed vascular response. Blue indicates areas with steal physiology and are excluded from analysis.

2.5.4 Partial volume correction

Progressive cortical atrophy is a cornerstone pathological feature of AD. Within our own CVR studies, we have observed a substantially different average CVR and speed of cerebrovascular response between GM and WM. Therefore, CVR studies comparing AD and MCI patients to healthy controls will incur a partial volume effect if atrophy is not considered. To address this potential confound, the analysis was confined to cortical GM and the following correction was applied to both the CVR and τ values in each voxel. Note: outlined is the correction for CVR, though the correction for τ is identical (simply substitute τ for CVR).

$$\boldsymbol{CVR_{VOX} = \left(CVR_{GM}\ x\ P_{GM}\right) + \left(CVR_{WM}\ x\ P_{WM}\right)}$$

$$\boldsymbol{\therefore CVR_{GM} = \frac{\left(CVR_{VOX} - \left(CVR_{WM}\ x\ P_{WM}\right)\right)}{P_{GM}}}$$

CVR_{VOX} refers to the CVR value measured in a voxel, CVR_{GM} and CVR_{WM} are the intrinsic CVR of the GM and WM in the voxel, and p_{GM} and p_{WM} are the proportions of GM and WM in the voxel, respectively. Simply put, the CVR value measured can be resolved in components arising from the GM and WM individually, assuming the contribution of the CSF to CVR is negligible. Therefore, by estimating the intrinsic CVR of WM as well as the proportion of GM and WM in a given voxel, a correction can be applied that accounts for variable levels of cortical atrophy across subjects. This correction is similar to that used by Johnson et al. and Du et al. when measuring CBF in AD patients using ASL MRI (Du et al., 2006; Johnson et al., 2005). As well, Cantin and colleagues applied a comparable correction when studying CVR in AD and MCI patients, however they assumed that WM produced negligible CVR, reducing the correction to a division of CVR_{VOX} by p_{GM} (Cantin et al., 2011). To generate an estimate of CVR_{WM}, a cerebral WM mask was generated using Freesurfer (covered later), then eroded to produce a cerebral WM volume with minimal GM contamination. Mean CVR was then calculated across the eroded mask for each patient, yielding an estimate of CVR_{WM}. To calculate p_{GM} and p_{WM}, T1-weighted anatomical images were segmented using SPM8 (Wellcome Trust Centre for Neuroimaging, University College London, London, UK). The resultant GM and WM probability maps were used as estimates of p_{GM} and p_{WM}, respectively.

2.6 Generation of ROIs

Two ROIs were included in the analysis, namely the temporal and parietal cortices. These two regions were selected due to the high level of involvement of these two regions in AD. The ROIs were generated from the T1-weighted anatomical images using the Freesurfer suite (http://surfer.nmr.mgh.harvard.edu/, as reviewed by Fischl, 2012). First, anatomical images underwent skull stripping, a bias field correction, and GM/WM segmentation. Then, cortical surface models of the GM/WM boundary and pial surface were reconstructed, followed by parcellation and labelling of the cortical surface. Whole-lobe cortical ROIs were then constructed for the temporal and parietal cortex for each subject and visually inspected for quality (Figure 2.7).

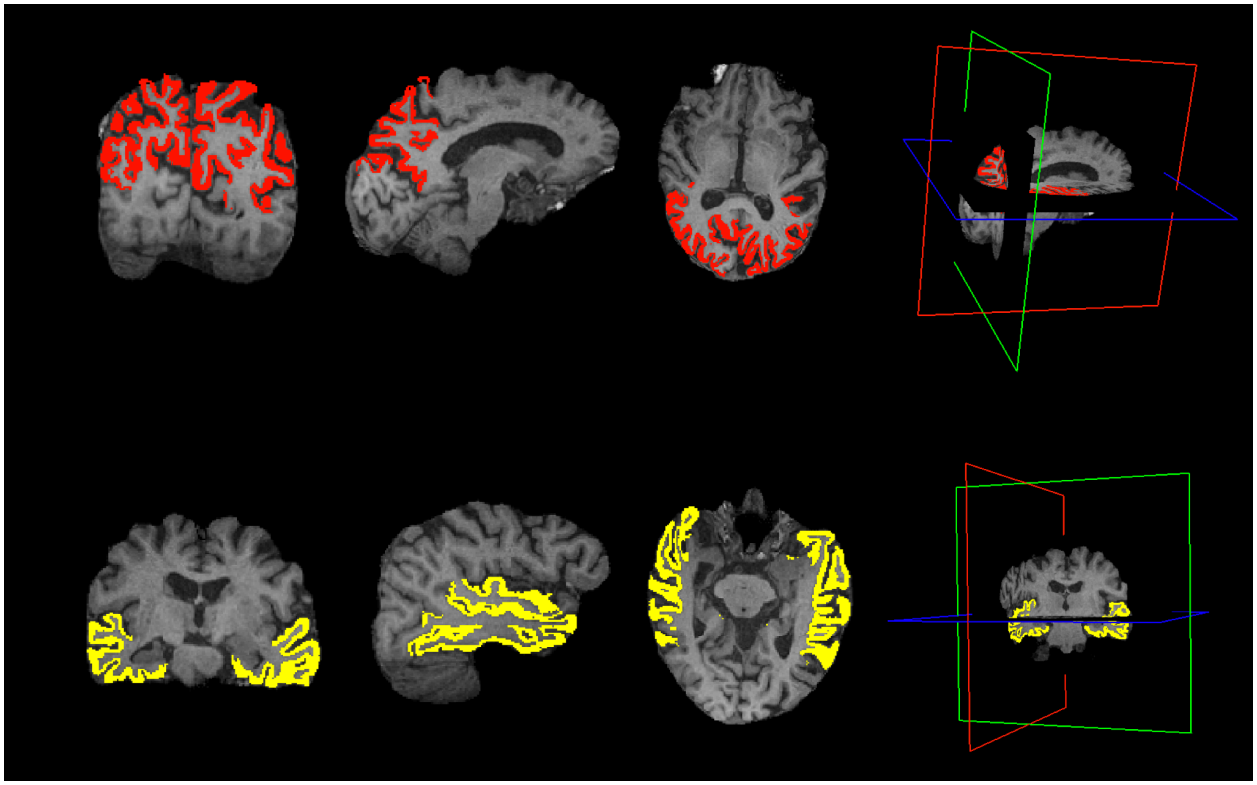

Figure 2.7. Sample of cortical ROIs for the parietal lobes (red) and temporal lobes (yellow).

2.7 Assessment of WMH Burden

To ensure that any group differences in CVR or the speed of cerebrovascular response were not the result of group differences in ischemic small vessel disease, the WMH burden was scored for each patient as a surrogate measure of microvascular disease and added to subsequent statistical analyses as a covariate of no interest. To accomplish this, proton density/T2-weighted images and 2D FLAIR images of all patients were screened by an experienced neuroradiologist who was blinded to group membership and scored using the Fazekas scale (Fazekas et al., 1987).

2.8 Statistical Analyses

All statistical analyses were completed using IBM SPSS Statistics v21 (IBM Corp. Released 2012. IBM SPSS Statistics for Macintosh, Version 21.0. Armonk, NY). To assess differences in CVR and speed of cerebrovascular response among AD, MCI and HC groups, a one-way analysis of covariance (ANCOVA) was carried out for both measures, CVR and speed of cerebrovascular response, in both ROIs, temporal and parietal cortices, while correcting for age and Fazekas score. Also, the assumptions of homogeneity of variances and normality of residuals were tested using Levene's test and the Shapiro-Wilk test, respectively. In the event of a statistically significant finding, Bonferroni-corrected post-hoc testing assessed pairwise comparisons.

To assess the relationship between CVR and memory, a partial correlation was completed between each vascular metric and each ROI, while also correcting for age and Fazekas score. Regarding multiple comparisons, a Holms-Bonferonni correction was used to adjust alpha values to address tests being carried out.

Chapter 3
Results

3 Results

3.1 Subject Demographics

A total of thirty-three individuals (age range: 52-83, 20 males) were recruited to participate in the study, consisting of seven AD subjects, twelve MCI subjects, and fourteen older healthy controls (HC). All participants tolerated the study protocol and there were no adverse events or subject motion greater than 2mm. However, one AD subject was discarded because of scanner-related artifact during BOLD acquisition, one MCI subject failed to complete the requisite imaging protocol, and one HC subject was removed due to poor stimulus control. Therefore, six early AD subjects, eleven MCI subjects, and thirteen older HC were included in the analysis.

Subject demographics are presented in Table 3.1. Experimental groups were not significantly different with regards to gender, however there was a significant age effect. The mean age of the MCI group was significantly higher than the HC group, though the AD group was not significantly different in age from either the MCI or HC group. In comparison to HC participants, MCI and AD participants had more vascular risk factors including hypertension and dyslipidemia. In addition, one AD subject had diabetes mellitus and one MCI subject had a remote history of smoking. In both the MCI and AD groups, two individuals were on an antihypertensive and one individuals was taking a statin, whereas in the HC group only one person was taking each of those drugs. A single subject from the MCI and HC groups and two individuals from the AD group were taking an antidepressant, however none were diagnosed with major depressive disorder. Fazekas score was significantly different between groups. The mean Fazekas score in the MCI group was significantly higher than in the HC group, but the mean Fazekas score in the AD group was not significantly different from the other groups. Both

the MCI and AD groups exhibited significantly reduced immediate and delayed memory scores, though were not significantly different from one another. None of the participants had a history of strokes, TIAs or other neurological disorders involving the central nervous system.

Table 3.1. Subject Demographics.

		HC (n=13)	MCI (n=11)	AD (n=6)	Statistics	Post-hoc
Age		63.9 ± 10.2	73.1 ± 5.7	70.5 ± 5.8	F=4.074, p=0.028*	MCI>NC
Gender	**Female**	4	4	2		
	Male	9	7	4	F=0.257, p=1.000	
Vascular Risk Factors	**Hypertension**	1	2	2		
	Dyslipidemia	1	2	3		
	Diabetes mellitus	0	0	1		
	Smoking	0	1	0		
Medications	**AChE Inhibitor**	0	0	1		
	Antidepressant	1	1	2		
	Antihypertensive	1	2	2		
	Statin	1	1	1		
	Beta-Blocker	0	1	2		
	Platelet Drug	0	0	2		
	Insulin/Metformin	0	0	1		
Fazekas Score		0.69± 0.75	1.64 ± 0.81	1.00 ± 0.63	F=4.747, p=0.017*	MCI>NC
Memory[1]	**Immediate Memory**	21.4 ± 3.1	16.3 ± 3.3	17.0 ± 2.6	F=8.044, p=0.002*	NC>MCI&AD
	Delayed Memory	72.5 ± 20.7	39.2 ± 22.1	21.4 ± 21.8	F=11.86, p<0.001*	NC>MCI&AD

[1] Sample size differs for memory scoring, NC=11, MCI=11, AD=5

3.2 CVR in AD, MCI, and HC Groups

Descriptive statistics of CVR are summarized in Table 3.2 and group maps of mean CVR in cortical GM are presented in Figure 3.1. In can be seen that in both the temporal and parietal cortices, mean CVR was greatest in the MCI group and lowest in the AD group, with HC possessing an intermediate mean CVR value. In order to test the hypothesis that group membership (HC, MCI, AD) had an effect on CVR, a between-groups ANCOVA was performed for each ROI, while correcting for age and Fazekas score. The assumptions of homogeneity of variances and normality of residuals were tested using Levene's test and the Shapiro-Wilk test, respectively, and found to be satisfactory.

The between-groups ANCOVAs found no significant main effect in either temporal cortex, $F(2,29) = 1.3$, $p=0.29$, or the parietal cortex, $F(2,29) = 1.469$, $p=0.249$ (Table 3.3). Thus, the null hypothesis was not rejected and no post-hoc testing was performed.

Table 3.2. CVR in temporal and parietal ROIs across HC, MCI, and AD groups.

Cortical ROI	Group	Mean (%/mmHg)	Std. Deviation	Est. Marg. Mean
Temporal	**HC**	0.504	0.064	0.492
	MCI	0.550	0.141	0.564
	AD	0.490	0.061	0.489
Parietal	**HC**	0.393	0.067	0.378
	MCI	0.410	0.121	0.426
	AD	0.341	0.067	0.344

Table 3.3. ANCOVA results for effect of group membership (HC, MCI, AD) on CVR.

Cortical ROI	F	p-value	Partial η^2
Temporal	1.30	0.290	0.094
Parietal	1.47	0.249	0.105

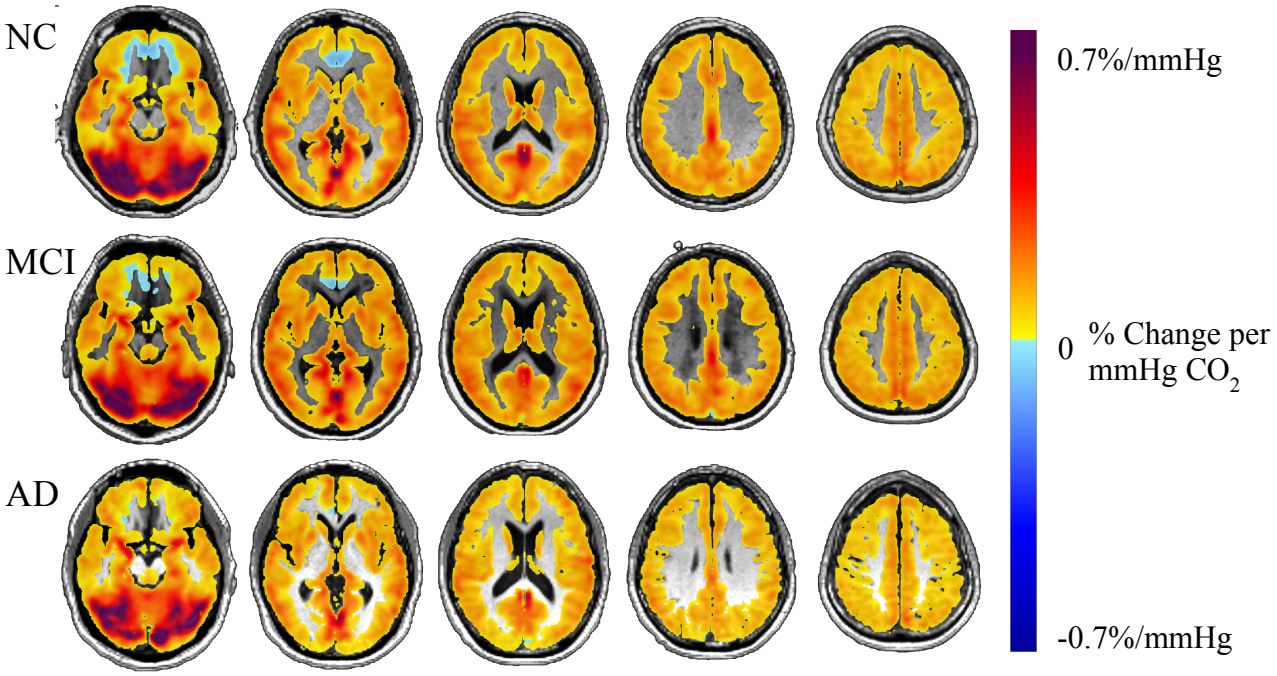

Figure 3.1. Maps of mean CVR in cortical GM in each group. Colour-coded map of mean CVR superimposed on a T1-weighted anatomical map in standard space. Reds and purples indicate a strong positive CVR response, while blues indicate a drop in blood flow, known as steal physiology.

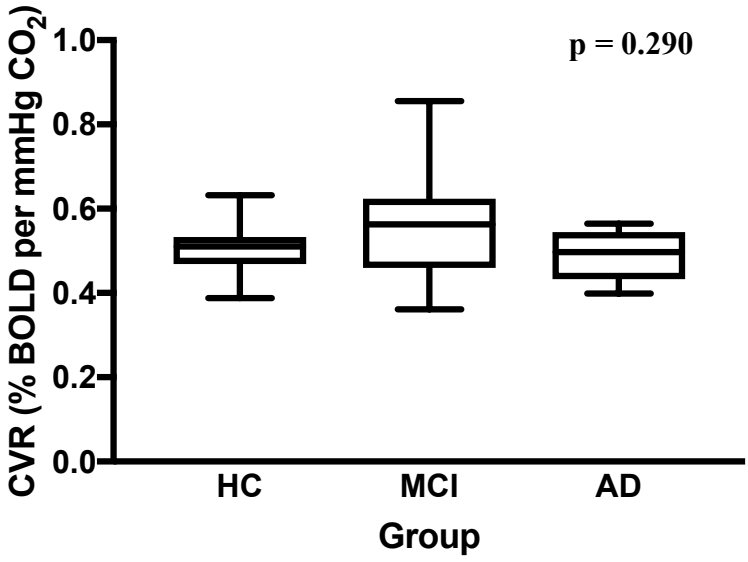

Figure 3.2. CVR in the temporal cortex across groups.
CVR values are reported as % change in BOLD per mmHg change on P_{ETCO_2}. Bars indicate minimum and maximum, boxes indicate the interquartile range, and the middle line denotes the median. No significant group differences were found in CVR.

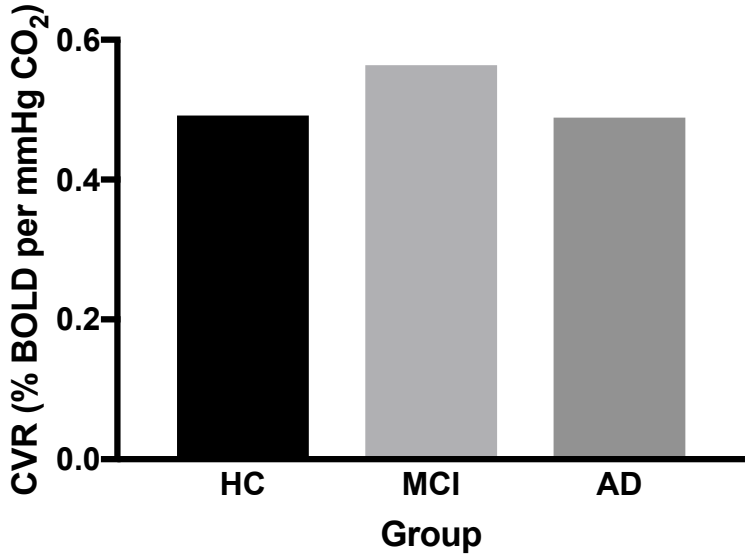

Figure 3.3. Estimated marginal mean CVR in the temporal cortex across groups.
Mean CVR estimates are corrected for age and Fazekas score and are reported as % change in BOLD per mmHg change on P_{ETCO_2}. Estimates are produced by the general linear model used for ANCOVA testing.

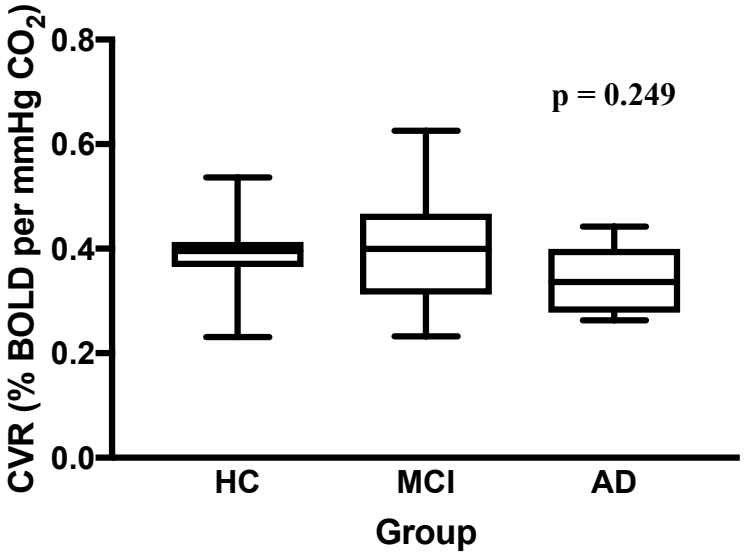

Figure 3.4. CVR in the parietal cortex across groups.
CVR values are reported as % change in BOLD per mmHg change on P_{ETCO_2}. Bars indicate minimum and maximum, boxes indicate the interquartile range, and the middle line denotes the median. No significant group differences were found in CVR.

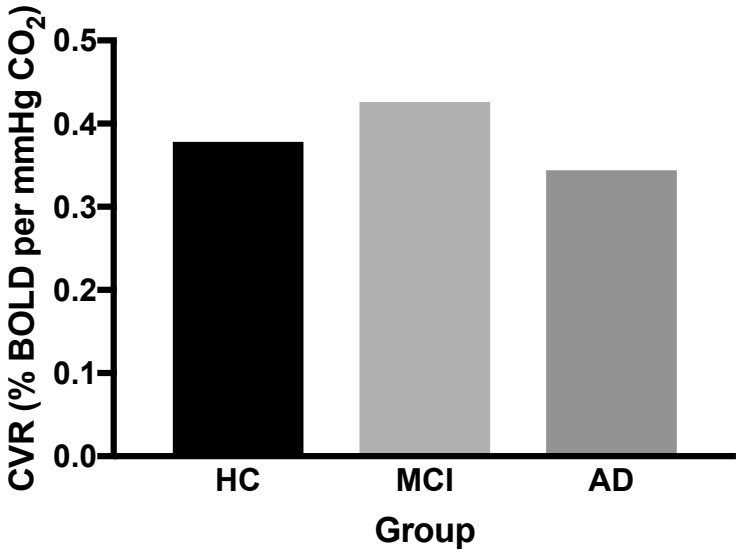

Figure 3.5 Estimated marginal mean CVR in the parietal cortex across groups.
Mean CVR estimates are corrected for age and Fazekas score and are reported as % change in BOLD per mmHg change on P_{ETCO_2}. Estimates are produced by the general linear model used for ANCOVA testing.

3.3 Speed of Cerebrovascular Response in AD, MCI and HC Groups

Descriptive statistics for speed of cerebrovascular response are summarized in Table 3.4 and group maps of time constant (τ) of the cerebrovascular response in cortical GM are presented in Figure 3.4. It can be seen that in both the temporal and parietal cortices, mean τ of the vascular response was greatest in the AD group and lowest in the HC group, with MCI possessing an intermediate τ value. In other words, mean speed of cerebrovascular response was fastest in the HC group and slowest in the AD group. In order to test the hypothesis that group membership (HC, MCI, AD) had an effect on CVR, a between-groups ANCOVA was performed for each cortical ROI, while correcting for age and Fazekas score. The assumptions of homogeneity of variances and normality of residuals were tested using Levene's test and the Shapiro-Wilk test, respectively, and found to be satisfactory.

ANCOVA statistics are summarized in Table 3.5. Between-groups ANCOVA found a significant effect in both temporal and parietal cortices (temporal: $F(2,29) = 3.93$, $p=0.033$; parietal: $F(2,29) = 5.05$, $p=0.014$). Therefore, the null hypothesis was rejected. Group membership accounted for 23.9% and 28.8% of the variance in τ in the temporal and parietal cortices, respectively. To further investigate the nature of group difference in τ, Bonferroni-corrected post-hoc testing was performed (Table 3.6). The AD group and HC group were significantly different in both the temporal ($p=0.031$) and parietal cortex ($p=0.013$), however the MCI group was not significantly different from either group.

Table 3.4. Time constant (τ) of the vascular response to CO_2 across HC, MCI, and AD groups.

Cortical ROI	Group	Mean (s)	Std. Deviation	Est. Marg. Mean (s)
Temporal	**HC**	26.4	11.5	27.6
	MCI	34.2	12.9	32.7
	AD	44.5	7.8	44.6
Parietal	**HC**	23.7	12.9	25.1
	MCI	34.3	16.5	32.5
	AD	48.3	11.6	48.6

Table 3.5. ANCOVA result testing effect of group membership (HC, MCI, AD) on the time constant (τ) of vascular response.

Cortical ROI	F	p-value	Partial η^2
Temporal	3.93	0.033 *	0.239
Parietal	5.05	0.014 *	0.288

Table 3.6. Bonferroni-corrected post-hoc testing of group differences in the time constant (τ) of the vascular response. p-value is adjusted to account for multiple comparisons

Cortical ROI	Comparison	Mean Difference (s)	p-value	
Temporal	**AD>HC**	17.0	0.031	*
	AD>MCI	11.9	0.212	
	MCI>HC	5.1	1.000	
Parietal	**AD>HC**	23.6	0.013	*
	AD>MCI	16.1	0.138	
	MCI>HC	7.4	0.932	

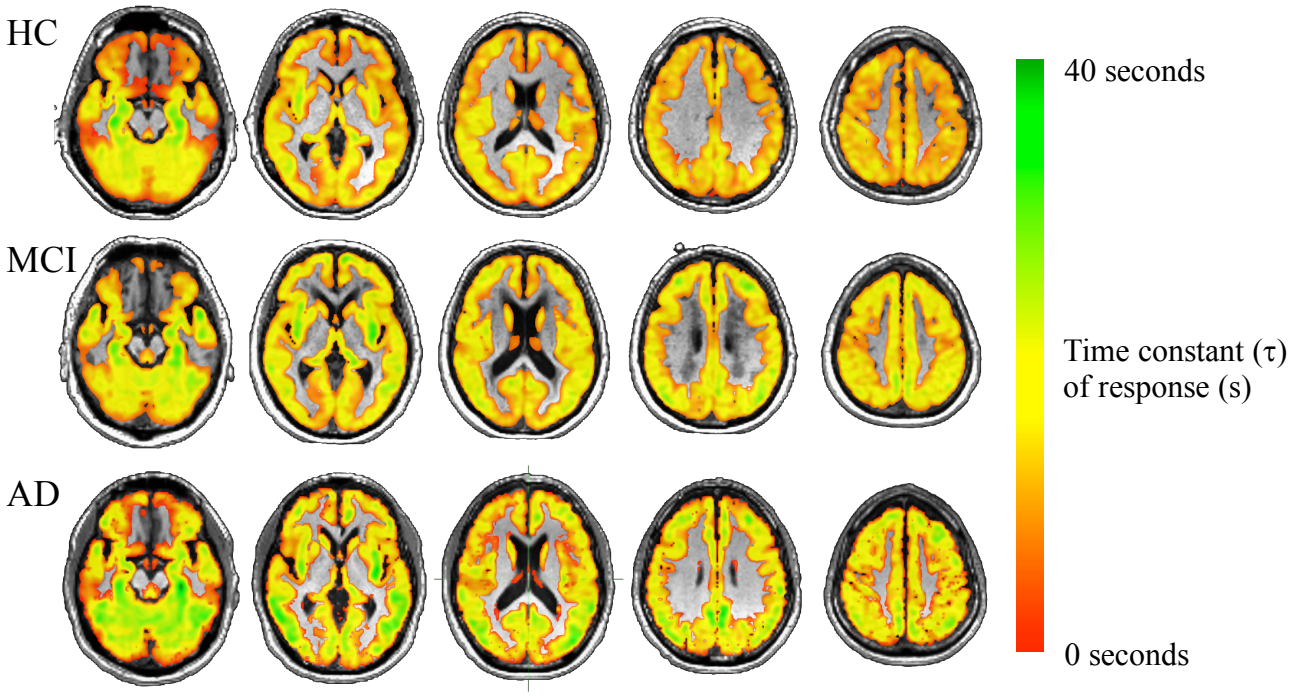

Figure 3.6. Maps of mean time constant (τ) of the cerebrovascular response in cortical GM in each group. Colour-coded map of mean τ superimposed on a T1-weighted anatomical map in standard space. Reds and yellows indicate a fast speed of response, while greens indicate a slowed vascular response.

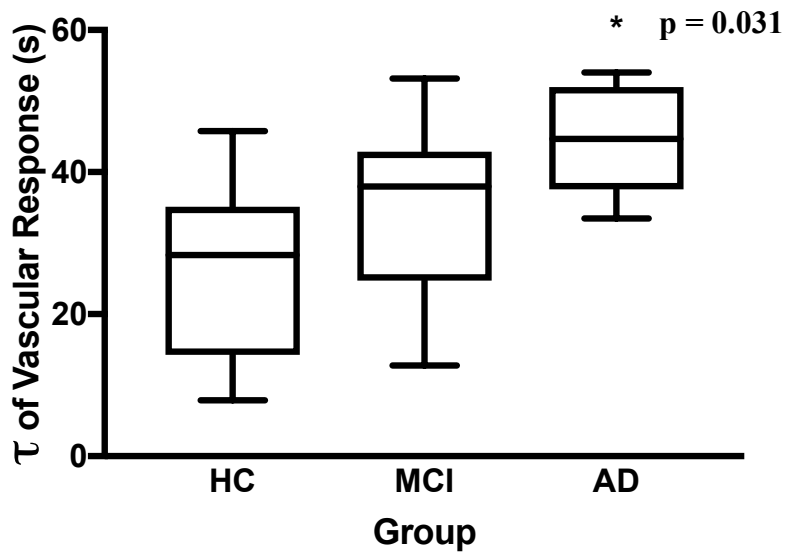

Figure 3.7. Time constant (τ) of the vascular response to CO_2 in temporal cortex across groups. τ values are reported in seconds. Bars indicate minimum and maximum, boxes indicate the interquartile range, and the middle line denotes the median value. Higher values indicate a slower speed of response. ANCOVA testing yielded a significant group effect on τ (p=0.031), and Bonferroni-corrected post-hoc testing determined that τ was significantly greater in the AD group than the HC group.

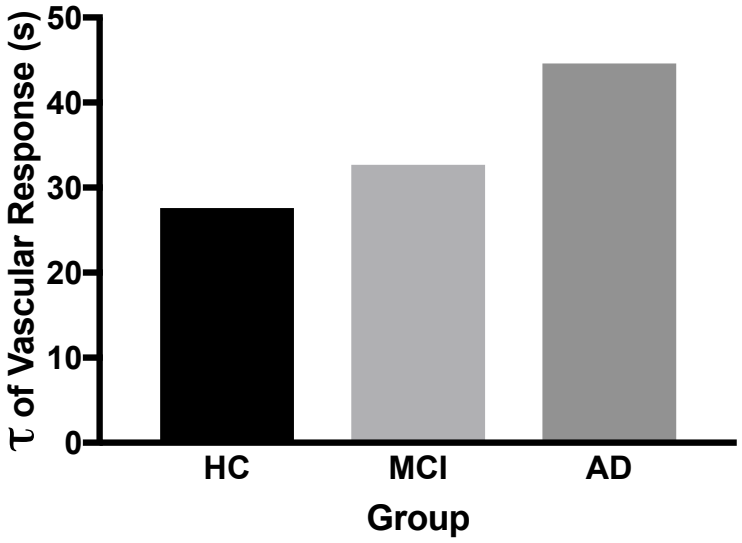

Figure 3.8. Estimated marginal mean τ in the temporal cortex across groups.
Mean τ estimates are corrected for age and Fazekas score and are reported in seconds. Higher values indicate a slower speed of response. Estimates are produced by the general linear model used for ANCOVA testing.

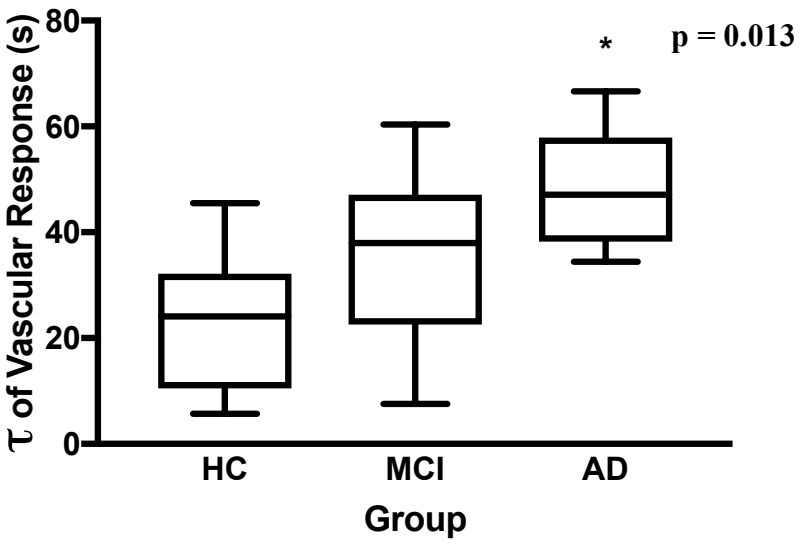

Figure 3.9. Time constant (τ) of the vascular response to CO_2 in parietal cortex across groups. τ values are reported in seconds. Bars indicate minimum and maximum, boxes indicate the interquartile range, and the middle line denotes the median value. Higher values indicate a slower speed of response. ANCOVA testing yielded a significant group effect on τ (p=0.013), and Bonferroni-corrected post-hoc testing determined that τ was significantly greater in the AD group than the HC group.

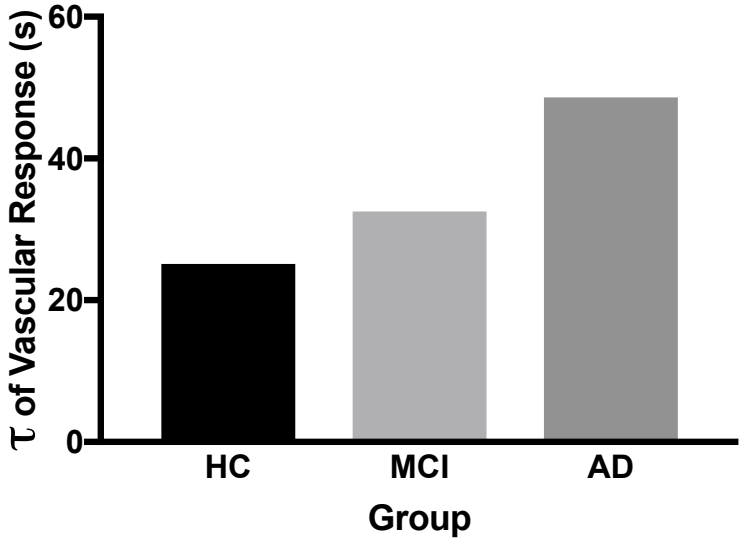

Figure 3.10. Estimated marginal mean τ in the parietal cortex across groups.
Mean τ estimates are corrected for age and Fazekas score and are reported in seconds. Higher values indicate a slower speed of response. Estimates are produced by the general linear model used for ANCOVA testing.

3.4 CVR, Speed of Cerebrovascular Response, and Episodic Memory

3.4.1 CVR and episodic memory

To test the hypothesis that CVR correlates with episodic memory across all subjects, a partial correlation was performed between CVR and both immediate and delayed memory scores for each cortical ROI, while correcting for age and Fazekas score. Analyses yielded no significant correlation between CVR and either immediate or delayed memory. Thus, the null hypothesis was not rejected. Partial correlation results are summarized in Table 3.7. Scatter plots were used to visualize the relationship between CVR and memory scoring.

Table 3.7. Partial correlations between CVR and episodic memory scoring.

Cortical ROI (n=27)	Memory type	Correlation (r)	p-value
Temporal	**Immediate**	-0.156	0.457
	Delayed	-0.027	0.897
Parietal	**Immediate**	-0.077	0.716
	Delayed	0.129	0.539

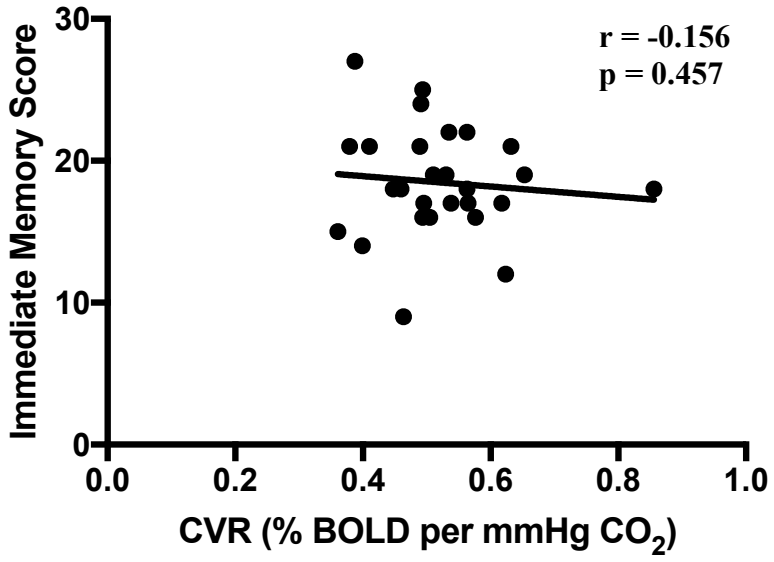

Figure 3.11. CVR in the temporal cortex vs immediate memory score across all subjects. Pearson r coefficient and p-value are corrected for age and Fazekas score. There is no relationship between CVR in the temporal cortex and immediate memory.

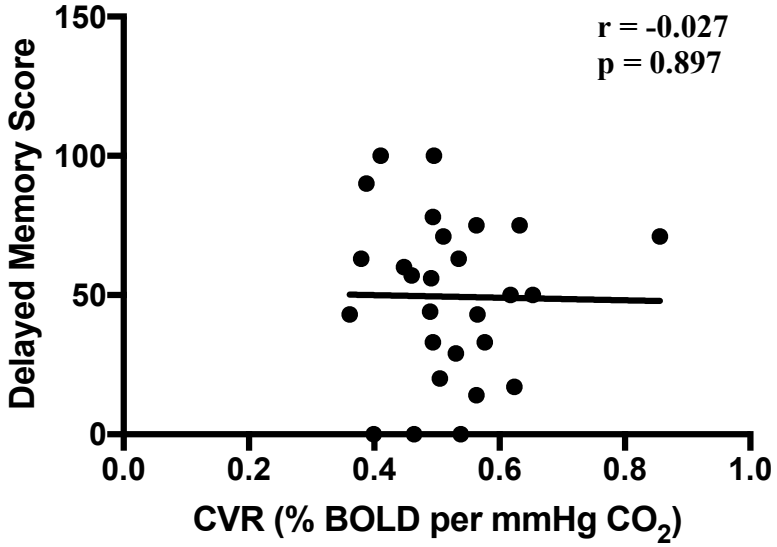

Figure 3.12. CVR in the temporal cortex vs delayed memory score across all subjects. Pearson r coefficient and p-value are corrected for age and Fazekas score. There is no relationship between CVR in the temporal cortex and delayed memory.

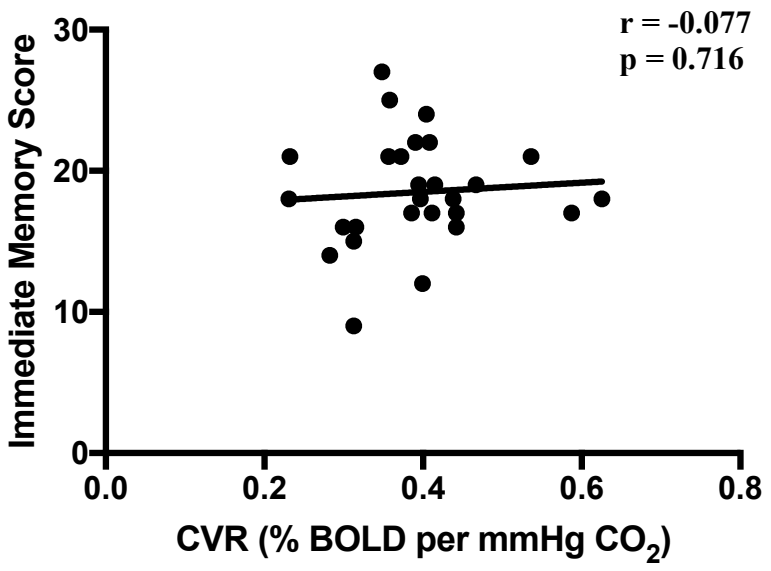

Figure 3.13. CVR in the parietal cortex vs immediate memory score across all subjects. Pearson r coefficient and p-value are corrected for age and Fazekas score. There is no relationship between CVR in the parietal cortex and immediate memory.

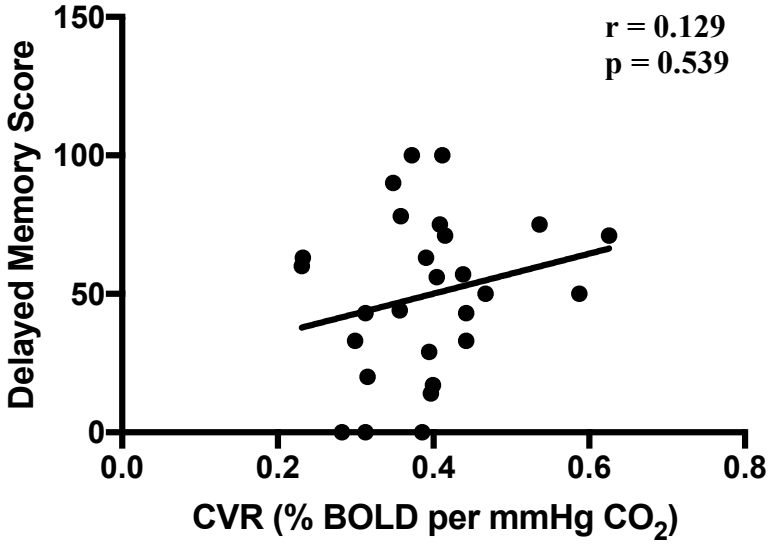

Figure 3.14. CVR in the parietal cortex vs delayed memory score across all subjects. Pearson r coefficient and p-value are corrected for age and Fazekas score. There is no relationship between CVR in the parietal cortex and delayed memory.

3.4.2 Speed of the cerebrovascular response and episodic memory

To test the hypothesis that τ correlates with episodic memory across all subjects, a partial correlation was performed between τ of the vascular response and both immediate and delayed memory scores for each cortical ROI, while correcting for age and Fazekas score. Analyses yielded a significant correlation between τ in the parietal cortex and delayed memory scoring, however after correction for multiple comparisons no significant findings remained. Thus, the null hypothesis was not rejected. Partial correlation results are summarized in Table 3.8. Scatter plots were used to visualize the relationship between CVR and memory scoring.

Table 3.8. Partial correlations of the time constant (τ) of the vascular response and episodic memory scoring.

Cortical ROI (n=27)	Memory type	Correlation (r)	p-value	Corrected p-value
Temporal	**Immediate**	-0.130	0.535	1.000
	Delayed	-0.298	0.148	0.592
Parietal	**Immediate**	-0.261	0.208	0.832
	Delayed	-0.432	0.031*	0.124

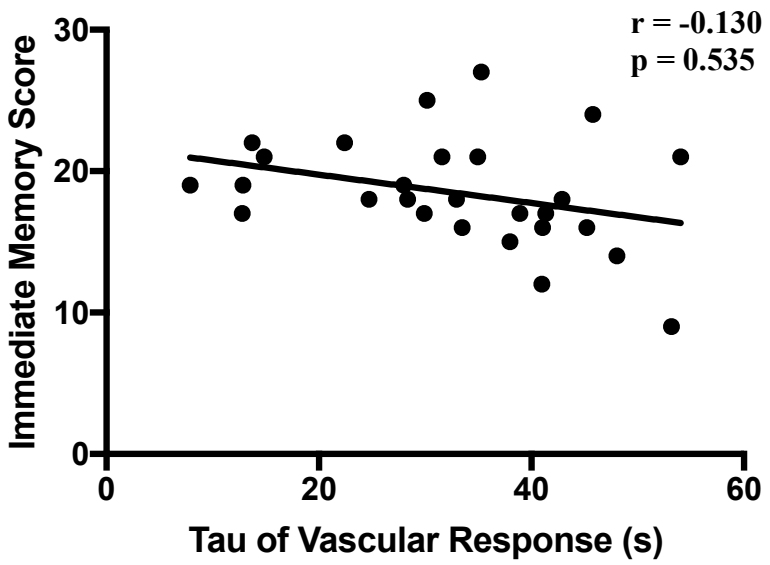

Figure 3.15. Time constant (τ) of the vascular response in the temporal cortex vs immediate memory score across all subjects. Larger τ values indicate a slower speed of vascular response. Pearson r coefficient and p-value are corrected for age and Fazekas score. It appears that slowing of the vascular response in the temporal cortex has no relation to immediate memory.

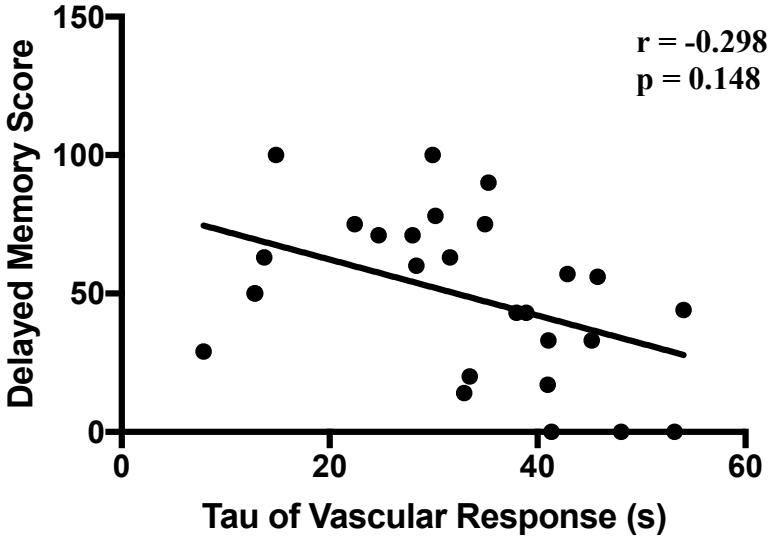

Figure 3.16. Time constant (τ) of the vascular response in the temporal cortex vs delayed memory score across all subjects. Larger τ values indicate a slower speed of vascular response. Pearson r coefficient and p-value are corrected for age and Fazekas score. Slowing of the vascular response in the temporal cortex was associated with a decline in delayed memory. However, this effect is not significant.

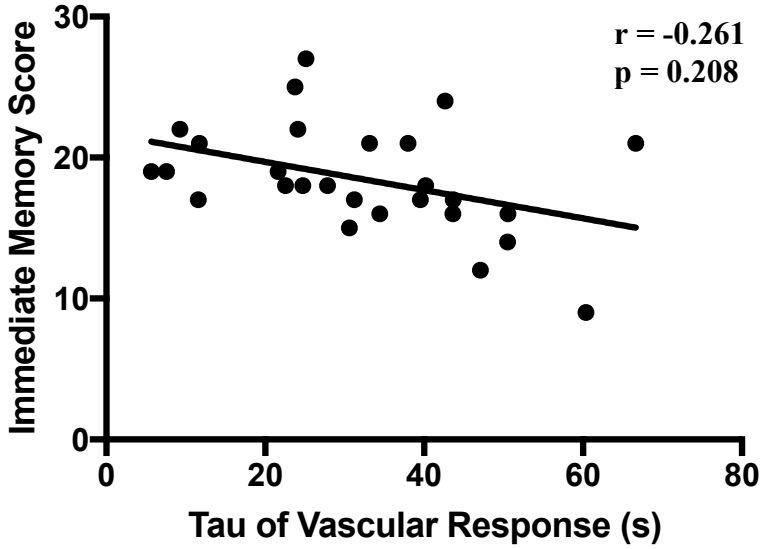

Figure 3.17. Time constant (τ) of the vascular response in the parietal cortex vs immediate memory score across all subjects. Larger τ values indicate a slower speed of vascular response. Pearson r coefficient and p-value are corrected for age and Fazekas score. Slowing of the vascular response in the parietal cortex was associated with a decline in immediate memory. However, this effect is not significant.

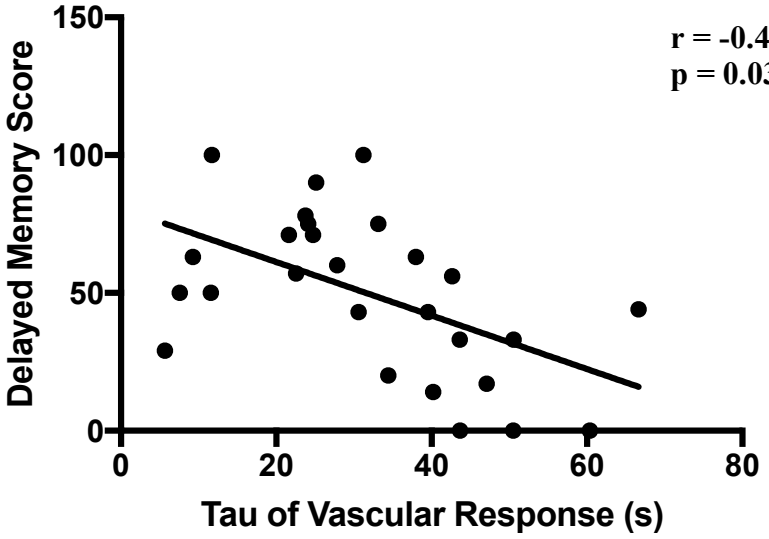

Figure 3.18. Time constant (τ) of the vascular response in the parietal cortex vs delayed memory score across all subjects. Larger τ values indicate a slower speed of vascular response. Pearson r coefficient and p-value are corrected for age and Fazekas score. Slowing of the vascular response in the parietal cortex was strongly associated with a decline in delayed memory. However, this relationship was not statistically significant after multiple comparisons correction.

Chapter 4
Discussion

4 Discussion

4.1 Summary of Key Findings

The objective of this study was to evaluate both CVR and the speed of cerebrovascular response to CO_2 in MCI and AD patients using a repeatable and reproducible methodology. By leveraging a specially-designed gas blending apparatus and a recently developed analysis of speed of vascular response, this was achieved. We found that development of AD is associated with a progressive slowing of the cerebrovascular response, and that this deficit cannot be explained by differences in age or microangiopathy. Interestingly, the magnitude of response, as measured by CVR, appears not to be significantly impaired at any stage of the disease. Furthermore, some evidence suggests that the speed of cerebrovascular response may also relate to the clinical presentation of episodic memory impairment, namely delayed recall. This section will discuss these findings in further detail and outline the strengths, limitations, and potential future directions of the work completed in this thesis.

4.1.1 No difference in CVR between groups

We did not observe a significant difference in CVR between HC, MCI and AD groups in either the temporal or parietal cortex. In fact, the relationship of CVR with group membership was dramatically different than what was predicted by our *a priori* hypothesis. We hypothesized that CVR would demonstrate a negative trend in both ROIs in relation to AD progression. Thus, we

predicted that the HC group would exhibit the highest mean CVR and the AD group would exhibit the lowest, with the MCI group falling in between the two. Instead, we found that the MCI group possessed the highest mean CVR and the AD group possessed the lowest; a trend that could be described as an inverse-U when considered against disease progression (HC, MCI, AD). In any case, the null hypothesis could not be rejected.

To our knowledge, only one other study, by Cantin et al., has explicitly examined regional CVR in both MCI and AD patients using CO_2 (Cantin et al., 2011). Interestingly, our findings conflict with those reported by Cantin and colleagues, who observed widespread CVR reductions, including in temporal and parietal ROIs, in both MCI (n=7) and AD (n=9) patients when compared to controls (n=11) (ie. NC>MCI=AD) (Cantin et al., 2011). However, a second study by Yezhuvath et al. also assessed regional CVR, though only in AD patients (n=17) and older controls (n=17) (Yezhuvath et al., 2012). Our findings are more consistent with those reported by Yezhuvath and colleagues, who found no significant difference in CVR between AD patients and controls in the temporal or parietal cortex. It is unclear why these two studies failed to produce the same results as they used similar methodologies, both employing fixed inspired CO_2 vasodilatory challenges and assessing changes in CBF using BOLD MRI. One key difference was the method used to correct for cortical atrophy in AD patients. Cantin et al. chose to divide CVR by an estimate of the proportion of GM in each voxel to normalize for atrophy, while Yezhuvath and colleagues registered each subject's images to the Montreal Neurological Institute (MNI) template then applied an algorithm from the Hierarchical Attribute Matching Mechanism for Elastic Registration (HAMMER, University of Pennsylvania, PA) software package that is thought correct for brain atrophy effects (Shen & Davatzikos, 2002).

The true nature of CVR in AD becomes increasingly blurred when considering the conflicting reports of older CVR studies in AD samples that did not apply a correction for GM atrophy. Employing acetazolamide and HMPAO-SPET imaging, Stoppe and colleagues reported significantly reduced CVR in both the temporal and parietal cortices of AD subjects (n=12) compared to elderly controls (n=9) (Stoppe et al., 1995). Another study by Oishi et. al using acetazolamide and xenon CT supported these findings, observing CVR in these cortical regions to be significantly reduced in AD (n=10) versus control (n=10) as well (Oishi et al., 1999). Conversely, CVR studies in AD samples by Kuwabara et al. and Jagust et al. both failed to observe any difference in CVR between AD participants (n=5 for both) and normal controls (n=5

and n=16, respectively) (Jagust et al., 1997; Kuwabara et al., 1992). Potentially of interest is that these studies differed from their contemporaries by utilizing fixed inspired CO_2 and PET imaging to assess CVR. Lastly, TCD studies of CVR in AD patients appear to lend credence to the notion that CVR is significantly impaired by the disease (Bär et al., 2007; Vicenzini et al., 2007). However, these studies lack spatial coverage, thus have limited utility in a discussion of specific regional changes in CVR. Also of note, no study has reported a potential increase in CVR in either AD or MCI patients.

4.1.2 AD is associated with a progressive slowing of the cerebrovascular response

When accessing the cerebrovascular response to CO_2, subjects with early AD have significantly longer τ values than older healthy controls in both the temporal and parietal cortex. In other words, AD patients exhibit, on average, a significantly slower speed of cerebrovascular response compared to controls. Moreover, the MCI group demonstrated an intermediate speed of cerebrovascular response, falling in between that of the AD and HC groups. While post-hoc testing was unable to declare a statistically significant difference in speed of cerebrovascular response between the MCI and HC groups, it is clear that a slowing of the response was detectable in the MCI group. These findings strongly suggest that AD is associated with a progressive slowing of the cerebrovascular response, which may even be detectable in prodromal stages of the disease.

To our knowledge, only one study has explicitly sought to assess the speed of cerebrovascular response to CO_2. In a sample of 20 AD patients, 15 MCI patients, and 28 healthy controls, Richiardi and colleagues used a 7% CO_2 inspiratory stimulus and BOLD fMRI to assess the speed of the cerebrovascular response (Richiardi et al., 2015). Of note, the authors chose not to monitor P_{ETCO_2}, instead opting to generate a stimulus regressor analytically. In any case, our findings are highly consistent with the results of their analysis. Globally, the authors reported that healthy controls demonstrated a significantly faster speed of cerebrovascular response than both MCI and AD subjects. Following up with a lobe-level analysis, they found the speed of response to be reduced in MCI and AD groups across all lobes, however after correction for

multiple comparisons, only the AD group remained statistically significantly different across all lobes, whereas the MCI group was no longer significantly different from the control group in any lobe. In addition, Cantin et al. also observed that a different slope of dynamic response to hypercapnia in MCI and AD groups compared to controls, suggesting that the temporal dynamics of CVR may be altered by the disease (Cantin et al., 2011).

The idea that the cerebrovascular response is progressively slowed by AD is further supported by findings that AD is associated with delayed BOLD fMRI responses to task-based stimuli. Rombouts and colleagues assessed the BOLD response to visual encoding in 18 AD patients, 28 MCI patients, and 41 elderly controls (Rombouts et al., 2005). Once again, the BOLD response was significantly delayed in the AD and MCI groups compared to controls and the delay was greater in the AD group than in the MCI group. Importantly, these differences in the speed of BOLD response could not be explained by differences in reaction times between groups. Also of note, the significantly delayed BOLD response to visual encoding in the MCI group was restricted to the occipital cortex, whereas in the AD group demonstrated a widespread delay in BOLD response. The spatial pattern of the BOLD delay can be at least partially explained by the fact that a visual encoding task will have the strongest activation, and therefore signal-to-noise ratio, in the occipital cortex, which would increase sensitivity of their experiment to detect changes in the BOLD signal in this region. Nonetheless, the fact that spatial extent of the delay increases from MCI to AD is consistent with the notion that MCI is a transitional state between healthy aging and AD dementia, and suggests that changes in the speed of cerebrovascular response may reflect the underlying progression of AD pathophysiology. Ultimately, the authors concluded that a delayed rather than a reduced BOLD response may be a stronger marker of early AD.

4.1.3 CVR metrics and episodic memory scoring

4.1.3.1 No correlation between CVR and episodic memory scoring

Across all participants of our study, there was no significant correlation between CVR and episodic memory scoring in either the temporal or parietal cortex. Considering that impairment of episodic memory is widely recognized as the earliest and most profound cognitive symptom of AD and given our focus on cortical structures intimately involved in memory function, particularly the temporal cortex, we hypothesized that changes in CVR would predict memory scoring, however this simply was not the case. Instead, our findings suggest that the magnitude of the cerebrovascular response in the temporal or parietal cortex, as measured by CVR, has little bearing on the presentation of episodic memory deficits in AD.

In the literature, correlating CVR in AD patients with cognitive scoring has resulted in mixed results. Cantin et al. found that in most ROIs, CVR values across 9 AD patients, 7 MCI patients, and 11 older controls were significantly correlated with the MMSE scoring, a general measure of cognitive impairment (Cantin et al., 2011). Conversely, Yezhuvath and colleagues were unable to find a relationship between CVR in AD patients and several measures of global cognitive function, including MMSE, CERAD Battery, and CDR (Yezhuvath et al., 2012). However, they did find a significant correlation between CVR in the frontal lobe and Boston Naming Test score, a measure of word retrieval performance. Despite performing multiple correlations, the authors also did not report any correction for multiple comparisons, thus this analysis may suffer from an increase probability of type I error. Another study by Stoppe and colleagues failed to find a significant correlation between MMSE and CVR across 12 AD patients and 9 elderly controls (Stoppe et al., 1995).

4.1.3.2 No correlation between speed of cerebrovascular response and episodic memory scoring, but potential relationship

Across all participants, we were unable to find a significant correlation between speed of cerebrovascular response (as measured by τ) and episodic memory in either the temporal or parietal cortex. However, this appears to be a product of inadequate sensitivity of the analysis rather than a lack of any relationship between the speed of cerebrovascular response and episodic memory. To the eye, it is apparent that the τ of the vascular response in both the temporal and parietal cortices relates well with delayed memory. In fact, prior to a Bonferroni correction for multiple comparisons, the negative correlation between mean τ of the vascular response in the parietal cortex and delayed memory was statistically significant. These results are generally consistent with the findings of Richiardi et al., who reported that the speed of the cerebrovascular response was significantly correlated with MMSE scores (Richiardi et al., 2015). In contrast, Rombouts and colleagues failed to find a significant correlation between performance on a visual recognition task and BOLD response delay in 18 AD patients, 28 MCI patients, and 41 elderly controls (Rombouts et al., 2005), however it was suggested that the use of a visual stimulus may have reduced the sensitivity of this test to detect a relationship with memory.

4.2 Implications of Findings

To our knowledge, this study is the first to employ a reproducible and quantifiable hypercapnic stimulus to assess both CVR and the speed of cerebrovascular response to CO_2 in AD and MCI patients. The findings presented in this thesis advance our understanding of vascular contribution to AD, and support an alternative model of how hemodynamic function is altered over the course of the disease.

While our CVR findings conflict with those recently reported by Cantin and colleagues (Cantin et al., 2011), they are not totally unsurprising given the inconsistent reports that preceded it. While is it reasonable to suspect that AD will have an appreciable effect on cerebrovascular

function, it is possible that any loss of the dynamic range of the cerebral vessels caused by AD-related injury may be counteracted by the hallmark cerebral hypoperfusion seen in AD. Simply put, any reduction in CBF due to hypometabolism or the vasoactive properties of amyloid-β could lead to an increase in the dynamic range of the related vessels and, by extension, the cerebrovascular reserve. Therefore, if the effect of hypoperfusion on cerebrovascular reserve is comparable to any simultaneous loss of reserve due to AD-related vascular injury, we may not see a significant change in CVR. With that in mind, our findings in the MCI group may indicate that the magnitude of the cerebrovascular response (as measured by CVR) is not significantly impaired early in the disease.

Our findings in CVR may also provide insight into the nature of cerebral hypoperfusion in AD. No group differences in CVR suggests that at least early in the disease, reduced CBF may not be associated with significant ischemia, otherwise cerebrovascular reserve would have been consumed to maintain ideal resting CBF. However, this concept must be considered cautiously, because hypoperfusion may have important consequences that are overlooked by this line of thought. For instance, hypoperfusion may reduce clearance of amyloid-β, thereby contributing significantly to the pathogenesis and progression of AD, irrespective of ischemia. Also, our study may simply be underpowered to detect subtle changes in CVR.

Perhaps more importantly, a slowed vascular response may directly confer an ischemic burden present in AD by adding a significant delay between neural activity and the resultant increase in CBF to support it. While the associated vascular deficit would be fleeting, the highly dynamic nature of the brain means that these short ischemic “events” may occur with tremendous frequency. Due to the highly protracted latent period of AD, the relatively small burden of these events may gradually accumulate over years or even decades, contributing to the total ischemic burden in AD in a meaningful way. In addition, reduced speed of response in cerebral vessels may partially explain findings of impaired cerebral autoregulation in AD. As reviewed earlier, transgenic mouse models of AD that overexpress APP have been shown to have significantly impaired cerebral autoregulation (Niwa et al., 2002). Furthermore, TCD studies in humans have also found that dynamic cerebral autoregulation in response to postural maneuvers is diminished compared to healthy controls (den Abeelen et al., 2014). Coherence and gain between intravascular pressure and CBF are dependent on the frequency of blood pressure changes (Gonzalez et al., 2014; Hamner et al., 2004). In other words, faster fluctuations in CPP more

readily produce changes in CBF because the cerebral vessels are unable to respond quickly enough. With that, AD patients may become increasingly susceptible to blood pressure-related changes in CBF as the responsivity of their cerebral vessels slows. Lastly, reduced speed of vascular response may also reflect a mechanism for impaired glymphatic flow in AD. A recent study by Peng et al. found that in a mouse model of AD, glymphatic transport was significantly reduced compared to wild-type (Peng et al., 2016). The driving force of glymphatic transport is still not fully understood, but recent evidence indicates that smooth muscle pulsation may drive CSF into the interstitial compartment (Iliff et al., 2013; Iliff et al., 2012). Slowed vasoreactivity may indicate impaired arterial pulsatility and, potentially, poor clearance of amyloid-β and other waste products. Together, these represent three plausible mechanisms by which reduced speed of cerebrovascular response could contribute to the vascular component of AD.

A major objective of this thesis was to assess the potential use of CVR imaging as a complement to current neurologic assessment in AD and MCI patients to ameliorate diagnostic and prognostic accuracy. The motivation for this spawned from a growing belief that our clinical diagnostic framework should better reflect our understanding that the cause of dementia is often multifactorial, with many compounding factors (Scheltens et al., 2016). While in the future, a multitude of biomarkers may be capable of a binary diagnosis of AD, ultimately this may be insufficient for addressing a disease with multiple parallel processes, each with a varying level of contribution. Accordingly, rather than trying to use our clinical tools to fit a patient into a rigid clinical label, our tools should be designed and employed to individually assess each patient's specific pathological features, which would ultimately yield a better characterization of the disease. In this context, our CVR imaging technique is a very promising tool for use in clinical assessment. Firstly, by applying an inspired CO_2 vasodilatory stimulus that acts directly on the cerebral blood vessels, CVR imaging provides a non-invasive, whole-brain measurement of cerebrovascular function that is not confounded by functional alterations in associated neurons and glial cells. In contrast, task fMRI assessments of neurovascular function or functional hyperemia (Machulda et al., 2003; Rombouts et al., 2005) may not provide an accurate measure of vascular function, as these techniques are sensitive to neurovascular uncoupling caused by injury to non-vascular components of the NVU. Moreover, the CVR imaging techniques presented in this thesis produce reliable measurements of CVR and speed of cerebrovascular response, in part due to the well-controlled delivery of a hypercapnic stimulus. A study by

Kassner and colleagues reported excellent between-day reproducibility in a cohort of 19 healthy volunteers (Kassner et al., 2010), while more recently Sobczyk and colleagues demonstrated reproducibility over longer periods of time using a near identical methodology to that used in this thesis (Sobczyk et al., 2016), firmly supporting its use for assessment of disease status over time. Finally, this thesis has demonstrated that our highly refined CVR imaging technique is able to confidently detect changes in the speed of cerebrovascular response associated with progression of AD. This effect could not be explained by differences in age or microangiopathy, and appears to be potentially associated with delayed memory dysfunction, a hallmark feature and strong diagnostic indicator of AD (Welsh et al., 1991), suggesting an intimate association between speed of cerebrovascular response and disease severity. Therefore, CVR imaging may provide clinicians with a valuable tool for specifically characterizing a patient's vascular burden, as well, may be useful in monitoring disease progression, at least from a vascular stand point. Recent studies of vascular medications in mouse models of AD, including those used to combat hypertension and hypercholesterolemia, show considerable promise towards improving cerebrovascular function (Hamel et al., 2016). These drugs have been shown to restore the vasodilatory function of cerebral blood vessels mediated by ion channels on endothelial and VSMCs, and improve bioavailability of NO in the brain. This could help to normalize perfusion in ischemic tissues and may improve neurovascular coupling, which together might slow progression of the disease. In our opinion, CVR imaging may be able to help clinicians assess need for these therapies in the future.

4.3 Strengths and Limitations

The primary strength of this thesis is the well-standardized and reproducible vasodilatory CO_2 stimulus achieved by employing a computerized gas-blender (RespirAct^{TM}, Thornhill Research Inc., Toronto, Canada) to prospectively target P_{ETCO_2}. A consistent stimulus is of paramount importance in CVR imaging as larger increases in P_{aCO_2} yield smaller CVR values upon analysis than smaller increases in P_{aCO_2} because of the sigmoidal relationship between P_{aCO_2} and CBF (Sobczyk et al., 2014). Moreover, by incorporating rebreathing of expired gas, P_{ETCO_2} could be

used as a reliable surrogate measure of P_{aCO_2} in this study. This feature is particularly useful when assessing the speed of vascular response, as quantifying this metric invariably requires the fitting of a response signal to an input signal. Additionally, in this study, each subject received two different CO_2 challenges, (i) an abrupt step change in P_{aCO_2} of 10 mmHg above baseline and (ii) a ramp stimulus spanning from 5 mmHg CO_2 below resting to 15 mmHg above, while remaining normoxic and independent of minute ventilation. This paradigm is ideal for assessing both CVR and the speed of cerebrovascular response. The step change is the optimal design for measuring the speed of cerebrovascular response as a gradual increase in P_{aCO_2} will make it difficult to resolve responses with a time course shorter than that of the stimulus. On the other hand, the ramp component is delay insensitive, allowing for the CVR to be assessed with minimal confound due to delayed responses. In comparison, previous studies have generally used a fixed inspired CO_2 challenge, which results in a biexponential rise in P_{aCO_2} that is influenced by minute ventilation and cannot be accurately quantified by measuring P_{ETCO_2}. Altogether, this limits the accuracy of this method, especially in assessing the speed of cerebrovascular response.

The methodology presented in this thesis has proven to be decidedly robust in assessing CVR and related metrics (Fierstra et al., 2013; Kassner et al., 2010), however there are still several limitations that must be considered. The main limitation of this thesis is related to the study sample. Due to the intensive nature of the imaging studies, subject recruitment is often challenging, which in turn limits the achievable sample size. This is partially the case with this study, however when compared to previous CVR studies in AD patients, the sample size in this study is relatively good and the inclusion of an MCI group is a notable strength. Also, this sample does suffer somewhat from a discrepancy in ages and prevalence of vascular risk factors between the groups. Despite efforts to balance groups, the HC group is on average younger than the MCI group and the prevalence of vascular risk factors was higher in the MCI and AD groups compared to the HC group. These potential confounds were addressed by adding age and Fazekas score to the statistical analyses as covariates of no interest.

Another potential limitation of this thesis is associated with the use of BOLD MRI as a surrogate measure of CBF. It is well understood that BOLD MRI does not directly measure changes in CBF. Instead, BOLD is sensitive to changes in the voxel concentration of deoxyhemoglobin (dHb). Changes in CBF will influence the concentration of dHb, however, changes in $CMRO_2$ and cerebral blood volume can also impact dHb concentration, and by extension, may create a

nonlinearity effect in the BOLD signal or create a between-subject CVR scaling effect due to variable concentrations of dHb at rest. Generally, it is assumed that $CMRO_2$ is unaffected and changes in blood volume are negligible during a hypercapnic stimulus, however this cannot be definitively ruled out in this study. Nevertheless, evidence in healthy subjects indicates that the BOLD signal response to CO_2 stimuli is dominated by the CBF effects (Shiino et al., 2003). As well, Mandell and colleagues found that the BOLD signal remained tightly associated with CBF even in severe steno-occlusive disease (Mandell et al., 2008).

Olfactory-mediated effects of hypercapnia may also be a potential consideration or limitation of this work. In testing vasoreactivity, our methodology employed abrupt and marked changes in inspired concentration of CO_2. Some evidence suggests that hypercapnia may modulate activity in the olfactory cortex by stimulating the trigeminal nerve (Chevy & Klingler, 2014). Given reports of olfactory dysfunction in AD patients, it is plausible that some differences in BOLD response to CO_2 between the AD and HC group may be explainable by differences in olfactory activation. However, the potential contribution of olfactory activation in the vascular response to CO_2 has yet to be fully evaluated and is thought to be minimal.

Finally, both AD and the administration of CO_2 have been found to alter cerebral autoregulation, increasing susceptibility to blood pressure effects on CBF. No blood pressure data was collected in this study to evaluate the influence of potential fluctuations in blood pressure during BOLD CVR MRI. However, our group have performed blood pressure recordings in other CVR studies using identical methodologies and have generally found changes in blood pressure to be minimal (ie. ~10-15 mmHg increase during hypercapnia). Nonetheless, this may constitute a limitation of this thesis.

4.4 Future Directions

First and foremost, a long-term follow-up of MCI patients, including CVR imaging and neuropsychological assessment, would be highly valuable. Only a fraction of individuals diagnosed with MCI will convert to clinical AD over the next 5-10 years. A meta-analysis by

Mitchell and Shiri-Feshki found that the annual conversion rate is approximately 5-10%, and the majority of MCI patients will not progress to dementia even after 10 years of follow-up (Mitchell & Shiri-Feshki, 2009). Interestingly, a second study by Ganguli and colleagues found that in a cohort of 40 patients diagnosed with MCI, over one-third actually reverted to normal at 10-year follow-up (Ganguli et al., 2004). Therefore, it is exceedingly important to be able to accurately identify those who will ultimately progress to clinical AD, illustrating the need for predictive biomarkers supporting conversion from preclinical and MCI stages of AD to full clinical dementia. Follow-up CVR imaging and neuropsychological testing would enable an analysis of the evolution of CVR metrics as they relate to the progression of AD. This may provide valuable insights into the potential contribution of hemodynamic impairment to development of AD and possibly yield a reliable prognosticator for clinical use.

Another potential future study includes transfer function analysis (TFA) of the BOLD signal and P_{ETCO_2} stimulus in an AD cohort, as demonstrated by Duffin and colleagues (Duffin et al., 2015). This analysis yields measures of gain and phase, which reflect the magnitude and speed of the vascular response, respectively. Therefore, carrying out a TFA on BOLD CVR MRI data could be used to verify the findings reported in this thesis, namely a progressive slowing of the cerebrovascular response in AD.

Lastly, BOLD MRI CVR may be useful in assessing the efficacy of vascular therapies in AD and MCI patients. As previously mentioned, several drugs, including those used for hypertension and hypercholesterolemia, have been shown to improve cerebrovascular function in mouse models of AD (Hamel et al., 2016), however their effect in humans is still a matter of considerable debate. BOLD MRI CVR provides a direct physiological measure of cerebrovascular function, thereby making it an ideal tool for investigating the vascular effects of current and future therapies.

CVR speed could also become a diagnostic metric with potentially greater specificity than existing PET tracers for detecting the earliest stages of AD. It is also far less expensive and more available than PET. The need to accurately detect the disease earlier in order to delay or prevent progression will be essential especially when allocating expensive treatments and monitoring their efficacy. Together these observations make a compelling argument for supporting CVR research in this area.

4.5 Conclusions

To my knowledge, this thesis was the first to investigate CVR and the speed of cerebrovascular response to CO_2 in AD and MCI patients using a reliable and quantifiable vasodilatory stimulus, and the first to assess the relationship between speed of response and episodic memory impairment. Importantly, this thesis demonstrates that AD is associated with a progressive slowing of the cerebrovascular response in the temporal and parietal cortex, with additional findings indicating that speed of response may relate to delayed memory performance. The inability to augment CBF in a timely manner may constitute neurovascular uncoupling, and could also impair cerebral autoregulation to abrupt changes in intravascular pressure. Ultimately, these changes may significantly contribute to the ischemic burden present in AD. With that, the findings of this thesis suggest that slowing of the cerebrovascular response may be intimately related with disease severity and, possibly, contribute to progression of the disease.

This thesis is also an important first step in the validation of BOLD CVR imaging as a tool for characterizing each patient's vascular contribution to guide clinicians in developing a treatment strategy. Future research should look to evaluate the evolution of CVR and the speed of vascular response longitudinally over the course of the disease, to assess the utility of CVR imaging as a disease prognosticator. Furthermore, CVR imaging may be valuable in monitoring the efficacy of vascular-based therapies in stabilizing or even rescuing cerebrovascular function.

References

Ahmed, Z., Cooper, J., Murray, T. K., Garn, K., McNaughton, E., Clarke, H., … O'Neill, M. J. (2014). A novel in vivo model of tau propagation with rapid and progressive neurofibrillary tangle pathology: The pattern of spread is determined by connectivity, not proximity. *Acta Neuropathologica*, *127*(5), 667–683.

Ainslie, P. N., & Duffin, J. (2009). Integration of cerebrovascular CO2 reactivity and chemoreflex control of breathing: mechanisms of regulation, measurement, and interpretation. *American Journal of Physiology. Regulatory, Integrative and Comparative Physiology*, *296*(5), R1473-95.

Aizenstein, H. J., Nebes, R. D., Saxton, J. a, Price, J. C., Mathis, C. a, Tsopelas, N. D., … Klunk, W. E. (2008). Frequent amyloid deposition without significant cognitive impairment among the elderly. *Archives of Neurology*, *65*(11), 1509–1517.

Albert, M. S. (1996). Cognitive and neurobiologic markers of early Alzheimer disease. *Proceedings of the National Academy of Sciences of the United States of America*, *93*(24), 13547–13551.

Albert, M. S., DeKosky, S. T., Dickson, D., Dubois, B., Feldman, H. H., Fox, N. C., … Phelps, C. H. (2011). The diagnosis of mild cognitive impairment due to Alzheimer's disease: Recommendations from the National Institute on Aging-Alzheimer's Association workgroups on diagnostic guidelines for Alzheimer's disease. *Alzheimer's and Dementia*, *7*(3), 270–279.

Alonso-Galicia, M., Drummond, H. a., Reddy, K. K., Falck, J. R., & Roman, R. J. (1997). Inhibition of 20-HETE production contributes to the vascular responses to nitric oxide. *Hypertension*, *29*(1 Pt 2), 320–325.

Alonso, A. del C., Zaidi, T., Novak, M., Grundke-Iqbal, I., & Iqbal, K. (2001). Hyperphosphorylation Induces Self-Assembly of Tau into Tangles of Paired Helical Filaments/Shraight Filaments. *Proceedings of the National Academy of Sciences*, *98*(12), 6923–6928.

Alzheimer's Association. (2016). 2016 Alzheimer's disease facts and figures. *Alzheimer's & Dementia : The Journal of the Alzheimer's Association*, *12*(4), 459–509.

Amruthesh, S. C., Boerschel, M. F., McKinney, J. S., Willoughby, K. A., & Ellis, E. F. (1993). Metabolism of Arachidonic Acid to Epoxyeicosatrienoic Acids. Hydroxyeicosatetraenoic Acids, and Prostaglandins in Cultured Rat Hippocampal Astrocytes. *Journal of Neurochemistry*, *61*(1), 150–159.

Apostolova, L. G., Mosconi, L., Thompson, P. M., Green, A. E., Hwang, K. S., Ramirez, A., … de Leon, M. J. (2010). Subregional hippocampal atrophy predicts Alzheimer's dementia in the cognitively normal. *Neurobiology of Aging*, *31*(7), 1077–1088.

Aronoff, J. M., Gonnerman, L. M., Almor, A., Arunachalam, S., Kempler, D., & Andersen, E. S.

(2006). Information content versus relational knowledge: Semantic deficits in patients with Alzheimer's disease. *Neuropsychologia*, *44*(1), 21–35.

Ashford, J. W., & Bayley, P. J. (2013). Retrogenesis: A model of dementia progression in Alzheimer's disease related to neuroplasticity. *Journal of Alzheimer's Disease*, *33*(4), 1191–1193.

Attems, J., & Jellinger, K. A. (2014). The overlap between vascular disease and Alzheimer's disease – lessons from pathology. *BMC Medicine*, *12*(1), 206.

Attwell, D., Buchan, A., Charpak, S., Lauritzen, M., MacVicar, B., & Newman, E. (2010). Glial and neuronal control of brain blood flow. *Nature*, *468*(7321), 232–243.

Attwell, D., & Laughlin, S. B. (2001). An energy budget for signaling in the grey matter of the brain. *Journal of Cerebral Blood Flow and Metabolism : Official Journal of the International Society of Cerebral Blood Flow and Metabolism*, *21*(10), 1133–45.

Baker, H. F., Ridley, R. M., Duchen, L. W., Crow, T. J., & Bruton, C. J. (1993). Evidence for the experimental transmission of cerebral beta-amyloidosis to primates. *International Journal of Experimental Pathology*, *74*(5), 441–54.

Ballatore, C., Lee, V., & J, T. (2007). Tau-mediated neurodegeneration in Alzheimer's disease and related disorders. *Nature Reviews. Neuroscience*, *8*(9), 663–672.

Balucani, C., Viticchi, G., Falsetti, L., & Silvestrini, M. (2012). Cerebral hemodynamics and cognitive performance in bilateral asymptomatic carotid stenosis. *Neurology*, *79*(17), 1788–1795.

Banzett, R. B., Garcia, R. T., & Moosavi, S. H. (2000). Simple contrivance "clamps" end-tidal PCO(2) and PO(2) despite rapid changes in ventilation. *Journal of Applied Physiology*, *88*(5), 1597–600.

Bär, K. J., Boettger, M. K., Seidler, N., Mentzel, H. J., Terborg, C., & Sauer, H. (2007). Influence of galantamine on vasomotor reactivity in alzheimer's disease and vascular dementia due to cerebral microangiopathy. *Stroke*, *38*(12), 3186–3192.

Baracchini, C., Mazzalai, F., Gruppo, M., Lorenzetti, R., Ermani, M., & Ballotta, E. (2012). Carotid endarterectomy protects elderly patients from cognitive decline: A prospective study. *Surgery*, *151*(1), 99–106.

Barker, W. W., Luis, C. a, Kashuba, A., Luis, M., Harwood, D. G., Loewenstein, D., … Duara, R. (2002). Relative frequencies of Alzheimer disease, Lewy body, vascular and frontotemporal dementia, and hippocampal sclerosis in the State of Florida Brain Bank. *Alzheimer Disease and Associated Disorders*, *16*(4), 203–212.

Barnes, J., Bartlett, J. W., van de Pol, L. A., Loy, C. T., Scahill, R. I., Frost, C., … Fox, N. C. (2009). A meta-analysis of hippocampal atrophy rates in Alzheimer's disease. *Neurobiology of Aging*, *30*(11), 1711–1723.

Bayliss, W. M. (1902). On the local reactions of the arterial wall to changes of internal pressure. *The Journal of Physiology*, *28*(3), 220–31.

Beach, T. G., Monsell, S. E., Phillips, L. E., & Kukull, W. (2012). Accuracy of the Clinical Diagnosis of Alzheimer Disease at National Institute on Aging Alzheimer Disease Centers, 2005–2010. *Journal of Neuropathology & Experimental Neurology*, *71*(4), 266–273.

Beach, T. G., Wilson, J. R., Sue, L. I., Newell, A., Poston, M., Cisneros, R., … Roher, A. E. (2007). Circle of Willis atherosclerosis: Association with Alzheimer's disease, neuritic plaques and neurofibrillary tangles. *Acta Neuropathologica*, *113*(1), 13–21.

Bell, R. D., Deane, R., Chow, N., Long, X., Sagare, A., Singh, I., … Zlokovic, B. V. (2009). SRF and myocardin regulate LRP-mediated amyloid-β clearance in brain vascular cells. *Nature Cell Biology*, *11*(2), 143–153.

Berger, M. G., Vandier, C., Bonnet, P., Jackson, W. F., & Rusch, N. J. (1998). Intracellular acidosis differentially regulates KV channels in coronary and pulmonary vascular muscle. *The American Journal of Physiology*, *275*(37), H1351–H1359.

Berliocchi, L., Bano, D., & Nicotera, P. (2005). Ca2+ signals and death programmes in neurons. *Philosophical Transactions of the Royal Society of London. Series B, Biological Sciences*, *360*(1464), 2255–8.

Beyreuther, K., & Masters, C. L. (1991). Amyloid precursor protein (APP) and beta A4 amyloid in the etiology of Alzheimer's disease: precursor-product relationships in the derangement of neuronal function. *Brain Pathology*, *1*(4), 241–251.

Binnewijzend, M. a a, Kuijer, J. P. a, Benedictus, M. R., van der Flier, W. M., Wink, A. M., Wattjes, M. P., … Barkhof, F. (2013). Cerebral blood flow measured with 3D pseudocontinuous arterial spin-labeling MR imaging in Alzheimer disease and mild cognitive impairment: a marker for disease severity. *Radiology*, *267*(1), 221–30.

Bloom, G. S. (2014). Amyloid-β and Tau. *JAMA Neurology*, *71*(4), 505.

Bobinski, M., de Leon, M. J., Convit, A., De Santi, S., Wegiel, J., Tarshish, C. Y., … Wisniewski, H. M. (1999). MRI of entorhinal cortex in mild Alzheimer's disease. *Lancet (London, England)*, *353*(9146), 38–40.

Bookheimer, S. Y., Strojwas, M. H., Cohen, M. S., Saunders, A. M., Pericak-Vance, M. A., Mazziotta, J. C., & Small, G. W. (2000). Patterns of brain activation in people at risk for Alzheimer's disease. *N.Engl.J Med*, *343*(7), 450–456.

Braak, H., & Braak, E. (1991). Neuropathological stageing of Alzheimer-related changes. *Acta Neuropathologica*, *82*(4), 239–59.

Braak, H., & Braak, E. (1997). Frequency of stages of Alzheimer-related lesions in different age categories. *Neurobiology of Aging*, *18*(4), 351–357.

Braak, H., Braak, E., & Bohl, J. (1993). Staging of Alzheimer-related cortical destruction.

European Neurology, *33*(6), 403–8.

Braak, H., & Del Tredici, K. (2011). The pathological process underlying Alzheimer's disease in individuals under thirty. *Acta Neuropathologica*, *121*(2), 171–181.

Braak, H., & Del Tredici, K. (2014). *Neuroanatomy and Pathology of Sporadic Alzheimer's Disease*. Springer International Publishing.

Brayden, J. E., & Nelson, M. T. (1992). Regulation of arterial tone by activation of calcium-dependent potassium channels. *Science (New York, N.Y.)*, *256*(5056), 532–535.

Brian, J. E. (1998). Carbon Dioxide and the Cerebral Circulation. *Anesthesiology*, *88*(5), 1365–1386.

Brodal, P. (2010). The central nervous system: structure and function. New York: Oxford University Press.

Burgmans, S., Van De Haar, H. J., Verhey, F. R. J., & Backes, W. H. (2013). Amyloid-Beta interacts with blood-brain barrier function in dementia: A systematic review. *Journal of Alzheimer's Disease*, *35*(4), 859–873.

Cantin, S., Villien, M., Moreaud, O., Tropres, I., Keignart, S., Chipon, E., … Krainik, A. (2011). Impaired cerebral vasoreactivity to CO 2 in Alzheimer's disease using BOLD fMRI. *NeuroImage*, *58*(2), 579–587.

Carmichael, O. T., Kuller, L. H., Lopez, O. L., Thompson, P. M., Dutton, R. A., Lu, A., … Becker, J. T. (2007). Ventricular volume and dementia progression in the Cardiovascular Health Study. *Neurobiology of Aging*, *28*(3), 389–397.

Carvalho, C., Correia, S. C., Santos, R. X., Cardoso, S., Moreira, P. I., Clark, T. A., … Perry, G. (2009). Role of mitochondrial-mediated signaling pathways in Alzheimer disease and hypoxia. *Journal of Bioenergetics and Biomembranes*, *41*(5), 433–440.

Chalmers, K., Wilcock, G. K., & Love, S. (2003). APOE e4 influences the pathological phenotype of Alzheimer's disease by favouring cerebrovascular over parenchymal accumulation of ABeta protein. *Neuropathology and Applied Neurobiology*, *29*(3), 231–238.

Chandel, N. S., McClintock, D. S., Feliciano, C. E., Wood, T. M., Melendez, J. A., Rodriguez, A. M., & Schumacker, P. T. (2000). Reactive oxygen species generated at mitochondrial Complex III stabilize hypoxia-inducible factor-1?? during hypoxia: A mechanism of O2 sensing. *Journal of Biological Chemistry*, *275*(33), 25130–25138.

Chen, P., Ratcliff, G., SH, B., JA, C., ST, D., & Ganguli, M. (2001). Patterns of cognitive decline in presymptomatic alzheimer disease: A prospective community study. *Archives of General Psychiatry*, *58*(9), 853–858.

Chesler, M. (2003). Regulation and Modulation of pH in the Brain. *Physiological Reviews*, *83*(4), 1183–1221.

Chevy, Q., & Klingler, E. (2014). Odorless Trigeminal Stimulus CO₂ Triggers Response in the Olfactory Cortex. *The Journal of Neuroscience*, *34*(2), 341 LP-342.

Cipolla, M.J. (2009). The Cerebral Circulation. San Rafael, CA: Morgan & Claypool Life Sciences.

Chow, N., Bell, R. D., Deane, R., Streb, J. W., Chen, J., Brooks, A., … Zlokovic, B. V. (2007). Serum response factor and myocardin mediate arterial hypercontractility and cerebral blood flow dysregulation in Alzheimer's phenotype. *Proceedings of the National Academy of Sciences of the United States of America*, *104*(3), 823–828.

Chui, H. C., Zarow, C., Mack, W. J., Ellis, W. G., Zheng, L., Jagust, W. J., … Vinters, H. V. (2006). Cognitive impact of subcortical vascular and Alzheimer's disease pathology. *Annals of Neurology*, *60*(6), 677–687.

Chun, T. H., Itoh, H., Ogawa, Y., Tamura, N., Takaya, K., Igaki, T., … Nakao, K. (1997). Shear stress augments expression of C-type natriuretic peptide and adrenomedullin. *Hypertension*, *29*(6), 1296–302.

Claassen, J. A. H. R., Diaz-Arrastia, R., Martin-Cook, K., Levine, B. D., & Zhang, R. (2009). Altered Cerebral Hemodynamics in Early Alzheimer Disease: A Pilot Study Using Transcranial Doppler. *Journal of Alzheimer's Disease : JAD*, *17*(3), 621–629.

Claassen, J. A., & Zhang, R. (2011). Cerebral autoregulation in Alzheimer's disease. *Journal of Cerebral Blood Flow & Metabolism*, *31*(7), 1572–1577.

Clavaguera, F., Bolmont, T., Crowther, R. A., Abramowski, D., Frank, S., Probst, A., … Tolnay, M. (2009). Transmission and spreading of tauopathy in transgenic mouse brain. *Nature Cell Biology*, *11*(7), 909–13.

Cohen, R. & Sweet, L. (2011). Brain imaging in behavioral medicine and clinical neuroscience. New York London: Springer.

Conklin, J., Fierstra, J., Crawley, A. P., Han, J. S., Poublanc, J., Silver, F. L., … Mikulis, D. J. (2011). Mapping white matter diffusion and cerebrovascular reactivity in carotid occlusive disease. *Neurology*, *77*(5), 431–8.

Cox, R. W. (1996). AFNI: Software for Analysis and Visualization of Functional Magnetic Resonance Neuroimages. *Computers and Biomedical Research*, *29*(3), 162–173.

Crawford, F., Suo, Z., Fang, C., Sawar, A., Su, G., Arendash, G., & Mullan, M. (1997). The vasoactivity of A beta peptides. *Ann.N.Y.Acad.Sci.*, *826*, 35–46.

Dai, W., Lopez, O. L., Carmichael, O. T., Becker, J. T., Kuller, L. H., & Gach, H. M. (2009). Mild Cognitive Impairment and Alzheimer Disease: Patterns of Altered Cerebral Blood Flow at MR Imaging. *Radiology*, *250*(3), 856–866.

Davis, T. L., Kwong, K. K., Weisskoff, R. M., & Rosen, B. R. (1998). Calibrated functional

MRI: mapping the dynamics of oxidative metabolism. *Proceedings of the National Academy of Sciences of the United States of America*, *95*(4), 1834–9.

de Flores, R., la Joie, R., & Chetelat, G. (2015). Review Structural Imaging of Hippocampal Subfields in Healthy Aging and Alzheimer ' S Disease. *Neuroscience*, *309*, 29–50.

de la Torre, J. C. (2010). Vascular risk factor detection and control may prevent Alzheimer's disease. *Ageing Research Reviews*, *9*(3), 218–225.

de Leon, M. J., Li, Y., Okamura, N., Tsui, W. H., Saint-Louis, L. A., Glodzik, L., … Rusinek, H. (2017). CSF clearance in Alzheimer Disease measured with dynamic PET 2) Running title: Impaired CSF clearance in. *Journal of Nuclear Medicine*, jnumed.116.187211.

Delis, D. C., Massman, P. J., Butters, N., Salmon, D. P., Cermak, L. S., & Kramer, J. H. (1991). Profiles of Demented and Amnesic Patients on the California Verbal Learning Test: Implications for the Assessment of Memory Disorders. *Psychological Assessment; A Journal of Consulting and Clinical Psychology*, *3*(1), 19–26.

den Abeelen, A. S., Lagro, J., van Beek, A. H., & Claassen, J. A. (2014). Impaired cerebral autoregulation and vasomotor reactivity in sporadic Alzheimer's disease. *Curr Alzheimer Res*, *11*(1), 11–17.

Derdeyn, C. P., Videen, T. O., Fritsch, S. M., Carpenter, D. a., Grubb, R. L., & Powers, W. J. (1999). Compensatory mechanisms for chronic cerebral hypoperfusion in patients with carotid occlusion. *Stroke; a Journal of Cerebral Circulation*, *30*(5), 1019–1024.

Dickey, P. S., Kailasnath, P., Bloomgarden, G., Goodrich, I., & Chaloupka, J. (1996). Computer modeling of cerebral blood flow following internal carotid artery occlusion. *Neurological Research*, *18*(3), 259–266.

Dietrich, H. H., & Dacey Jr, R. G. (1994). Effects of extravascular acidification and extravascular alkalinization on constriction and depolarization in rat cerebral arterioles in vitro. *Journal of Neurosurgery*, *81*(3), 437–442.

Dinggang Shen, D., & Davatzikos, C. (2002). HAMMER: hierarchical attribute matching mechanism for elastic registration. *IEEE Transactions on Medical Imaging*, *21*(11), 1421–1439.

Du, A., Schuff, N., & Amend, D. (2001). Magnetic resonance imaging of the entorhinal cortex and hippocampus in mild cognitive impairment and Alzheimer's disease. *Journal of Neurology, Neurosurgery & Psychiatry*, *71*(1), 441–447.

Du, A. T., Jahng, G. H., Hayasaka, S., Kramer, J. H., Rosen, H. J., Gorno-Tempini, M. L., … Schuff, N. (2006). Hypoperfusion in frontotemporal dementia and Alzheimer disease by arterial spin labeling MRI. *Neurology*, *67*(7), 1215–1220.

Dubois, B., Feldman, H. H., Jacova, C., Hampel, H., Molinuevo, J. L., Blennow, K., … Cummings, J. L. (2014). Advancing research diagnostic criteria for Alzheimer's disease: The IWG-2 criteria. *The Lancet Neurology*, *13*(6), 614–629.

Duchemin, S., Boily, M., Sadekova, N., & Girouard, H. (2012). The complex contribution of NOS interneurons in the physiology of cerebrovascular regulation. *Frontiers in Neural Circuits*, *6*(August), 51.

Duffin, J., Sobczyk, O., Crawley, A. P., Poublanc, J., Mikulis, D. J., & Fisher, J. A. (2015). The dynamics of cerebrovascular reactivity shown with transfer function analysis. *NeuroImage*, *114*, 207–216.

Duyckaerts, C., & Hauw, J. J. (1997). Diagnosis and staging of Alzheimer disease. *Neurobiology of Aging*, *18*(4 SUPPL.), S33-42.

Eberling, J. L., Jagust, W. J., Reed, B. R., & Baker, M. G. (1992). Reduced temporal lobe blood flow in alzheimer's disease. *Neurobiology of Aging*, *13*(4), 483–491.

Eisele, Y. S., Bolmont, T., Heikenwalder, M., Langer, F., Jacobson, L. H., Yan, Z.-X., … Jucker, M. (2009). Induction of cerebral beta-amyloidosis: intracerebral versus systemic Abeta inoculation. *Proceedings of the National Academy of Sciences of the United States of America*, *106*(31), 12926–12931.

Erickson, M. A., & Banks, W. A. (2013). Blood-brain barrier dysfunction as a cause and consequence of Alzheimer's disease. *Journal of Cerebral Blood Flow and Metabolism : Official Journal of the International Society of Cerebral Blood Flow and Metabolism*, *33*(10), 1500–13.

Esiri, M. M., Nagy, Z., Smith, M. Z., Barnetson, L., Smith, A. D., & Joachim, C. (1999). Cerebrovascular disease and threshold for dementia in the early stages of Alzheimer's disease. *Lancet*, *354*(9182), 919–920.

Fagan, A. M., Mintun, M. A., Mach, R. H., Lee, S. Y., Dence, C. S., Shah, A. R., … Holtzman, D. M. (2006). Inverse relation between in vivo amyloid imaging load and cerebrospinal fluid Abeta;42 in humans. *Annals of Neurology*, *59*(3), 512–519.

Fang, H., Zhang, L. F., Meng, F. T., Du, X., & Zhou, J. N. (2010). Acute hypoxia promote the phosphorylation of tau via ERK pathway. *Neuroscience Letters*, *474*(3), 173–177.

Farkas, E., & Luiten, P. G. M. (2001). Cerebral microvascular pathology in aging and Alzheimer's disease. *Progress in Neurobiology*, *64*(6), 575–611.

Farrall, A. J., & Wardlaw, J. M. (2009). Blood-brain barrier: Ageing and microvascular disease - systematic review and meta-analysis. *Neurobiology of Aging*, *30*(3), 337–352.

Fazekas, F., Chawluk, J. B., & Alavi, A. (1987). MR signal abnormalities at 1.5 T in Alzheimer's dementia and normal aging. *American Journal of Neuroradiology*, *8*(3), 421–426.

Ferri, C. P., Prince, M., Brayne, C., Brodaty, H., Fratiglioni, L., Ganguli, M., … Scazufca, M. (2005). Global prevalence of dementia: A Delphi consensus study. *Lancet*, *366*(9503), 2112–2117.

Fiala, J. C. (2007). Mechanisms of amyloid plaque pathogenesis. *Acta Neuropathologica*, *114*(6), 551–571.

Fierstra, J., Maclean, D. B., Fisher, J. A., Han, J. S., Mandell, D. M., Conklin, J., … Tymianski, M. (2011). Surgical Revascularization Reverses Cerebral Cortical Thinning in Patients With Severe Cerebrovascular Steno-Occlusive Disease. *Stroke*, *42*(6), 1631 LP-1637.

Fierstra, J., Poublanc, J., Han, J. S., Silver, F., Tymianski, M., Crawley, A. P., … Mikulis, D. J. (2010). Steal physiology is spatially associated with cortical thinning. *Journal of Neurology, Neurosurgery, and Psychiatry*, *81*(3), 290–293.

Fierstra, J., Sobczyk, O., Battisti-Charbonney, A., Mandell, D. M., Poublanc, J., Crawley, A. P., … Fisher, J. A. (2013). Measuring cerebrovascular reactivity: what stimulus to use? *The Journal of Physiology*, *591*(23), 5809–21.

Fischl, B. (2012). FreeSurfer. *NeuroImage*, *62*(2), 774–781.

Fisher, J. A. (2016). The CO2 stimulus for cerebrovascular reactivity: Fixing inspired concentrations vs. targeting end-tidal partial pressures. *Journal of Cerebral Blood Flow & Metabolism*, *36*(6), 1004–1011.

Fleming, I. (2014). The Pharmacology of the Cytochrome P450 Epoxygenase/Soluble Epoxide Hydrolase Axis in the Vasculature and Cardiovascular Disease. *Pharmacol. Rev.*, *66*(4), 1106–1140.

Fox, P. T., & Raichle, M. E. (1986). Focal physiological uncoupling of cerebral blood flow and oxidative metabolism during somatosensory stimulation in human subjects. *Proceedings of the National Academy of Sciences of the United States of America*, *83*(4), 1140–1144.

Freedman, M., Leach, L., Stokes, K. A., Goldberg, Y., Alhaj, M., Greenberg, B. D., … Tang-Wai, D. F. (2016). Behavioural Neurology Assessment – Revised: Validation in Amnestic Mild Cognitive Impairment (Amci). *Alzheimer's & Dementia*, *12*(7), P1160–P1161.

Friedhoff, P., von Bergen, M., Mandelkow, E.-M., & Mandelkow, E. (2000). Structure of tau protein and assembly into paired helical filaments. *Biochimica et Biophysica Acta (BBA) - Molecular Basis of Disease*, *1502*(1), 122–132.

Fujimoto, Y., Uno, E., & Sakuma, S. (2004). Effects of reactive oxygen and nitrogen species on cyclooxygenase-1 and -2 activities. *Prostaglandins Leukotrienes and Essential Fatty Acids*, *71*(5), 335–340.

Ganguli, M., Dodge, H. H., Shen, C., & DeKosky, S. T. (2004). Mild cognitive impairment, amnestic type: an epidemiologic study. *Neurology*, *63*(1), 115–121.

Garthwaite, J., & Boulton, C. L. (1995). Nitric Oxide Signaling in the Central Nervous System. *Annu. Rev. Physiol*, *57*(1), 683–706.

Gilbert, J. J., & Vinters, H. V. (1983). Cerebral amyloid angiopathy: incidence and complications in the aging brain. II. The Distribution of Amyloid Vascular Changes. *Stroke*,

14(6), 915–923.

Glenner, G. G., & Wong, C. W. (1984). Alzheimer's disease: Initial report of the purification and characterization of a novel cerebrovascular amyloid protein. *Biochemical and Biophysical Research Communications*, *120*(3), 885–890.

Glodzik, L., Randall, C., Rusinek, H., & De Leon, M. J. (2013). Cerebrovascular reactivity to carbon dioxide in alzheimer's disease. *Journal of Alzheimer's Disease*, *35*(3), 427–440.

Goate A, Chartier-Harlin MC, Mullan M, Brown J, Crawford F, Fidani L, Giuffra L, Haynes A, Irving N, James L, et al. (1991). Segregation of a missense mutation in the amyloid precursor protein gene with familial Alzheimer's disease. *Nature*, *349*(6311), 704–6.

Goedert, M. (2015). NEURODEGENERATION. Alzheimer's and Parkinson's diseases: The prion concept in relation to assembled Abeta, tau, and alpha-synuclein. *Science*, *349*(6248), 1255555.

Goedert, M., Jakes, R., Crowther, R. a, Six, J., Lübke, U., Vandermeeren, M., … Lee, V. M. (1993). The abnormal phosphorylation of tau protein at Ser-202 in Alzheimer disease recapitulates phosphorylation during development. *Proceedings of the National Academy of Sciences of the United States of America*, *90*(11), 5066–5070.

Goldblum, M. C., Gomez, C. M., Dalla Barba, G., Boller, F., Deweer, B., Hahn, V., & Dubois, B. (1998). The influence of semantic and perceptual encoding onb recognition memory in Alzheimer's disease. *Neuropsychologia*, *36*(8), 717–729.

Golding, E. M., Marrelli, S. P., You, J., & Bryan, R. M. (2002). Endothelium-derived hyperpolarizing factor in the brain: a new regulator of cerebral blood flow? *Stroke; a Journal of Cerebral Circulation*, *33*(3), 661–3.

Gong, Y., Chang, L., Viola, K. L., Lacor, P. N., Lambert, M. P., Finch, C. E., … Klein, W. L. (2003). Alzheimer's disease-affected brain: Presence of oligomeric Aβ ligands (ADDLs) suggests a molecular basis for reversible memory loss. *Proceedings of the National Academy of Sciences of the United States of America*, *100*(18), 10417–10422.

Gonzalez, M. J., Miranda-Massari, J. R., Berdiel, M. J., Duconge, J., Rodr??guez-L??pez, J. L., Hunninghake, R., & Cobas-Rosario, V. J. (2014). High dose intraveneous Vitamin C and chikungunya fever: A case report. *Journal of Orthomolecular Medicine*, *29*(4), 154–156.

Goode, S. D., Krishan, S., Alexakis, C., Mahajan, R., & Auer, D. P. (2009). Precision of cerebrovascular reactivity assessment with use of different quantification methods for hypercapnia functional MR imaging. *American Journal of Neuroradiology*, *30*(5), 972–977.

Gordon, G. R. J., Choi, H. B., Rungta, R. L., Ellis-Davies, G. C. R., & MacVicar, B. A. (2008). Brain metabolism dictates the polarity of astrocyte control over arterioles. *Nature*, *456*(7223), 745–9.

Gorelick, P. B., Scuteri, A., Black, S. E., Decarli, C., Greenberg, S. M., Iadecola, C., … Seshadri, S. (2011). Vascular contributions to cognitive impairment and dementia: A

statement for healthcare professionals from the American Heart Association/American Stroke Association. *Stroke*, *42*(9), 2672–2713.

Greenberg, S. M., Gurol, M. E., Rosand, J., & Smith, E. E. (2004). Amyloid angiopathy-related vascular cognitive impairment. *Stroke*, *35*(11 SUPPL. 1), 2616–2619.

Grimmer, T., Faust, M., Auer, F., Alexopoulos, P., Förstl, H., Henriksen, G., … Kurz, A. (2012). White matter hyperintensities predict amyloid increase in Alzheimer's disease. *Neurobiology of Aging*, *33*(12), 2766–2773.

Grundke-Iqbal, I., Iqbal, K., Tung, Y. C., Quinlan, M., Wisniewski, H. M., & Binder, L. I. (1986). Abnormal phosphorylation of the microtubule-associated protein tau (tau) in Alzheimer cytoskeletal pathology. *Proceedings of the National Academy of Sciences of the United States of America*, *83*(13), 4913–7.

Gurol, M. E., Irizarry, M. C., Smith, E. E., Raju, S., Diaz-Arrastia, R., Bottiglieri, T., … Greenberg, S. M. (2006). Plasma -amyloid and white matter lesions in AD, MCI, and cerebral amyloid angiopathy. *Neurology*, *66*(1), 23–29.

Haass, C., Kaether, C., Thinakaran, G., & Sisodia, S. (2012). Trafficking and proteolytic processing of APP. *Cold Spring Harbor Perspectives in Medicine*, *2*(5), a006270.

Haass, C., Koo, E. H., Mellon, A., Hung, a Y., & Selkoe, D. J. (1992). Targeting of cell-surface beta-amyloid precursor protein to lysosomes: alternative processing into amyloid-bearing fragments. *Nature*, *357*(6378), 500–3.

Haass, C., Lemere, C. a., Capell, A., Citron, M., Seubert, P., Schenk, D., … Selkoe, D. J. (1995). The Swedish mutation causes early-onset Alzheimer's disease by β-secretase cleavage within the secretory pathway. *Nature Medicine*, *1*(12), 1291–1296.

Hall, C. N., Reynell, C., Gesslein, B., Hamilton, N. B., Mishra, A., Sutherland, B. A., … Attwell, D. (2014). Capillary pericytes regulate cerebral blood flow in health and disease. *Nature*, *508*(7494), 55–60.

Hamel, E., Royea, J., Ongali, B., & Tong, X.-K. (2016). Neurovascular and Cognitive failure in Alzheimer's Disease: Benefits of Cardiovascular Therapy. *Cellular and Molecular Neurobiology*, *36*(2), 219–232.

Hamner, J. W., Cohen, M. A., Mukai, S., Lipsitz, L. A., & Taylor, J. A. (2004). Spectral indices of human cerebral blood flow control: responses to augmented blood pressure oscillations. *The Journal of Physiology*, *559*(Pt 3), 965–73.

Han, J. S., Abou-Hamden, A., Mandell, D. M., Poublanc, J., Crawley, A. P., Fisher, J. A., … Tymianski, M. (2011). Impact of extracranial-intracranial bypass on cerebrovascular reactivity and clinical outcome in patients with symptomatic moyamoya vasculopathy. *Stroke*, *42*(11), 3047–3054.

Hardy, J., & Selkoe, D. J. (2002). The amyloid hypothesis of Alzheimer's disease: progress and problems on the road to therapeutics. *Science (New York, N.Y.)*, *297*(5580), 353–6.

Herzig, M. C., Van Nostrand, W. E., & Jucker, M. (2006). Mechanism of cerebral beta-amyloid angiopathy: murine and cellular models. *Brain Pathology (Zurich, Switzerland)*, *16*(1), 40–54.

Hill, R. A., Tong, L., Yuan, P., Murikinati, S., Gupta, S., & Grutzendler, J. (2015). Regional Blood Flow in the Normal and Ischemic Brain Is Controlled by Arteriolar Smooth Muscle Cell Contractility and Not by Capillary Pericytes. *Neuron*, *87*(1), 95–110.

Hodges, J. R., Salmon, D. P., & Butters, N. (1991). The nature of the naming deficit in alzheimer's and huntington's disease. *Brain*, *114*(4), 1547–1558.

Honig, L. S., Kukull, W., & Mayeux, R. (2005). Atherosclerosis and AD: analysis of data from the US National Alzheimer's Coordinating Center. *Neurology*, *64*(3), 494–500.

Hossmann, K. ???A. (1994). Viability thresholds and the penumbra of focal ischemia. *Annals of Neurology*, *36*(4), 557–565.

Hsia, A. Y., Masliah, E., McConlogue, L., Yu, G. Q., Tatsuno, G., Hu, K., … Mucke, L. (1999). Plaque-independent disruption of neural circuits in Alzheimer's disease mouse models. *Proc. Natl. Acad. Sci. USA*, *96*(6), 3228–3233.

Hsieh, H., Boehm, J., Sato, C., Iwatsubo, T., Tomita, T., Sisodia, S., & Malinow, R. (2006). AMPAR Removal Underlies A??-Induced Synaptic Depression and Dendritic Spine Loss. *Neuron*, *52*(5), 831–843.

Hughes, T. M., Kuller, L. H., Barinas-Mitchell, E. J. M., Mackey, R. H., McDade, E. M., Klunk, W. E., … Lopez, O. L. (2013). Pulse wave velocity is associated with β-amyloid deposition in the brains of very elderly adults. *Neurology*, *81*(19), 1711–1718.

Hughes, T. M., Kuller, L. H., Barinas-Mitchell, E. J. M., McDade, E. M., Klunk, W. E., Cohen, A. D., … Lopez, O. L. (2014). Arterial stiffness and β-amyloid progression in nondemented elderly adults. *JAMA Neurology*, *71*(5), 562–8.

Iadecola, C. (2004). Neurovascular regulation in the normal brain and in Alzheimer's disease. *Nature Reviews. Neuroscience*, *5*(5), 347–360.

Iadecola, C., & Nedergaard, M. (2007). Glial regulation of the cerebral microvasculature. *Nature Neuroscience*, *10*(11), 1369–76.

Iadecola, C., Yang, G., Ebner, T. J., & Chen, G. (1997). Local and propagated vascular responses evoked by focal synaptic activity in cerebellar cortex. *Journal of Neurophysiology*, *78*(2), 651–659.

Iadecola, C., Zhang, F., Niwa, K., Eckman, C., Turner, S. K., Fischer, E., … Carlson, G. A. (1999). SOD1 rescues cerebral endothelial dysfunction in mice overexpressing amyloid precursor protein. *Nature Neuroscience*, *2*(2), 157–161.

Ignarro, L. J., Cirino, G., Casini, A., & Napoli, C. (1999). Nitric oxide as a signaling molecule in the vascular system: an overview. *Journal of Cardiovascular Pharmacology*, *34*(6), 879–86.

Iliff, J. J., & Nedergaard, M. (2013). Is there a cerebral lymphatic system? *Stroke*, *44*(SUPPL. 1), S93–S95.

Iliff, J. J., Wang, M., Liao, Y., Plogg, B. A., Peng, W., Gundersen, G. A., … Nedergaard, M. (2012). A Paravascular Pathway Facilitates CSF Flow Through the Brain Parenchyma and the Clearance of Interstitial Solutes, Including Amyloid β. *Science Translational Medicine*, *4*(147), 147ra111.

Iliff, J. J., Wang, M., Zeppenfeld, D. M., Venkataraman, A., Plog, B. A., Liao, Y., … Nedergaard, M. (2013). Cerebral Arterial Pulsation Drives Paravascular CSF-Interstitial Fluid Exchange in the Murine Brain. *Journal of Neuroscience*, *33*(46), 18190–18199.

Imran, M. B., Kawashima, R., Awata, S., Sato, K., Kinomura, S., Ono, S., … Fukuda, H. (1999). Tc-99m HMPAO SPECT in the evaluation of Alzheimer's disease: correlation between neuropsychiatric evaluation and CBF images. *Journal of Neurology, Neurosurgery, and Psychiatry*, *66*(2), 228–32.

Ito, S., Mardimae, A., Han, J., Duffin, J., Wells, G., Fedorko, L., … Fisher, J. A. (2008). Non-invasive prospective targeting of arterial P CO 2 in subjects at rest. *The Journal of Physiology*, *586*(15), 3675–3682.

Jack, C. R., Knopman, D. S., Jagust, W. J., Petersen, R. C., Weiner, M. W., Aisen, P. S., … Trojanowski, J. Q. (2013). Tracking pathophysiological processes in Alzheimer's disease: An updated hypothetical model of dynamic biomarkers. *The Lancet Neurology*, *12*(2), 207–216.

Jack, C. R., Petersen, R. C., O'Brien, P. C., & Tangalos, E. G. (1992). MR-based hippocampal volumetry in the diagnosis of Alzheimer's disease. *Neurology*, *42*(1), 183–188.

Jack, C. R., Petersen, R. C., Xu, Y. C., Waring, S. C., O'Brien, P. C., Tangalos, E. G., … Kokmen, E. (1997). Medial temporal atrophy on MRI in normal aging and very mild Alzheimer's disease. *Neurology*, *49*(3), 786–794.

Jack Jr, C. R., Petersen, R. C., Xu, Y. C., Waring, S. C., O'Brien, P. C., Tangalos, E. G., … Kokmen, E. (1997). Medial temporal atrophy on MRI in normal aging and very mild Alzheimer's disease. *Neurology*, *49*(3), 786–794.

Jackman, K., & Iadecola, C. (2014). Neurovascular Regulation in the Ischemic Brain. *Antioxidants & Redox Signaling*, *0*(0), 1–12.

Jackson, W. F. (2005). Potassium Channels in the Peripheral Microcirculation. *Microcirculation (New York, N.Y. : 1994)*, *12*(1), 113–127.

Jacobs, D. (1990). Intrusion Errors in the Figural Memory of and Huntington ' s Disease Patients with Alzheimer ' s. *Archives of Clinical Neuropsychology*, *5*(1), 49–57.

Jacobson, S., & Marcus, E. M. (2008). Neuroanatomy for the neuroscientist. *Neuroanatomy for the Neuroscientist*, 1–498.

Jagust, W. J., Bandy, D., Chen, K., Foster, N. L., Landau, S. M., Mathis, C. A., … Koeppe, R. A. (2010). The Alzheimer's Disease Neuroimaging Initiative positron emission tomography core. *Alzheimer's and Dementia*, *6*(3), 221–229.

Jagust, W. J., Eberling, J. L., Reed, B. R., Mathis, C. A., & Budinger, T. F. (1997). Clinical studies of cerebral blood flow in Alzheimer's disease. *Annals of the New York Academy of Sciences*, *826*, 254–62.

Jellinger, K. a, & Attems, J. (2003). Incidence of cerebrovascular lesions in Alzheimer's disease: a postmortem study. *Acta Neuropathologica*, *105*(1), 14–7.

Johnson, D. K., Storandt, M., Morris, J. C., & Galvin, J. E. (2009). Longitudinal study of the transition from healthy aging to Alzheimer disease. *Archives of Neurology*, *66*(10), 1254–9.

Johnson, N. A., Jahng, G. H., Weiner, M. W., Miller, B. L., Chui, H. C., Jagust, W. J., … Schuff, N. (2005). Pattern of cerebral hypoperfusion in Alzheimer disease and mild cognitive impairment measured with arterial spin-labeling MR imaging: initial experience. *Radiology*, *234*(3), 851–859.

Johnston, M., Zakharov, A., Papaiconomou, C., Salmasi, G., & Armstrong, D. (2004). Evidence of connections between cerebrospinal fluid and nasal lymphatic vessels in humans, non-human primates and other mammalian species. *Cerebrospinal Fluid Research*, *1*(1), 2.

Jones, E. G. (1970). On the mode of entry of blood vessels into the cerebral cortex. *Journal of Anatomy*, *106*(Pt 3), 507–520.

Jones, N. L., Campbell, E. J., Edwards, R. H., & Wilkoff, W. G. (1969). Alveolar-to-blood PCO2 difference during rebreathing in exercise. *J Appl Physiol*, *27*(3), 356–360.

Kalaria, R. N., & Ballard, C. (1999). Overlap between pathology of Alzheimer disease and vascular dementia. *Alzheimer Disease and Associated Disorders*, *13*(3), S115-23.

Kassner, A., Winter, J. D., Poublanc, J., Mikulis, D. J., & Crawley, A. P. (2010). Blood-oxygen level dependent MRI measures of cerebrovascular reactivity using a controlled respiratory challenge: Reproducibility and gender differences. *Journal of Magnetic Resonance Imaging*, *31*(2), 298–304.

Kerchner, G. A., Berdnik, D., Shen, J. C., Bernstein, J. D., Fenesy, M. C., Deutsch, G. K., … Rutt, B. K. (2014). APOE e4 worsens hippocampal CA1 apical neuropil atrophy and episodic memory. *Neurology*, *82*(8), 691–697.

Kety, S. S., & Schmidt, C. F. (1948). the Effects of Altered Arterial Tensions of Carbon Dioxide and Oxygen on Cerebral Blood Flow and Cerebral Oxygen Consumption of Normal Young Men 1. *Journal of Clinical Investigation*, *27*(4), 484–492.

Kiliç, T., & Akakin, A. (2008). Anatomy of cerebral veins and sinuses. *Frontiers of Neurology and Neuroscience*, *23*, 4–15.

Kimbrough, I. F., Robel, S., Roberson, E. D., & Sontheimer, H. (2015). Vascular amyloidosis

impairs the gliovascular unit in a mouse model of Alzheimer's disease. *Brain*, *138*(12), 3716–3733.

Knopman, D. S., & Ryberg, S. (1989). A verbal memory test with high predictive accuracy for dementia of the Alzheimer type. *Archives of Neurology*, *46*(2), 141–145.

Knot, H. J., & Nelson, M. T. (1998). Regulation of arterial diameter and wall [Ca2+] in cerebral arteries of rat by membrane potential and intravascular pressure. *The Journal of Physiology*, (Pt 1), 199–209.

Kocharyan, A., Fernandes, P., Tong, X.-K., Vaucher, E., & Hamel, E. (2008). Specific subtypes of cortical GABA interneurons contribute to the neurovascular coupling response to basal forebrain stimulation. *Journal of Cerebral Blood Flow and Metabolism : Official Journal of the International Society of Cerebral Blood Flow and Metabolism*, *28*(2), 221–231.

Koike, M. A., Green, K. N., Blurton-Jones, M., & LaFerla, F. M. (2010). Oligemic Hypoperfusion Differentially Affects Tau and Amyloid-β. *The American Journal of Pathology*, *177*(1), 300–310.

Kopeikina, K. J., Hyman, B. T., & Spires-Jones, T. L. (2012). Soluble forms of tau are toxic in Alzheimer's disease. *Translational Neuroscience*, *3*(3), 223–233.

Kovacech, B., Skrabana, R., & Novak, M. (2010). Transition of tau protein from disordered to misordered in alzheimer's disease. *Neurodegenerative Diseases*, *7*(1–3), 24–27.

Kress, B. T., Iliff, J. J., Xia, M., Wang, M., Wei Bs, H. S., Zeppenfeld, D., … Nedergaard, M. (2014). Impairment of paravascular clearance pathways in the aging brain. *Annals of Neurology*, *76*(6), 845–861.

Kroetz, D. L., & Xu, F. (2005). Regulation and Inhibition of Arachidonic Acid Ω-Hydroxylases and 20-Hete Formation. *Annual Review of Pharmacology and Toxicology*, *45*(1), 413–438.

Kullmann, D. M., & Lamsa, K. P. (2007). Long-term synaptic plasticity in hippocampal interneurons. *Nat Rev Neurosci*, *8*(9), 687–699.

Kuwabara, Y., Ichiya, Y., Otsuka, M., Masuda, K., Ichimiya, A., & Fujishima, M. (1992). Cerebrovascular responsiveness to hypercapnia in Alzheimer's dementia and vascular dementia of the Binswanger type. *Stroke; a Journal of Cerebral Circulation*, *23*(4), 594–598.

Landau, S. M., Harvey, D., Madison, C. M., Koeppe, R. A., Reiman, E. M., Foster, N. L., … Jagust, W. J. (2011). Associations between cognitive, functional, and FDG-PET measures of decline in AD and MCI. *Neurobiology of Aging*, *32*(7), 1207–1218.

Lange, A., Gebremedhin, D., Narayanan, J., & Harder, D. (1997). 20-Hydroxyeicosatetraenoic acid-induced vasoconstriction and inhibition of potassium current in cerebral vascular smooth muscle is dependent on activation of protein kinase C. *The Journal of Biological Chemistry*, *272*(43), 27345–52.

Lavi, S., Gaitini, D., Milloul, V., & Jacob, G. (2006). Impaired cerebral CO2 vasoreactivity: association with endothelial dysfunction. *American Journal of Physiology. Heart and Circulatory Physiology*, *291*(4), H1856–H1861.

Leffler, C. W., Mirro, R., Pharris, L. J., & Shibata, M. (1994). Permissive role of prostacyclin in cerebral vasodilation to hypercapnia in newborn pigs. *Am J Physiol*, *267*(1 Pt 2), H285-91.

Lehericy, S., Baulac, M., Chiras, J., Pierot, L., Martin, N., Pillon, B., … Marsault, C. (1994). Amygdalohippocampal MR volume measurements in the early stages of Alzheimer disease. *American Journal of Neuroradiology*, *15*(5), 929–937.

Lemke, H., Castro, A. G. C. de, Schlattmann, P., Heuser, I., & Neu, P. (2010). Cerebrovascular reactivity over time-course - From major depressive episode to remission. *Journal of Psychiatric Research*, *44*(3), 132–136.

Leroy, K., Ando, K., Laporte, V., Dedecker, R., Suain, V., Authelet, M., … Brion, J. P. (2012). Lack of tau proteins rescues neuronal cell death and decreases amyloidogenic processing of APP in APP/PS1 mice. *American Journal of Pathology*, *181*(6), 1928–1940.

Li, B., Chohan, M. O., Grundke-Iqbal, I., & Iqbal, K. (2007). Disruption of microtubule network by Alzheimer abnormally hyperphosphorylated tau. *Acta Neuropathologica*, *113*(5), 501–511.

Li, J., Pan, P., Huang, R., & Shang, H. (2012). A meta-analysis of voxel-based morphometry studies of white matter volume alterations in Alzheimer's disease. *Neuroscience and Biobehavioral Reviews*, *36*(2), 757–763.

Li, J., Wang, Y. J., Zhang, M., Xu, Z. Q., Gao, C. Y., Fang, C. Q., … Zhou, H. D. (2011). Vascular risk factors promote conversion from mild cognitive impairment to Alzheimer disease. *Neurology*, *76*(17), 1485–1491.

Li, S., Hong, S., Shepardson, N. E., Walsh, D. M., Shankar, G. M., & Selkoe, D. (2009). Soluble Oligomers of Amyloid-Beta Protein Facilitate Hippocampal Long-Term Depression by Disrupting Neuronal Glutamate Uptake. *Neuron*, *62*(6), 788–801.

Li, S., Jin, M., Koeglsperger, T., Shepardson, N. E., Shankar, G. M., & Selkoe, D. J. (2011). Soluble A{beta} Oligomers Inhibit Long-Term Potentiation through a Mechanism Involving Excessive Activation of Extrasynaptic NR2B-Containing NMDA Receptors. *The Journal of Neuroscience : The Official Journal of the Society for Neuroscience*, *31*(18), 6627–38.

Locascio, J. J., Growdon, J. H., & Corkin, S. (1995). Cognitive test performance in detecting, staging, and tracking Alzheimer's disease. *Archives of Neurology*, *52*(11), 1087–1099.

Logothetis, N. K. (2003). The underpinnings of the BOLD functional magnetic resonance imaging signal. *The Journal of Neuroscience : The Official Journal of the Society for Neuroscience*, *23*(10), 3963–71.

Logothetis, N. K., Pauls, J., Augath, M., Trinath, T., & Oeltermann, A. (2001).

Neurophysiological investigation of the basis of the fMRI signal. *Nature*, *412*(6843), 150–157.

Love, S., & Miners, J. S. (2016). Cerebral Hypoperfusion and the Energy Deficit in Alzheimer's Disease. *Brain Pathology*, *26*(5), 607–617.

Lu, D. C., Soriano, S., Bredesen, D. E., & Koo, E. H. (2003). Caspase cleavage of the amyloid precursor protein modulates amyloid beta-protein toxicity. *Journal of Neurochemistry*, *87*(3), 733–41.

Luchsinger, J. A., Reitz, C., Honig, L. S., Tang, M. X., Shea, S., & Mayeux, R. (2005). Aggregation of vascular risk factors and risk of incident Alzheimer disease. *Neurology*, *65*(4), 545–551.

Lyketsos, C. G., Carrillo, M. C., Ryan, J. M., Khachaturian, A. S., Trzepacz, P., Amatniek, J., … Miller, D. S. (2011). Neuropsychiatric symptoms in Alzheimer's disease. *Alzheimer's & Dementia : The Journal of the Alzheimer's Association*, *7*(5), 532–539.

Machulda, M. M., Ward, H. a, Borowski, B., Gunter, J. L., Cha, R. H., O'Brien, P. C., … Jack, C. R. (2003). Comparison of memory fMRI response among normal, MCI, and Alzheimer's patients. *Neurology*, *61*(4), 500–6.

Makani, S., & Chesler, M. (2010). Rapid rise of extracellular pH evoked by neural activity is generated by the plasma membrane calcium ATPase. *Journal of Neurophysiology*, *103*(2), 667–76.

Mandelkow, E. M., & Mandelkow, E. (1998). Tau in Alzheimer's disease. *Trends in Cell Biology*, *8*(11), 425–427.

Mandelkow, E., Von Bergen, M., Biernat, J., & Mandelkow, E. M. (2007). Structural principles of tau and the paired helical filaments of Alzheimer's disease. *Brain Pathology*, *17*(1), 83–90.

Mandell, D. M., Han, J. S., Poublanc, J., Crawley, A. P., Kassner, A., Fisher, J. A., & Mikulis, D. J. (2008). Selective reduction of blood flow to white matter during hypercapnia corresponds with leukoaraiosis. *Stroke*, *39*(7), 1993–1998.

Mandell, D. M., Han, J. S., Poublanc, J., Crawley, A. P., Stainsby, J. A., Fisher, J. A., & Mikulis, D. J. (2008). Mapping cerebrovascular reactivity using blood oxygen level-dependent MRI in patients with arterial steno-occlusive disease: Comparison with arterial spin labeling MRI. *Stroke*, *39*(7), 2021–2028.

Marchesi, V. T. (2011). Alzheimer's dementia begins as a disease of small blood vessels, damaged by oxidative-induced inflammation and dysregulated amyloid metabolism: implications for early detection and therapy. *FASEB Journal : Official Publication of the Federation of American Societies for Experimental Biology*, *25*(1), 5–13.

Mark, C. I., Slessarev, M., Ito, S., Han, J., Fisher, J. A., & Pike, G. B. (2010). Precise control of end-tidal carbon dioxide and oxygen improves BOLD and ASL cerebrovascular reactivity

measures. *Magnetic Resonance in Medicine*, *64*(3), 749–756.

Markus, H., & Cullinane, M. (2001). Severely impaired cerebrovascular reactivity predicts stroke and TIA risk in patients with carotid artery stenosis and occlusion. *Brain : A Journal of Neurology*, *124*(Pt 3), 457–67.

Masuda, J., Tanaka, K., Ueda, K., & Omae, T. (1988). Autopsy study of incidence and distribution of cerebral amyloid angiopathy in Hisayama, Japan. *Stroke; a Journal of Cerebral Circulation*, *19*(2), 205–210.

Mattson, M. P. (2004). Pathways towards and away from Alzheimer's disease. *Nature*, *430*(7000), 631–639.

Mawuenyega, K. G., Sigurdson, W., Ovod, V., Munsell, L., Kasten, T., Morris, J. C., … Bateman, R. J. (2010). Decreased clearance of CNS beta-amyloid in Alzheimer's disease. *Science (New York, N.Y.)*, *330*(6012), 1774.

Mayeux, R., & Stern, Y. (2012). Epidemiology of Alzheimer disease. *Cold Spring Harbor Perspectives in Medicine*, *2*(8), 10.1101/cshperspect.a006239 a006239.

McCulloch, T. J., Visco, E., & Lam, A. M. (2000). Graded hypercapnia and cerebral autoregulation during sevoflurane or propofol anesthesia. *Anesthesiology*, *93*(5), 1205–9.

McKhann, G. M., Knopman, D. S., Chertkow, H., Hyman, B. T., Jack, C. R., Kawas, C. H., … Phelps, C. H. (2011). The diagnosis of dementia due to Alzheimer's disease: Recommendations from the National Institute on Aging-Alzheimer's Association workgroups on diagnostic guidelines for Alzheimer's disease. *Alzheimer's and Dementia*, *7*(3), 263–269.

McLean, C. A., Cherny, R. A., Fraser, F. W., Fuller, S. J., Smith, M. J., Beyreuther, K., … Masters, C. L. (1999). Soluble pool of Abeta amyloid as a determinant of severity of neurodegeneration in Alzheimer's disease. *Annals of Neurology*, *46*(6), 860–6.

Meng, L., & Gelb, A. W. (2015). Regulation of cerebral autoregulation by carbon dioxide, (1), 196–205.

Meng, X.-F., Yu, J.-T., Wang, H.-F., Tan, M.-S., Wang, C., Tan, C.-C., & Tan, L. (2014). Midlife Vascular Risk Factors and the Risk of Alzheimer's Disease: A Systematic Review and Meta-Analysis. *Journal of Alzheimer's Disease*, *42*(4), 1295–1310.

Metea, M. R. (2006). Glial Cells Dilate and Constrict Blood Vessels: A Mechanism of Neurovascular Coupling. *Journal of Neuroscience*, *26*(11), 2862–2870.

Mielke, M. M., Rosenberg, P. B., Tschanz, J., Cook, L., Corcoran, C., Hayden, K. M., … Lyketsos, C. G. (2007). Vascular factors predict rate of progression in Alzheimer disease. *Neurology*, *69*(19), 1850–1858.

Mikulis, D. J. (2013). Chronic neurovascular uncoupling syndrome. *Stroke*, *44*(SUPPL. 1), 55–58.

Mikulis, D. J., Krolczyk, G., Desal, H., Logan, W., Deveber, G., Dirks, P., … Fisher, J. a. (2005). Preoperative and postoperative mapping of cerebrovascular reactivity in moyamoya disease by using blood oxygen level-dependent magnetic resonance imaging. *Journal of Neurosurgery*, *103*(2), 347–355.

Mintun, M. a, Lundstrom, B. N., Snyder, a Z., Vlassenko, a G., Shulman, G. L., & Raichle, M. E. (2001). Blood flow and oxygen delivery to human brain during functional activity: theoretical modeling and experimental data. *Proceedings of the National Academy of Sciences of the United States of America*, *98*(12), 6859–6864.

Mistridis, P., Krumm, S., Monsch, A. U., Berres, M., & Taylor, K. I. (2015). The 12 Years Preceding Mild Cognitive Impairment Due to Alzheimer's Disease: The Temporal Emergence of Cognitive Decline. *Journal of Alzheimer's Disease*, *48*(4), 1095–1107.

Mitchell, A. J., & Shiri-Feshki, M. (2009). Rate of progression of mild cognitive impairment to dementia - Meta-analysis of 41 robust inception cohort studies. *Acta Psychiatrica Scandinavica*, *119*(4), 252–265.

Monsch, A. U., Bondi, M. W., Butters, N., Salmon, D. P., Katzman, R., & Thal, L. J. (1992). Comparisons of verbal fluency tasks in the detection of dementia of the Alzheimer type. *Archives of Neurology*, *49*(12), 1253–1258.

Montagne, A., Barnes, S. R., Sweeney, M. D., Halliday, M. R., Sagare, A. P., Zhao, Z., … Zlokovic, B. V. (2015). Blood-Brain barrier breakdown in the aging human hippocampus. *Neuron*, *85*(2), 296–302.

Montagne, A., Nation, D. A., Pa, J., Sweeney, M. D., Toga, A. W., & Zlokovic, B. V. (2016). Brain imaging of neurovascular dysfunction in Alzheimer's disease. *Acta Neuropathologica*, *131*(5), 687–707.

Montine, T. J., Phelps, C. H., Beach, T. G., Bigio, E. H., Cairns, N. J., Dickson, D. W., … Hyman, B. T. (2012). National institute on aging-Alzheimer's association guidelines for the neuropathologic assessment of Alzheimer's disease: A practical approach. *Acta Neuropathologica*, *123*(1), 1–11.

Morales, R., Duran-Aniotz, C., Castilla, J., Estrada, L. D., & Soto, C. (2012). De novo induction of amyloid-β deposition in vivo. *Molecular Psychiatry*, *17*(12), 1347–53.

Morris, J. C., Heyman, A., Mohs, R. C., Hughes, J. P., van Belle, G., Fillenbaum, G., … Clark, C. (1989). The Consortium to Establish a Registry for Alzheimer's Disease (CERAD). Part I. Clinical and neuropsychological assessment of Alzheimer's disease. *Neurology*, *39*(9), 1159–65.

Moskowitz, M. A., Lo, E. H., & Iadecola, C. (2010). The science of stroke: Mechanisms in search of treatments. *Neuron*, *67*(2), 181–198.

Mucke, L., Masliah, E., Yu, G. Q., Mallory, M., Rockenstein, E. M., Tatsuno, G., … McConlogue, L. (2000). High-level neuronal expression of abeta 1-42 in wild-type human amyloid protein precursor transgenic mice: synaptotoxicity without plaque formation. *The*

Journal of Neuroscience : The Official Journal of the Society for Neuroscience, *20*(11), 4050–8.

Mucke, L., & Selkoe, D. J. (2012). Neurotoxicity of amyloid β-protein: Synaptic and network dysfunction. *Cold Spring Harbor Perspectives in Medicine*, *2*(7), a006338.

Muller, U. C., & Zheng, H. (2012). Physiological functions of APP family proteins. *Cold Spring Harbor Perspectives in Medicine*, *2*(2), a006288.

Mulligan, S. J., & MacVicar, B. A. (2004). Calcium transients in astrocyte endfeet cause cerebrovascular constrictions. *Nature*, *431*(7005), 195–199.

Muoio, V., Persson, P. B., & Sendeski, M. M. (2014). The neurovascular unit - concept review. *Acta Physiologica*, *210*(4), 790–798.

Nagata, K., Kondoh, Y., Atchison, R., Sato, M., Satoh, Y., Watahiki, Y., … Yokoyama, E. (2000). Vascular and metabolic reserve in Alzheimer's disease. *Neurobiology of Aging*, *21*(2), 301–307.

Nagelhus, E. A., Mathiisen, T. M., & Ottersen, O. P. (2004). Aquaporin-4 in the central nervous system: Cellular and subcellular distribution and coexpression with KIR4.1. *Neuroscience*, *129*(4), 905–913.

Nave, K.-A. (2010). Myelination and support of axonal integrity by glia. *Nature*, *468*(7321), 244–252.

Nedergaard, M. (2013). Garbage Truck of the Brain. *Science (New York, N.Y.)*, *340*(6140), 1529–1530.

Nelson, P. T., Alafuzoff, I., Bigio, E. H., Bouras, C., Braak, H., Cairns, N. J., … Beach, T. G. (2012). Correlation of Alzheimer Disease Neuropathologic Changes With Cognitive Status: A Review of the Literature. *J Neuropathol Exp Neurol*, *71*(5), 362–381.

Nishimura, N., Rosidi, N. L., Iadecola, C., & Schaffer, C. B. (2010). Limitations of collateral flow after occlusion of a single cortical penetrating arteriole. *Journal of Cerebral Blood Flow and Metabolism : Official Journal of the International Society of Cerebral Blood Flow and Metabolism*, *30*(12), 1914–1927.

Niwa, K., Kazama, K., Younkin, L., Younkin, S. G., Carlson, G. A., & Iadecola, C. (2002). Cerebrovascular autoregulation is profoundly impaired in mice overexpressing amyloid precursor protein. *American Journal of Physiology - Heart and Circulatory Physiology*, *283*(1), H315–H323.

Niwa, K., Porter, V. A., Kazama, K., Cornfield, D., Carlson, G. A., & Iadecola, C. (2001). A beta-peptides enhance vasoconstriction in cerebral circulation. *American Journal of Physiology. Heart and Circulatory Physiology*, *281*(6), H2417-24.

Nunomura, A., Perry, G., Aliev, G., Hirai, K., Takeda, A., Balraj, E. K., … Smith, M. A. (2001). Oxidative damage is the earliest event in Alzheimer disease. *Journal of Neuropathology*

and Experimental Neurology, *60*(8), 759–767.

Ogawa, S., Lee, T. M., Kay, A. R., & Tank, D. W. (1990). Brain magnetic resonance imaging with contrast dependent on blood oxygenation. *Proc.Natl Acad.Sci.U.S.A*, *87*(0027–8424 LA–eng PT–Journal Article RN–0 (Hemoglobins) RN–124–38–9 (Carbon Dioxide) RN–7782–44–7 (Oxygen) SB–IM), 9868–9872.

Oishi, Mochizuki, & Takasu. (1999). Regional differences in cerebrovascular reactivity to acetazolamide in Alzheimer's disease. *Journal of Clinical Neuroscience : Official Journal of the Neurosurgical Society of Australasia*, *6*(5), 380–381.

Okazawa, H., Yamauchi, H., Sugimoto, K., Toyoda, H., Kishibe, Y., & Takahashi, M. (2001). Effects of acetazolamide on cerebral blood flow, blood volume, and oxygen metabolism: a positron emission tomography study with healthy volunteers. *Journal of Cerebral Blood Flow and Metabolism : Official Journal of the International Society of Cerebral Blood Flow and Metabolism*, *21*(12), 1472–9.

Palmer, J. C., Barker, R., Kehoe, P. G., & Love, S. (2012). Endothelin-1 is elevated in Alzheimer's disease and upregulated by amyloid-β. *Journal of Alzheimer's Disease : JAD*, *29*(4), 853–61.

Paulson, O. B., Strandgaard, S., & Edvinsson, L. (1990). Cerebral autoregulation. *Cerebrovascular and Brain Metabolism Reviews*, *2*(2), 161–92.

Peña-Casanova, J., Sánchez-Benavides, G., de Sola, S., Manero-Borrás, R. M., & Casals-Coll, M. (2012). Neuropsychology of Alzheimer's Disease. *Archives of Medical Research*, *43*(8), 686–693.

Peng, W., Achariyar, T. M., Li, B., Liao, Y., Mestre, H., Hitomi, E., … Deane, R. (2016). Suppression of glymphatic fluid transport in a mouse model of Alzheimer's disease. *Neurobiology of Disease*, *93*, 215–225.

Pennanen, C., Kivipelto, M., Tuomainen, S., Hartikainen, P., H??nninen, T., Laakso, M. P., … Soininen, H. (2004). Hippocampus and entorhinal cortex in mild cognitive impairment and early AD. *Neurobiology of Aging*, *25*(3), 303–310.

Petrovitch, H., Ross, G. W., Steinhorn, S. C., Abbott, R. D., Markesbery, W., Davis, D., … White, L. R. (2005). AD lesions and infarcts in demented and non-demented Japanese-American men. *Annals of Neurology*, *57*(1), 98–103.

Pezzini, A., Del Zotto, E., Volonghi, I., Giossi, A., Costa, P., & Padovani, A. (2009). Cerebral amyloid angiopathy: a common cause of cerebral hemorrhage. *Curr Med Chem*, *16*(20), 2498–2513.

Pohanka, M. (2014). Alzheimer´s disease and oxidative stress: a review. *Current Medicinal Chemistry*, *21*(3), 356–64.

Potter, R., Patterson, B. W., Elbert, D. L., Ovod, V., Kasten, T., Sigurdson, W., … Tammie, L. S. (2013). Increased in vivo Amyloid-b42 production, exchange, and irreversible loss in

Presenilin Mutations Carriers. *Science Translational Medicine*, *5*(189), 10.1126/scitranslmed.3005615.

Poublanc, J., Crawley, A. P., Sobczyk, O., Montandon, G., Sam, K., Mandell, D. M., … Fisher, J. a. (2015). Measuring cerebrovascular reactivity: the dynamic response to a step hypercapnic stimulus. *Journal of Cerebral Blood Flow & Metabolism*, (April), 1–11.

Powers, W. J., Hirsch, I. B., & Cryer, P. E. (1996). Effect of stepped hypoglycemia on regional cerebral blood flow response to physiological brain activation. *Am J Physiol*, *270*(2 Pt 2), H554-9.

Prince, M., Bryce, R., Albanese, E., Wimo, A., Ribeiro, W., & Ferri, C. P. (2013). The global prevalence of dementia: A systematic review and metaanalysis. *Alzheimer's and Dementia*, *9*(1), 63–75.

Prisman, E., Slessarev, M., Han, J., Poublanc, J., Mardimae, A., Crawley, A., … Mikulis, D. (2008). Comparison of the effects of independently-controlled end-tidal PCO 2 and PO2 on Blood Oxygen Level-Dependent (BOLD) MRI. *Journal of Magnetic Resonance Imaging*, *27*(1), 185–191.

Reitz, C., & Mayeux, R. (2014). Alzheimer disease: Epidemiology, diagnostic criteria, risk factors and biomarkers. *Biochemical Pharmacology*, *88*(4), 640–651.

Rennels, M. L., & Nelson, E. (1975). Capillary innervation in the mammalian central nervous system: An electron microscopic demonstration. *American Journal of Anatomy*, *144*(2), 233–241.

Richiardi, J., Monsch, A. U., Haas, T., Barkhof, F., Van de Ville, D., Radü, E. W., … Haller, S. (2015). Altered cerebrovascular reactivity velocity in mild cognitive impairment and Alzheimer's disease. *Neurobiology of Aging*, *36*(1), 33–41.

Roberson, E. D., Scearce-Levie, K., Palop, J. J., Yan, F., Cheng, I. H., Wu, T., … Mucke, L. (2007). Reducing endogenous tau ameliorates amyloid beta-induced deficits in an Alzheimer's disease mouse model. *Science (New York, N.Y.)*, *316*(5825), 750–4.

Roher, A. E., Chaney, M. O., Kuo, Y. M., Webster, S. D., Stine, W. B., Haverkamp, L. J., … Emmerling, M. R. (1996). Morphology and toxicity of Abeta-(1-42) dimer derived from neuritic and vascular amyloid deposits of Alzheimer's disease. *The Journal of Biological Chemistry*, *271*(34), 20631–5.

Roher, A. E., Debbins, J. P., Malek-Ahmadi, M., Chen, K., Pipe, J. G., Maze, S., … Beach, T. G. (2012). Cerebral blood flow in Alzheimer's disease. *Vascular Health and Risk Management*, *8*(1), 596–611.

Rombouts, S. A. R. B., Goekoop, R., Stam, C. J., Barkhof, F., & Scheltens, P. (2005). Delayed rather than decreased BOLD response as a marker for early Alzheimer's disease. *NeuroImage*, *26*(4), 1078–1085.

Rosenberg, G. A. (2009). Matrix metalloproteinases and their multiple roles in

neurodegenerative diseases. *The Lancet Neurology*, *8*(2), 205–216.

Roy, S., Zhang, B., Lee, V. M. Y., & Trojanowski, J. Q. (2005). Axonal transport defects: A common theme in neurodegenerative diseases. *Acta Neuropathologica*, *109*(1), 5–13.

Rubial-Álvarez, S., de Sola, S., Machado, M.-C., Sintas, E., Böhm, P., Sánchez-Benavides, G., … Peña-Casanova, J. (2013). The comparison of cognitive and functional performance in children and Alzheimer's disease supports the retrogenesis model. *Journal of Alzheimer's Disease : JAD*, *33*(1), 191–203.

Ruhrberg, C., & Bautch, V. L. (2013). Neurovascular development and links to disease. *Cellular and Molecular Life Sciences*, *70*(10), 1675–1684.

Sabayan, B., Jansen, S., Oleksik, A. M., Osch, M. J. P. Van, Buchem, M. A. Van, Vliet, P. Van, … Westendorp, R. G. J. (2012). Cerebrovascular hemodynamics in Alzheimer ' s disease and vascular dementia : A meta-analysis of transcranial Doppler studies. *Ageing Research Reviews*, *11*(2), 271–277.

Sam, K., Conklin, J., Holmes, K. R., Sobczyk, O., Poublanc, J., Crawley, A. P., … Mikulis, D. J. (2016). Impaired dynamic cerebrovascular response to hypercapnia predicts development of white matter hyperintensities. *NeuroImage: Clinical*, *11*, 796–801.

Sam, K., Crawley, A. P., Conklin, J., Poublanc, J., Sobczyk, O., Mandell, D. M., … Mikulis, D. J. (2016). Development of White Matter Hyperintensity Is Preceded by Reduced Cerebrovascular Reactivity. *Annals of Neurology*, *80*(2), 277–285.

Sam, K., Peltenburg, B., Conklin, J., Sobczyk, O., Poublanc, J., Crawley, A. P., … Mikulis, D. J. (2016). Cerebrovascular reactivity and white matter integrity. *Neurology*, *87*(22), 2333–2339.

Sasse, S. A., Berry, R. B., Nguyen, T. K., Light, R. W., & Mahutte, C. K. (1996). Arterial blood gas changes during breath-holding from functional residual capacity. *Chest*, *110*(4), 958–964.

Saxton, W. M., & Hollenbeck, P. J. (2012). The axonal transport of mitochondria. *Journal of Cell Science*, *125*(Pt 9), 2095–104.

Scahill, R. I., Schott, J. M., Stevens, J. M., Rossor, M. N., & Fox, N. C. (2002). Mapping the evolution of regional atrophy in Alzheimer's disease: unbiased analysis of fluid-registered serial MRI. *Proceedings of the National Academy of Sciences of the United States of America*, *99*(7), 4703–7.

Schaffer, C. B., Friedman, B., Nishimura, N., Schroeder, L. F., Tsai, P. S., Ebner, F. F., … Kleinfeld, D. (2006). Two-photon imaging of cortical surface microvessels reveals a robust redistribution in blood flow after vascular occlusion. *PLoS Biology*, *4*(2), 258–270.

Scheibel, A. B., Duong, T. H., & Jacobs, R. (1989). Alzheimer's disease as a capillary dementia. *Annals of Medicine*, *21*(2), 103–107.

Scheltens, P., Blennow, K., Breteler, M. M. B., de Strooper, B., Frisoni, G. B., Salloway, S., & Van der Flier, W. M. aria. (2016). Alzheimer's disease. *Lancet (London, England)*, *388*(10043), 505–517.

Scheuner, D., Eckman, C., Jensen, M., Song, X., Citron, M., Suzuki, N., … Younkin, S. (1996). Secreted amyloid beta-protein similar to that in the senile plaques of Alzheimer's disease is increased in vivo by the presenilin 1 and 2 and APP mutations linked to familial Alzheimer's disease. *Nature Medicine*, *2*(8), 864–870.

Schmechel, D. E., Saunders, A. M., Strittmatter, W. J., Crain, B. J., Hulette, C. M., Joo, S. H., … Roses, A. D. (1993). Increased amyloid beta-peptide deposition in cerebral cortex as a consequence of apolipoprotein E genotype in late-onset Alzheimer disease. *Proceedings of the National Academy of Sciences of the United States of America*, *90*(20), 9649–53.

Schneider, J. A., Arvanitakis, Z., Leurgans, S. E., & Bennett, D. A. (2009). The neuropathology of probable Alzheimer disease and mild cognitive impairment. *Annals of Neurology*, *66*(2), 200–208.

Schneider, J. a, Wilson, R. S., Bienias, J. L., Evans, D. a, & Bennett, D. a. (2004). Cerebral infarctions and the likelihood of dementia from Alzheimer disease pathology. *Neurology*, *62*(7), 1148–1155.

Schubert, R., Lidington, D., & Bolz, S. S. (2008). The emerging role of Ca2+ sensitivity regulation in promoting myogenic vasoconstriction. *Cardiovascular Research*, *77*(1), 8–18.

Seeley, W. W., Crawford, R. K., Zhou, J., Miller, B. L., & Greicius, M. D. (2009). Neurodegenerative Diseases Target Large-Scale Human Brain Networks. *Neuron*, *62*(1), 42–52.

Selkoe, D. J. (1991). The molecular pathology of Alzheimer's disease. *Neuron*, *6*(4), 487–98.

Selkoe, D. J. (2008). Biochemistry and Molecular Biology of Amyloid ??-Protein and the Mechanism of Alzheimer's Disease. In *Handbook of Clinical Neurology* (Vol. 89, pp. 245–260).

Serrano-Pozo, A., Frosch, M. P., Masliah, E., & Hyman, B. T. (2011). Neuropathological alterations in Alzheimer disease. *Cold Spring Harbor Perspectives in Medicine*, *1*(1), a006189.

Shankar, G. M., Bloodgood, B. L., Townsend, M., Walsh, D. M., Selkoe, D. J., & Sabatini, B. L. (2007). Natural Oligomers of the Alzheimer Amyloid-β Protein Induce Reversible Synapse Loss by Modulating an NMDA-Type Glutamate Receptor-Dependent Signaling Pathway. *J Neurosci*, *27*(11), 2866–2875.

Shankar, G. M., Li, S., Mehta, T. H., Garcia-Munoz, A., Shepardson, N. E., Smith, I., … Selkoe, D. J. (2008). Amyloid-beta protein dimers isolated directly from Alzheimer's brains impair synaptic plasticity and memory. *Nature Medicine*, *14*(8), 837–42.

Sheline, Y. I., Morris, J. C., Snyder, A. Z., Price, J. L., Yan, Z., D'Angelo, G., … Mintun, M. a.

(2010). APOE4 allele disrupts resting state fMRI connectivity in the absence of amyloid plaques or decreased CSF Aβ42. *The Journal of Neuroscience : The Official Journal of the Society for Neuroscience*, *30*(50), 17035–40.

Shiino, A., Morita, Y., Tsuji, A., Maeda, K., Ito, R., Furukawa, A., … Inubushi, T. (2003). Estimation of Cerebral Perfusion Reserve by Blood Oxygenation Level—Dependent Imaging: Comparison with Single-Photon Emission Computed Tomography. *Journal of Cerebral Blood Flow & Metabolism*, *23*(1), 121–135.

Shoji, M., Golde, T. E., Ghiso, J., Cheung, T. T., Estus, S., Shaffer, L. M., … Younkin, S. G. (1992). Production of the Alzheimer Amyloid β Protein by Normal Proteolytic Processing. *Science*, *258*(5079), 126–129.

Silvestrini, M., Vernieri, F., Pasqualetti, P., Matteis, M., Passarelli, F., Troisi, E., & Caltagirone, C. (2000). Impaired cerebral vasoreactivity and risk of stroke in patients with asymptomatic carotid artery stenosis. *JAMA*, *283*(16), 2122–7.

Silvestrini, M., Vernieri, F., Troisi, E., Passarelli, F., Matteis, M., Pasqualetti, P., … Caltagirone, C. (1999). Cerebrovascular reactivity in carotid artery occlusion: possible implications for surgical management of selected groups of patients. *Acta Neurologica Scandinavica*, *99*(3), 187–91.

Silvestrini, M., Viticchi, G., Altamura, C., Luzzi, S., Balucani, C., & Vernieri, F. (2012). Cerebrovascular assessment for the risk prediction of Alzheimer's disease. *Journal of Alzheimer's Disease*, *32*(3), 689–698.

Slessarev, M., Han, J., Mardimae, A., Prisman, E., Preiss, D., Volgyesi, G., … Fisher, J. a. (2007). Prospective targeting and control of end-tidal CO2 and O2 concentrations. *The Journal of Physiology*, *581*(Pt 3), 1207–19.

Small, B. J., Fratiglioni, L., Viitanen, M., Winblad, B., & Backman, L. (2000). The course of cognitive impairment in preclinical Alzheimer disease: three- and 6-year follow-up of a population-based sample. *Archives of Neurology*, *57*(6), 839–844.

Smith, C. D., Andersen, A. H., Kryscio, R. J., Schmitt, F. A., Kindy, M. S., Blonder, L. X., & Avison, M. J. (1999). Altered brain activation in cognitively intact individuals at high risk for Alzheimer's disease. *Neurology*, *53*(7), 1391–1396.

Snowdon, D. A., Greiner, L. H., Mortimer, J. A., Greiner, P. A., & Markesbery, W. R. (1997). Brain Infarction and the Clinical Expression of Alzheimer Disease Study. *Journal of the American Medical Association*, *277*(10), 813–817.

Snyder, E. M., Nong, Y., Almeida, C. G., Paul, S., Moran, T., Choi, E. Y., … Greengard, P. (2005). Regulation of NMDA receptor trafficking by amyloid-beta. *Nature Neuroscience*, *8*(8), 1051–8.

Sobczyk, O., Battisti-Charbonney, A., Fierstra, J., Mandell, D. M., Poublanc, J., Crawley, A. P., … Fisher, J. A. (2014). A conceptual model for CO2-induced redistribution of cerebral blood flow with experimental confirmation using BOLD MRI. *NeuroImage*, *92*, 56–68.

Sobczyk, O., Crawley, A. P., Poublanc, J., Sam, K., Mandell, D. M., Mikulis, D. J., … Fisher, J. A. (2016). Identifying Significant Changes in Cerebrovascular Reactivity to Carbon Dioxide. *American Journal of Neuroradiology*.

Spano, V. R., Mandell, D. M., Poublanc, J., Sam, K., Battisti-Charbonney, A., Pucci, O., … Mikulis, D. J. (2013). CO2 blood oxygen level-dependent MR mapping of cerebrovascular reserve in a clinical population: safety, tolerability, and technical feasibility. *Radiology*, *266*(2), 592–8.

Sperling, R. A., Aisen, P. S., Beckett, L. A., Bennett, D. A., Craft, S., Fagan, A. M., … Phelps, C. H. (2011). Toward defining the preclinical stages of Alzheimer's disease: Recommendations from the National Institute on Aging-Alzheimer's Association workgroups on diagnostic guidelines for Alzheimer's disease. *Alzheimer's and Dementia*, *7*(3), 280–292.

Spires-Jones, T. L., Meyer-Luehmann, M., Osetek, J. D., Jones, P. B., Stern, E. A., Bacskai, B. J., & Hyman, B. T. (2007). Impaired spine stability underlies plaque-related spine loss in an Alzheimer's disease mouse model. *The American Journal of Pathology*, *171*(4), 1304–11.

St Croix, C. M., Cunningham, D. a, Kowalchuk, J. M., McConnell, a K., Kirby, a S., Scheuermann, B. W., … Paterson, D. H. (1995). Estimation of arterial PCO2 in the elderly. *Journal of Applied Physiology (Bethesda, Md. : 1985)*, *79*(6), 2086–93.

Stancu, I.-C., Vasconcelos, B., Terwel, D., & Dewachter, I. (2014). Models of β-amyloid induced Tau-pathology: the long and "folded" road to understand the mechanism. *Molecular Neurodegeneration*, *9*, 51.

Stelzmann, R. A., Norman Schnitzlein, H., & Reed Murtagh, F. (1995). An english translation of alzheimer's 1907 paper, uber eine eigenartige erkankung der hirnrinde. *Clinical Anatomy*, *8*(6), 429–431.

Stöhr, J., Watts, J. C., Mensinger, Z. L., Oehler, A., Grillo, S. K., DeArmond, S. J., … Giles, K. (2012). Purified and synthetic Alzheimer's amyloid beta (Aβ) prions. *Proceedings of the National Academy of Sciences of the United States of America*, *109*(27), 11025–30.

Stoppe, G., Schütze, R., Kögler, A., Staedt, J., Munz, D. L., Emrich, D., & Rüther, E. (1995). Cerebrovascular reactivity to acetazolamide in (senile) dementia of Alzheimer's type: relationship to disease severity. *Dementia (Basel, Switzerland)*, *6*(2), 73–82.

Sun, C. W., Alonso-Galicia, M., Taheri, M. R., Falck, J. R., Harder, D. R., & Roman, R. J. (1998). Nitric oxide-20-hydroxyeicosatetraenoic acid interaction in the regulation of K+ channel activity and vascular tone in renal arterioles. *Circulation Research*, *83*(11), 1069–1079.

Sun, X., He, G., Qing, H., Zhou, W., Dobie, F., Cai, F., … Song, W. (2006). Hypoxia facilitates Alzheimer's disease pathogenesis by up-regulating BACE1 gene expression. *Proceedings of the National Academy of Sciences of the United States of America*, *103*(49), 18727–18732.

Suo, Z., Humphrey, J., Kundtz, A., Sethi, F., Placzek, A., Crawford, F., & Mullan, M. (1998).

Soluble Alzheimers β-amyloid constricts the cerebral vasculature in vivo. *Neuroscience Letters*, *257*(2), 77–80.

Suri, S., Mackay, C. E., Kelly, M. E., Germuska, M., Tunbridge, E. M., Frisoni, G. B., … Filippini, N. (2015). Reduced cerebrovascular reactivity in young adults carrying the APOE ??4 allele. *Alzheimer's and Dementia*, *11*(6), 648–657.e1.

Takano, T., Tian, G.-F., Peng, W., Lou, N., Libionka, W., Han, X., & Nedergaard, M. (2006). Astrocyte-mediated control of cerebral blood flow. *Nature Neuroscience*, *9*(2), 260–267.

Tan, C. O. (2012). Defining the characteristic relationship between arterial pressure and cerebral flow. *Journal of Applied Physiology*, *113*(8), 1194–1200.

Tarumi, T., Dunsky, D. I., Khan, M. A., Liu, J., Hill, C., Armstrong, K., … Zhang, R. (2014). Dynamic cerebral autoregulation and tissue oxygenation in amnestic mild cognitive impairment. *Journal of Alzheimer's Disease : JAD*, *41*(3), 765–78.

Thal, D. R., Rüb, U., Orantes, M., & Braak, H. (2002). Phases of Aβ-deposition in the human brain and its relevance for the development of AD. *Neurology*, *58*(12), 1791–800.

Thomas, T., Thomas, G., McLendon, C., Sutton, T., & Mullan, M. (1996). beta-Amyloid-mediated vasoactivity and vascular endothelial damage. *Nature*, *380*(6570), 168–171.

Thompson, P. M., Hayashi, K. M., De Zubicaray, G. I., Janke, A. L., Rose, S. E., Semple, J., … Toga, A. W. (2004). Mapping hippocampal and ventricular change in Alzheimer disease. *NeuroImage*, *22*(4), 1754–1766.

Thompson, P. M., Hayashi, K. M., Sowell, E. R., Gogtay, N., Giedd, J. N., Rapoport, J. L., … Toga, A. W. (2004). Mapping cortical change in Alzheimer's disease, brain development, and schizophrenia. *NeuroImage*, *23*(SUPPL. 1), S2-18.

Tiecks, F. P., Lam, A. M., Aaslid, R., & Newell, D. W. (1995). Comparison of Static and Dynamic Cerebral Autoregulation Measurements. *Stroke*, *26*(6).

Tohgi, H., Yonezawa, H., Takahashi, S., Sato, N., Kato, E., Kudo, M., … Sasaki, T. (1998). Cerebral blood flow and oxygen metabolism in senile dementia of Alzheimer's type and vascular dementia with deep white matter changes. *Neuroradiology*, *40*(3), 131–137.

Toledo, J. B., Arnold, S. E., Raible, K., Brettschneider, J., Xie, S. X., Grossman, M., … Trojanowski, J. Q. (2013). Contribution of cerebrovascular disease in autopsy confirmed neurodegenerative disease cases in the National Alzheimer's Coordinating Centre. *Brain*, *136*(9), 2697–2706.

Toledo, J. B., ıa Toledo, E., Weiner, M. W., Jack, C. R., Jagust, W., M-Y Lee, V., … Trojanowski, J. Q. (2012). Cardiovascular risk factors, cortisol, and amyloid-b deposition in Alzheimer's Disease Neuroimaging Initiative; for the Alzheimer's Disease Neuroimaging Initiative. *Alzheimer's & Dementia*, *8*(6), 483–489.

Tolppanen, A. M., Ngandu, T., Kåreholt, I., Laatikainen, T., Rusanen, M., Soininen, H., &

Kivipelto, M. (2014). Midlife and late-life body mass index and late-life dementia: Results from a prospective population-based cohort. *Journal of Alzheimer's Disease*, *38*(1), 201–209.

Tzeng, Y.-C., & Ainslie, P. N. (2014). Blood pressure regulation IX: cerebral autoregulation under blood pressure challenges. *European Journal of Applied Physiology*, *114*(3), 545–559.

van Beek, A. H. E. A., Sijbesma, J. C., Jansen, R. W. M. M., Rikkert, M. G. M. O., & Claassen, J. A. H. R. (2010). Cortical Oxygen Supply During Postural Hypotension is Further Decreased in Alzheimer's Disease, but Unrelated to Cholinesterase-Inhibitor Use. *Journal of Alzheimer's Disease*, *21*(2), 519–526.

van Westen, D., Lindqvist, D., Blennow, K., Minthon, L., Nägga, K., Stomrud, E., … Hansson, O. (2016). Cerebral white matter lesions - associations with Aβ isoforms and amyloid PET. *Scientific Reports*, *6*, 20709.

Vassar, R., Bennett, B. D., Babu-Khan, S., Kahn, S., Mendiaz, E. a, Denis, P., … Citron, M. (1999). Beta-secretase cleavage of Alzheimer's amyloid precursor protein by the transmembrane aspartic protease BACE. *Science (New York, N.Y.)*, *286*(5440), 735–41.

Verclytte, S., Lopes, R., Lenfant, P., Rollin, A., Semah, F., Leclerc, X., … Delmaire, C. (2016). Cerebral Hypoperfusion and Hypometabolism Detected by Arterial Spin Labeling MRI and FDG-PET in Early-Onset Alzheimer's Disease. *Journal of Neuroimaging*, *26*(2), 207–212.

Vernieri, F., Pasqualetti, P., Passarelli, F., Rossini, P. M., & Silvestrini, M. (1999). Outcome of carotid artery occlusion is predicted by cerebrovascular reactivity. *Stroke; a Journal of Cerebral Circulation*, *30*(3), 593–598.

Vicenzini, E., Ricciardi, M. C., Altieri, M., Puccinelli, F., Bonaffini, N., Di Piero, V., & Lenzi, G. L. (2007). Cerebrovascular reactivity in degenerative and vascular dementia: a transcranial Doppler study. *European Neurology*, *58*(2), 84–89.

Vinters, H. V. (1987). Cerebral amyloid angiopathy. A critical review. *Stroke; a Journal of Cerebral Circulation*, *18*(2), 311–24.

Viswanathan, A., & Greenberg, S. M. (2011). Cerebral amyloid angiopathy in the elderly. *Annals of Neurology*, *70*(6), 871–880.

Viswanathan, A., Patel, P., Rahman, R., Nandigam, R. N. K., Kinnecom, C., Bracoud, L., … Smith, E. E. (2008). Tissue Microstructural Changes Are Independently Associated With Cognitive Impairment in Cerebral Amyloid Angiopathy. *Stroke; a Journal of Cerebral Circulation*, *39*(7), 1988–1992.

Wang, Q., Pelligrino, D. A., Koenig, H. M., & Albrecht, R. F. (1994). The Role of Endothelium and Nitric Oxide in Rat Pial Arteriolar Dilatory Responses to CO_2 in vivo. *Journal of Cerebral Blood Flow & Metabolism*, *14*(6), 944–951.

Wang, X., Xing, A., Xu, C., Cai, Q., Liu, H., & Li, L. (2010). Cerebrovascular hypoperfusion

induces spatial memory impairment, synaptic changes, and amyloid-β oligomerization in rats. *Journal of Alzheimer's Disease*, *21*(3), 813–822.

Wang, Z., Yang, D., Zhang, X., Li, T., Li, J., Tang, Y., & Le, W. (2011). Hypoxia-induced Down-regulation of Neprilysin by histone modification in mouse primary cortical and Hippocampal neurons. *PLoS ONE*, *6*(4), e19229.

Wardlaw, J. M., Smith, E. E., Biessels, G. J., Cordonnier, C., Fazekas, F., Frayne, R., … Dichgans, M. (2013). Neuroimaging standards for research into small vessel disease and its contribution to ageing and neurodegeneration. *The Lancet Neurology*, *12*(8), 822–838.

Wei, E. P., Kontos, H. a, & Patterson, J. L. (1980). Dependence of pial arteriolar response to hypercapnia on vessel size. *The American Journal of Physiology*, *238*(5), 697–703.

Weintraub, S., Wicklund, A. H., & Salmon, D. P. (2012). The neuropsychological profile of Alzheimer disease. *Cold Spring Harbor Perspectives in Medicine*, *2*(4), a006171.

Welsh, K., Butters, N., Hughes, J., Mohs, R., & Heyman, A. (1991). Detection of abnormal memory decline in mild cases of Alzheimer's disease using CERAD neuropsychological measures. *Archives of Neurology*, *48*(3), 278–281.

Wintermark, M., Sesay, M., Barbier, E., Borbély, K., Dillon, W. P., Eastwood, J. D., … Yonas, H. (2005). Comparative overview of brain perfusion imaging techniques. *J Neuroradiol*, *32*(5), 294–314.

Xu, H., Cui, N., Yang, Z., Wu, J., Giwa, L. R., Abdulkadir, L., … Jiang, C. (2001). Direct Activation of Cloned KATP Channels by Intracellular Acidosis. *Journal of Biological Chemistry*, *276*(16), 12898–12902.

Yablonskiy, D. A., Ackerman, J. J. H., & Raichle, M. E. (2000). Coupling between changes in human brain temperature and oxidative metabolism during prolonged visual stimulation. *Proceedings of the National Academy of Sciences*, *97*(13), 7603–7608.

Yarchoan, M., Xie, S. X., Kling, M. A., Toledo, J. B., Wolk, D. A., Lee, E. B., … Arnold, S. E. (2012). Cerebrovascular atherosclerosis correlates with Alzheimer pathology in neurodegenerative dementias. *Brain*, *135*(12), 3749–3756.

Yezhuvath, U. S., Uh, J., Cheng, Y., Martin-Cook, K., Weiner, M., Diaz-Arrastia, R., … Lu, H. (2012). Forebrain-dominant deficit in cerebrovascular reactivity in Alzheimer's disease. *Neurobiology of Aging*, *33*(1), 75–82.

Yonas, H., & Pindzola, R. R. (1994). Physiological determination of cerebrovascular reserves and its use in clinical management. *Cerebrovascular and Brain Metabolism Reviews*, *6*(4), 325–340.

You, J. P., Wang, Q., Zhang, W., Jansen-Olesen, I., Paulson, O. B., Lassen, N. A., & Edvinsson, L. (1994). Hypercapnic vasodilatation in isolated rat basilar arteries is exerted via low pH and does not involve nitric oxide synthase stimulation or cyclic GMP production. *Acta Physiologica Scandinavica*, *152*(4), 391–397.

Zazulia, A. R., Videen, T. O., Morris, J. C., & Powers, W. J. (2010). Autoregulation of cerebral blood flow to changes in arterial pressure in mild Alzheimer's disease. *Journal of Cerebral Blood Flow & Metabolism*, *30*(11), 1883–1889.

Zekry, D., Duyckaerts, C., Belmin, J., Geoffre, C., Moulias, R., & Hauw, J. J. (2003). Cerebral amyloid angiopathy in the elderly: Vessel walls changes and relationship with dementia. *Acta Neuropathologica*, *106*(4), 367–373.

Zhang, B., Maiti, A., Shively, S., Lakhani, F., McDonald-Jones, G., Bruce, J., … Trojanowski, J. Q. (2005). Microtubule-binding drugs offset tau sequestration by stabilizing microtubules and reversing fast axonal transport deficits in a tauopathy model. *Proceedings of the National Academy of Sciences of the United States of America*, *102*(1), 227–31.

Zhang, X., Zhou, K., Wang, R., Cui, J., Lipton, S. A., Liao, F.-F., … Zhang, Y. -w. (2007). Hypoxia-inducible Factor 1 (HIF-1)-mediated Hypoxia Increases BACE1 Expression and beta-Amyloid Generation. *Journal of Biological Chemistry*, *282*(15), 10873–10880.

Zlokovic, B. V. (2005). Neurovascular mechanisms of Alzheimer's neurodegeneration. *Trends in Neurosciences*, *28*(4), 202–208.

Zlokovic, B. V. (2008). The Blood-Brain Barrier in Health and Chronic Neurodegenerative Disorders. *Neuron*, *57*(2), 178–201.

Zlokovic, B. V. (2010). Neurodegeneration and the neurovascular unit. *Nature Medicine*, *16*(12), 1370–1371.

Zlokovic, B. V. (2011). Neurovascular pathways to neurodegeneration in Alzheimer's disease and other disorders. *Nature Reviews. Neuroscience*, *12*(12), 723–38.

Zonta, M., Angulo, M. C., Gobbo, S., Rosengarten, B., Hossmann, K.-A., Pozzan, T., & Carmignoto, G. (2003). Neuron-to-astrocyte signaling is central to the dynamic control of brain microcirculation. *Nature Neuroscience*, *6*(1), 43–50.

Appendices

Appendix 1. Consent Forms

CONSENT TO PARTICIPATE IN A RESEARCH STUDY
(FOR HEALTHY PARTICIPANT)

Title: Developing an imaging biomarker for Alzheimer's dementia based on vascular dysfunction

Principal Investigator: Dr. David Mikulis, M.D.

Tel: 416 603-5800 Ext. 5612

Co-Investigators: Melanie Cohn, Ph.D. C. Psych
Adrian Crawley, Ph.D.
Paul Dufort, Ph.D.
Dr. Daniel Mandell
Dr. David Tang-Wai
Dr. Carmela Tartaglia

You are being asked to take part in a research study. Please read this explanation about the study and its risks and benefits before you decide if you would like to take part. You should take as much time as you need to make your decision. You should ask the study doctor or study staff to explain anything that you do not understand and make sure that all of your questions have been answered before signing this consent form. Before you make your decision, feel free to talk about this study with anyone you wish including your friends, family, and family doctor. Participation in this study is voluntary.

Background

As the population ages, more people are developing dementia. Dementia is a loss in certain mental abilities, including but not limited to memory, attention and understanding language. It is therefore increasingly important for the health care system to find solutions for slowing or even eliminating this condition. Individuals with declining brain function may be developing one of several different types of dementia that can be difficult to distinguish from each other early on. Knowledge of the dementia type is important for starting the right treatment as soon as possible. Certain types of dementia are actually caused by injury only to the blood vessels themselves. Yet, in the other dementias, the relationship between blood vessel injury and direct injury to nerve cells is less well understood, though it likely plays a role in Alzheimer's disease.

This research study will use a method to better understand the role that damaged blood vessels play in the development and progression of dementia. You are being invited to take part in the study because you are healthy.

Carbon dioxide content of the blood increases when you hold your breath and decreases when you hyperventilate (breathe rapidly). Interestingly, the blood flow to the brain is also controlled by the carbon dioxide level in the blood. Increases in carbon dioxide increase brain blood flow and vice versa. We make changes to the carbon dioxide in the blood by adding carbon dioxide to, and then taking it away from, the air you are breathing. While this is being done, we use the magnetic resonance scanner (MRI) to monitor the changes in blood flow in your brain. How the blood flow responds to the carbon dioxide changes tells us about the health of the blood vessels, and the brain.

We believe that the areas in the brain with unhealthy blood vessels will be seen at a very early stage of dementia allowing doctors to begin proper treatment sooner improving the future quality of life.

Purpose

The purpose of this study is to determine whether we can use advanced MRI to detect early changes in Alzheimer's disease and to distinguish these changes from other forms of dementia. If the study is successful, this new information would be a major advance in our understanding of the development of Alzheimer's disease. Ultimately, this may lead to earlier treatment of people with Alzheimer's disease. A total 60 study participants at UHN, 20 Alzheimer's patients, 20 MCI and 20 healthy controls will be enrolled to this study.

Procedure

We wish to compare the blood flow in people with Alzheimer's disease with blood flow in people who do not have Alzheimer's disease, to see if there is a difference

The study consists of two visits. All visits will be held at the Toronto Western Hospital. During the first visit your medical history will be obtained and reviewed by the study staff and a physician to ensure that you are healthy and eligible to participate in the study. You will also be seen by a clinical psychologist who will conduct an interview and administer some questionnaires to assess general functioning capacity. This session will last approximately two hours.

On your second visit, you will be asked to provide a blood sample for genetic testing. 5mL (1 teaspoon) of blood will be collected. Genetic testing is being done as part of a research study and results will not be provided to participants. You will also have an MRI. Before you enter the MRI scanner, a breathing mask will be applied to your face. Medical adhesive tape will be used as necessary to make sure there are no air leaks around the mask. The mask will be supplied by air, oxygen and carbon dioxide by a computer-controlled machine built specifically for this purpose. Attached to the mask on your face will be some tubing and valves and two clear bags that work with the machine. You will be able to touch the bag that gets the gas from the machine so you can tell when it collapses. You will be asked to make sure you breathe hard enough to keep emptying the bag. You will also be breathing in some of the gas from the other bag that

collects the gas you breathed out. Since it has your own breathed out gas, is warm and moist, you may feel this. However your inhaling of your breathed out gas is taken into account by the computer, which will make sure that you are getting the gas you require.

Before you enter the MRI scanner we will do a practice test where we make the same degree of changes in carbon dioxide as will occur in the MRI scanner. When your carbon dioxide levels are raised, it may cause you to feel like you are somewhat out of breath, like you feel after exercise or while holding your breath. However, your oxygen levels will remain normal throughout and you will be able to breathe as hard as you feel is necessary without affecting the test. At the end of the test the out of breath feeling will stop within 2 or 3 breaths. To be clear, you are not being given anything other than oxygen, nitrogen and carbon dioxide, the same gases that are in room air. We are only changing their concentrations. The RespirAct™ , which is the machine providing the gases was developed by the researchers specifically for studies such as this one and has been used in over 500 experiments. The RespirAct™ is an investigational device, which means it is being used for research only. Health Canada has not approved it for sale, but they have approved its use for this research study.

For the study you will be in the MRI scanner for approximately 45 minutes. Most of this time regular MRI images are generated and you will be breathing room air normally. MRI tests are associated with loud clicking noises indicating that the MRI scanner is taking pictures of your brain. There are some soft pillows which will help you keep your head still during scanning. There will be 1 test where carbon dioxide changes. It will be 13 minutes long performed at the beginning of the scan series. During this time, the procedure will be the same as the practice test, only this time you will be lying down in the MRI scanner.

Risks

Possible risks associated with drawing blood from your arm include pain, bruising, lightheadedness, and, on rare occasions, infection.

The changes in levels of carbon dioxide and breathing are in the range of that expected in most people in the course of normal living. If you have not noticed any symptoms related to breathing as part of your normal life, it is unlikely that you will have any during the test. The breathing of carbon dioxide is similar to briefly rebreathing your exhaled breath from a bag or even holding your breath, but with the test the oxygen is kept normal. Overall the changes in carbon dioxide in this test are considered to be very safe. During parts of the test you may need to breathe harder than you would normally, in order to empty the bag. During parts of the test it is possible for you to feel that you need to breathe harder to get enough air. If so, you can increase your breathing as much as you wish without affecting the study. In any event, such feelings would only last no more than 2 minutes and will be similar to the practice run. If during the test you feel too uncomfortable and do not wish to continue, you may press an alarm that will be placed in your hand and the study staff will end the test.

MRI is a standard brain imaging technique. It gives off no radiation and has no known risks. Except for the noise, it is painless and safe. If you have any metal in your body, you will need to tell the staff. However, to make images, the head must fit inside a plastic structure that fits close to the face. Most people undergo brain MRI without any problems. Some people may feel a

little 'closed-in' the MRI scanner, but you will be able to speak with someone at all times and can stop the test at any time. You will be given a "call button" to hold in your hand. Should you press the button you will be given 100% oxygen and will be taken out of the MRI scanner. You can stop the study any time you would like.

Pregnancy

If you think you may be pregnant, please inform the doctor, research coordinator, or MRI technologist. You cannot participate in this study if you are pregnant.

Benefits

This research will not benefit you personally, but it will improve our understanding of the development of Alzheimer's disease. This may lead to better treatment for people with Alzheimer's disease.

Confidentiality

Personal Health Information

If you agree to join this study, the study doctor and his/her study team will look at your personal health information and collect only the information they need for the study.

Personal health information is any information that could identify you and includes your:

- name,
- address,
- date of birth,
- new or existing medical records, that includes types, dates and results of medical tests and procedures.

The study doctor will keep any personal health information about you in a secure and confidential location for a minimum of 25 years. A list linking your study number with your name will be kept by the study doctor in a secure place, separate from your study file. Only the study team or the people or groups listed below will be allowed to look at your records. Your participation in this study also may be recorded in your medical record at this hospital. This is for clinical safety purposes.

The following people may come to the hospital to look at the study records and at your personal health information to check that the information collected for the study is correct and to make sure the study is following proper laws and guidelines:

- Representatives of the University Health Network (UHN) including the UHN Research Ethics Board
- Representatives of Health Canada

All information collected during this study, including your personal health information, will be kept confidential and will not be shared with anyone outside the study unless required by law. You will not be named in any reports, publications, or presentations that may come from this study.

This study is also being conducted at Sunnybrook Hospital and John Hopkins Hospital Data may be shared or transferred however no identifying information will be transferred or shared. Any information that will be transferred or shared will be done via a secure server.

Costs

You do not have to pay for any of the procedures associated with the study. You will be reimbursed $25 for parking, per study visit.

Participation

Your participation in this study is voluntary. You can choose not to participate or you may withdraw at any time. If you decide to withdraw from the study, the information that was collected before you leave the study will still be used in order to help answer the research question. No new information will be collected without your permission.

RIGHTS AS A PARTICIPANT

If you are harmed as a direct result of taking part in this study, all necessary medical treatment will be made available to you at no cost.

By signing this form you do not give up any of your legal rights against the investigators, sponsor or involved institutions for compensation, nor does this form relieve the investigators, sponsor or involved institutions of their legal and professional responsibilities

Conflict of Interest

Dr. David Mikulis is one of the inventors of the RespirAct™ breathing device being used in this study. The device is produced, and made available for the study, by Thornhill Research Inc. where Dr. David Mikulis is also a shareholder of Thornhill Research Inc. Dr. Mikulis stands to profit from this device if it is successfully commercialized. The University Health Network similarly stands to gain financially from the commercialization of the device.

Questions

If you have any questions, concerns or would like to speak to the study team for any reason, please call the study coordinator at 416-603-5800 extension 6586 or Dr. David Mikulis at 416-603-5800 extension 5612.

If you have any questions about your rights as a research participant or have concerns about this study, call the Chair of the University Health Network Research Ethics Board (REB) or the Research Ethics office at 416-581-7849. The REB is a group of people who oversee the ethical conduct of research studies. These people are not part of the study team. Everything that you discuss with the REB will be kept confidential.

Consent

This study has been explained to me and any questions I had have been answered.
I know that I may leave the study at any time. I agree to take part in this study.

_____	_____	_____
Print Study Participant's Name	Signature	Date

(You will be given a signed copy of this consent form)

My signature means that I have explained the study to the participant named above. I have answered all questions.

_____	_____	_____
Print Name of Person Obtaining Consent	Signature	Date

CONSENT TO PARTICIPATE IN A RESEARCH STUDY
(FOR PARTICIPANT WITH MILD COGNITIVE IMPAIRMENT)

Title: Developing an imaging biomarker for Alzheimer's dementia based on vascular dysfunction

Principal Investigator: Dr. David Mikulis, M.D.

Tel: 416 603-5800 Ext. 5612

Co-Investigators: Melanie Cohn, Ph.D. C. Psych
Adrian Crawley, Ph.D.
Paul Dufort, Ph.D.
Dr. Daniel Mandell
Dr. David Tang-Wai
Dr. Carmela Tartaglia

You are being asked to take part in a research study. Please read this explanation about the study and its risks and benefits before you decide if you would like to take part. You should take as much time as you need to make your decision. You should ask the study doctor or study staff to explain anything that you do not understand and make sure that all of your questions have been answered before signing this consent form. Before you make your decision, feel free to talk about this study with anyone you wish including your friends, family, and family doctor. Participation in this study is voluntary.

Background

As the population ages, more people are developing dementia. Dementia is a loss in certain mental abilities, including but not limited to memory, attention and understanding language. It is therefore increasingly important for the health care system to find solutions for slowing or even eliminating this condition. Individuals with declining brain function may be developing one of several different types of dementia that can be difficult to distinguish from each other early on. Knowledge of the dementia type is important for starting the right treatment as soon as possible. Certain types of dementia are actually caused by injury only to the blood vessels themselves. Yet, in the other dementias, the relationship between blood vessel injury and direct injury to nerve cells is less well understood, though it likely plays a role in Alzheimer's disease.

This research study will use a method to better understand the role that damaged blood vessels play in the development and progression of dementia. You are being invited to take part in the study because you are healthy.

Carbon dioxide content of the blood increases when you hold your breath and decreases when you hyperventilate (breathe rapidly). Interestingly, the blood flow to the brain is also controlled by the carbon dioxide level in the blood. Increases in carbon dioxide increase brain blood flow and vice versa. We make changes to the carbon dioxide in the blood by adding carbon dioxide

to, and then taking it away from, the air you are breathing. While this is being done, we use the magnetic resonance scanner (MRI) to monitor the changes in blood flow in your brain. How the blood flow responds to the carbon dioxide changes tells us about the health of the blood vessels, and the brain.

We believe that the areas in the brain with unhealthy blood vessels will be seen at a very early stage of dementia allowing doctors to begin proper treatment sooner improving the future quality of life.

Purpose

The purpose of this study is to determine whether we can use advanced MRI to detect early changes in Alzheimer's disease and to distinguish these changes from other forms of dementia. If the study is successful, this new information would be a major advance in our understanding of the development of Alzheimer's disease. Ultimately, this may lead to earlier treatment of people with Alzheimer's disease. A total 60 study participants at UHN, 20 Alzheimer's patients, 20 MCI and 20 healthy controls, will be enrolled to this study.

Procedures

The study consists of three visits. All visits will be held at the Toronto Western Hospital on different days. During the first visit your medical history will be obtained and reviewed by the study staff and a physician to ensure that you are healthy and eligible to participate in the study. You will also be seen by a clinical psychologist who will conduct an interview and administer some questionnaires to assess general functioning capacity. This session will last approximately two hours.

On your second visit, you will be asked to provide a blood sample for genetic testing. 5mL (1 teaspoon) of blood will be collected. Genetic testing is being done as part of a research study and results will not be provided to participants. You will also have an MRI. Before you enter the MRI scanner, a breathing mask will be applied to your face. Medical adhesive tape will be used as necessary to make sure there are no air leaks around the mask. The mask will be supplied by air, oxygen and carbon dioxide by a computer-controlled machine built specifically for this purpose. Attached to the mask on your face will be some tubing and valves and two clear bags that work with the machine. You will be able to touch the bag that gets the gas from the machine so you can tell when it collapses. You will be asked to make sure you breathe hard enough to keep emptying the bag. You will also be breathing in some of the gas from the other bag that collects the gas you breathed out. Since it has your own breathed out gas, is warm and moist, you may feel this. However your inhaling of your breathed out gas is taken into account by the computer, which will make sure that you are getting the gas you require.

Before you enter the MRI scanner we will do a practice test where we make the same degree of changes in carbon dioxide as will occur in the MRI scanner. When your carbon dioxide levels are raised, it may cause you to feel like you are somewhat out of breath, like you feel after exercise or while holding your breath. However, your oxygen levels will remain normal throughout and you will be able to breathe as hard as you feel is necessary without affecting the test. At the end of the test the out of breath feeling will stop within 2 or 3 breaths. To be clear, you are not being given anything other than oxygen, nitrogen and carbon dioxide, the same gases

that are in room air. We are only changing their concentrations. The RespirAct™ , which is the machine providing the gases was developed by the researchers specifically for studies such as this one and has been used in over 500 experiments. The RespirAct™ is an investigational device, which means it is being used for research only. Health Canada has not approved it for sale, but they have approved its use for this research study.

For the study you will be in the MRI scanner for approximately 45 minutes. Most of this time regular MRI images are generated and you will be breathing room air normally. MRI tests are associated with loud clicking noises indicating that the MRI scanner is taking pictures of your brain. There are some soft pillows which will help you keep your head still during scanning. There will be 1 test where carbon dioxide changes. It will be 13 minutes long performed at the beginning of the scan series. During this time, the procedure will be the same as the practice test, only this time you will be lying down in the MRI scanner.

Your third and final visit will be scheduled three years from the date of your first visit. During this visit you will be seen by the clinical psychologist who will conduct the same interview and questionnaires as the first visit.

Risks

Possible risks associated with drawing blood from your arm include pain, bruising, lightheadedness, and, on rare occasions, infection.

The changes in levels of carbon dioxide and breathing are in the range of that expected in most people in the course of normal living. If you have not noticed any symptoms related to breathing as part of your normal life, it is unlikely that you will have any during the test. The breathing of carbon dioxide is similar to briefly rebreathing your exhaled breath from a bag or even holding your breath, but with the test the oxygen is kept normal. Overall the changes in carbon dioxide in this test are considered to be very safe. During parts of the test you may need to breathe harder than you would normally, in order to empty the bag. During parts of the test it is possible for you to feel that you need to breathe harder to get enough air. If so, you can increase your breathing as much as you wish without affecting the study. In any event, such feelings would only last no more than 2 minutes and will be similar to the practice run. If during the test you feel too uncomfortable and do not wish to continue, you may press an alarm that will be placed in your hand and the study staff will end the test.

MRI is a standard brain imaging technique. It gives off no radiation and has no known risks. Except for the noise, it is painless and safe. If you have any metal in your body, you will need to tell the staff. However, to make images, the head must fit inside a plastic structure that fits close to the face. Most people undergo brain MRI without any problems. Some people may feel a little ‘closed-in’ the MRI scanner, but you will be able to speak with someone at all times and can stop the test at any time. You will be given a “call button” to hold in your hand. Should you press the button you will be given 100% oxygen and will be taken out of the MRI scanner. You can stop the study any time you would like. It will not affect your care.

Pregnancy

If you think you may be pregnant, please inform the doctor, research coordinator, or MRI technologist. You cannot participate in this study if you are pregnant.

Benefits

This research may not necessarily benefit you personally, but it will improve our understanding of the development of Alzheimer's disease. This may lead to better treatment for people with Alzheimer's disease.

Confidentiality

Personal Health Information

If you agree to join this study, the study doctor and his/her study team will look at your personal health information and collect only the information they need for the study.

Personal health information is any information that could identify you and includes your:

- name,
- address,
- date of birth,
- new or existing medical records, that includes types, dates and results of medical tests and procedures.

The study doctor will keep any personal health information about you in a secure and confidential location for a minimum of 25 years. A list linking your study number with your name will be kept by the study doctor in a secure place, separate from your study file. Only the study team or the people or groups listed below will be allowed to look at your records. Your participation in this study also may be recorded in your medical record at this hospital. This is for clinical safety purposes.

The following people may come to the hospital to look at the study records and at your personal health information to check that the information collected for the study is correct and to make sure the study is following proper laws and guidelines:

- Representatives of the University Health Network (UHN) including the UHN Research Ethics Board
- Representatives of Health Canada

All information collected during this study, including your personal health information, will be kept confidential and will not be shared with anyone outside the study unless required by law. You will not be named in any reports, publications, or presentations that may come from this study.

This study is also being conducted at Sunnybrook Hospital and John Hopkins Hospital. Data may be shared or transferred however no identifying information will be transferred or shared. Any information that will be transferred or shared will be done via a secure server.

Costs

You do not have to pay for any of the procedures associated with the study. You will be reimbursed $25 for parking, per study visit.

Participation

Your participation in this study is voluntary. You can choose not to participate or you may withdraw at any time without affecting your medical care. If you decide to withdraw from the study, the information that was collected before you leave the study will still be used in order to help answer the research question. No new information will be collected without your permission

RIGHTS AS A PARTICIPANT

If you are harmed as a direct result of taking part in this study, all necessary medical treatment will be made available to you at no cost.

By signing this form you do not give up any of your legal rights against the investigators, sponsor or involved institutions for compensation, nor does this form relieve the investigators, sponsor or involved institutions of their legal and professional responsibilities

Conflict of Interest

Dr. David Mikulis is one of the inventors of the RespirAct™ breathing device being used in this study. The device is produced, and made available for the study, by Thornhill Research Inc. where Dr. David Mikulis is also a shareholder of Thornhill Research Inc. Dr. Mikulis stands to profit from this device if it is successfully commercialized. The University Health Network similarly stands to gain financially from the commercialization of the device.

Questions

If you have any questions, concerns or would like to speak to the study team for any reason, please call the study coordinator 416-603-5800 extension 6586 or Dr. David Mikulis at 416-603-5800 extension 5612.

If you have any questions about your rights as a research participant or have concerns about this study, call the Chair of the University Health Network Research Ethics Board (REB) or the Research Ethics office at 416-581-7849. The REB is a group of people who oversee the ethical conduct of research studies. These people are not part of the study team. Everything that you discuss with the REB will be kept confidential.

Consent

This study has been explained to me and any questions I had have been answered.
I know that I may leave the study at any time. I agree to take part in this study.

_____	_____	_____
Print Study Participant's Name	Signature	Date

(You will be given a signed copy of this consent form)

My signature means that I have explained the study to the participant named above. I have answered all questions.

_____	_____	_____
Print Name of Person Obtain Consent	Signature	Date

CONSENT TO PARTICIPATE IN A RESEARCH STUDY
(FOR PARTICIPANT WITH ALZHEIMER'S DISEASE)

Title: Developing an imaging biomarker for Alzheimer's dementia based on vascular dysfunction

Principal Investigator: Dr. David Mikulis, M.D. FRCP(C)

Tel: 416 603-5800 Ext. 5612

Co-Investigators: Melanie Cohn, Ph.D. C. Psych
Adrian Crawley, Ph.D.
Paul Dufort, Ph.D.
Dr. Daniel Mandell
Dr. David Tang-Wai
Dr. Carmela Tartaglia

You are being asked to take part in a research study. Please read this explanation about the study and its risks and benefits before you decide if you would like to take part. You should take as much time as you need to make your decision. You should ask the study doctor or study staff to explain anything that you do not understand and make sure that all of your questions have been answered before signing this consent form. Before you make your decision, feel free to talk about this study with anyone you wish including your friends, family, and family doctor. Participation in this study is voluntary.

Background

As the population ages, more people are developing dementia. Dementia is a loss in certain mental abilities, including but not limited to memory, attention and understanding language. It is therefore increasingly important for the health care system to find solutions for slowing or even eliminating this condition. Individuals with declining brain function may be developing one of several different types of dementia that can be difficult to distinguish from each other early on. Knowledge of the dementia type is important for starting the right treatment as soon as possible. Certain types of dementia are actually caused by injury only to the blood vessels. Yet, in the other dementias, the relationship between blood vessel injury and direct injury to nerve cells is less well understood, though it likely plays a role in Alzheimer's disease.

This research study will use a method to better understand the role that damaged blood vessels play in the development and progression of dementia. You are being invited to participate in the study because you have been diagnosed with Alzheimer's Disease.

Carbon dioxide content of the blood increases when you hold your breath and decreases when you hyperventilate (breathe rapidly). Interestingly, the blood flow to the brain is also controlled by the carbon dioxide level in the blood. Increases in carbon dioxide increase brain blood flow and vice versa. We make changes to the carbon dioxide in the blood by adding carbon dioxide to, and then taking it away from, the air you are breathing. While this is being done, we use the magnetic resonance scanner (MRI) to monitor the changes in blood flow in your brain. How the

blood flow responds to the carbon dioxide changes tells us about the health of the blood vessels, and the brain.

We believe that the areas in the brain with unhealthy blood vessels will be seen at a very early stage of dementia allowing doctors to begin proper treatment sooner, improving the future quality of life.

Purpose

The purpose of this study is to determine whether we can use advanced MRI to detect early changes in Alzheimer's disease and to distinguish these changes from other forms of dementia. If the study is successful, this new information would be a major advance in our understanding of the development of Alzheimer's disease. Ultimately, this may lead to earlier treatment of people with Alzheimer's disease. A total 60 study participants at UHN, 20 Alzheimer's patients, 20 MCI and 20 healthy controls, will be enrolled to this study.

Procedures

The study consists of one visit which will be held at the Toronto Western Hospital. During this visit your medical history will be obtained and reviewed by the study staff and a physician to ensure that you are healthy and eligible to participate in the study. We are asking your permission to contact your treating and/or diagnosing phsycian to obtain your medical history and any pertaining information to determine your eligibility for this study. You will be asked to provide a blood sample for genetic testing. 5mL (1 teaspoon) of blood will be collected. Genetic testing is being done as part of a research study and results will not be provided to participants. If your clinical assessment was done more than 6 months ago, you will also be seen by a clinical psychologist who will conduct an interview and administer some questionnaires to assess general functioning capacity. This session will last approximately one hour. You will also have an MRI.

Before you enter the MRI scanner, a breathing mask will be applied to your face. Medical adhesive tape will be used as necessary to make sure there are no air leaks around the mask. The mask will be supplied by air, oxygen and carbon dioxide by a computer-controlled machine built specifically for this purpose. Attached to the mask on your face will be some tubing and valves and two clear bags that work with the machine. You will be able to touch the bag that gets the gas from the machine so you can tell when it collapses. You will be asked to make sure you breathe hard enough to keep emptying the bag. You will also be breathing in some of the gas from the other bag that collects the gas you breathed out. Since it has your own breathed out gas, is warm and moist, you may feel this. However your inhaling of your breathed out gas is taken into account by the computer, which will make sure that you are getting the gas you require.

Before you enter the MRI scanner we will do a practice test where we make the same degree of changes in carbon dioxide as will occur in the MRI scanner. When your carbon dioxide levels are raised, it may cause you to feel like you are somewhat out of breath, like you feel after exercise or while holding your breath. However, your oxygen levels will remain normal throughout and you will be able to breathe as hard as you feel is necessary without affecting the test. At the end of the test the out of breath feeling will stop within 2 or 3 breaths. To be clear, you are not being given anything other than oxygen, nitrogen and carbon dioxide, the same gases that are in room air. We are only changing their concentrations. The RespirAct™ , which is the machine providing the gases was developed by the researchers specifically for studies such as

this one and has been used in over 500 experiments. The RespirAct™ is an investigational device, which means it is being used for research only. Health Canada has not approved it for sale, but they have approved its use for this research study.

For the study you will be in the MRI scanner for approximately 45 minutes. Most of this time, regular MRI images are generated and you will be breathing room air normally. MRI tests are associated with loud clicking noises indicating that the MRI scanner is taking pictures of your brain. There are some soft pillows which will help you keep your head still during scanning. There will be 1 test where carbon dioxide changes. It will be 13 minutes long performed at the beginning of the scan series. During this time, the procedure will be the same as the practice test, only this time you will be lying down in the MRI scanner.

Risks

Possible risks associated with drawing blood from your arm include pain, bruising, lightheadedness, and, on rare occasions, infection.

The changes in levels of carbon dioxide and breathing are in the range of that expected in most people in the course of normal living. If you have not noticed any symptoms related to breathing as part of your normal life, it is unlikely that you will have any during the test. The breathing of carbon dioxide is similar to briefly rebreathing your exhaled breath from a bag or even holding your breath, but with the test the oxygen is kept normal. Overall the changes in carbon dioxide in this test are considered to be very safe. During parts of the test you may need to breathe harder than you would normally, in order to empty the bag. During parts of the test it is possible for you to feel that you need to breathe harder to get enough air. If so, you can increase your breathing as much as you wish without affecting the study. In any event, such feelings would only last no more than 2 minutes and will be similar to the practice run. If during the test you feel too uncomfortable and do not wish to continue, you may press an alarm that will be placed in your hand and the study staff will end the test.

MRI is a standard brain imaging technique. It gives off no radiation and has no known risks. Except for the noise, it is painless and safe. If you have any metal in your body, you will need to tell the staff. However, to make images, the head must fit inside a plastic structure that fits close to the face. Most people undergo brain MRI without any problems. Some people may feel a little 'closed-in' the MRI scanner, but you will be able to speak with someone at all times and can stop the test at any time. You will be given a "call button" to hold in your hand. Should you press the button you will be given 100% oxygen and will be taken out of the MRI scanner. You can stop the study any time you would like. It will not affect your care.

Pregnancy

If you think you may be pregnant, then please inform the doctor, research coordinator, or MRI technologist. You cannot participate in this study if you are pregnant.

Benefits

This research may not necessarily benefit you personally, but it will improve our understanding of the development of Alzheimer's disease. This may lead to better treatment for people with Alzheimer's disease.

Confidentiality

Personal Health Information

If you agree to join this study, the study doctor and his/her study team will look at your personal health information and collect only the information they need for the study.

Personal health information is any information that could identify you and includes your:

- name,
- address,
- date of birth,
- new or existing medical records, that includes types, dates and results of medical tests and procedures.

The study doctor will keep any personal health information about you in a secure and confidential location for a minimum of 25 years. A list linking your study number with your name will be kept by the study doctor in a secure place, separate from your study file. Only the study team or the people or groups listed below will be allowed to look at your records. Your participation in this study also may be recorded in your medical record at this hospital. This is for clinical safety purposes.

The following people may come to the hospital to look at the study records and at your personal health information to check that the information collected for the study is correct and to make sure the study is following proper laws and guidelines:

- Representatives of the University Health Network (UHN) including the UHN Research Ethics Board
- Representatives of Health Canada

All information collected during this study, including your personal health information, will be kept confidential and will not be shared with anyone outside the study unless required by law. You will not be named in any reports, publications, or presentations that may come from this study.

This study is also being conducted at Sunnybrook Hospital and John Hopkins Hospital. Data may be shared or transferred however no identifying information will be transferred or shared. Any information that will be transferred or shared will be done via a secure server.

Costs

You do not have to pay for any of the procedures associated with the study. You will be reimbursed $25 for parking, per study visit.

Participation

Your participation in this study is voluntary. You can choose not to participate or you may withdraw at any time without affecting your medical care.
If you decide to withdraw from the study, the information that was collected before you leave the study will still be used in order to help answer the research question. No new information will be collected without your permission.

RIGHTS AS A PARTICIPANT

If you are harmed as a direct result of taking part in this study, all necessary medical treatment will be made available to you at no cost.

By signing this form you do not give up any of your legal rights against the investigators, sponsor or involved institutions for compensation, nor does this form relieve the investigators, sponsor or involved institutions of their legal and professional responsibilities

Conflict of Interest

Dr. David Mikulis is one of the inventors of the RespirAct™ breathing device being used in this study. The device is produced, and made available for the study, by Thornhill Research Inc. where Dr. David Mikulis is also a shareholder of Thornhill Research Inc. Dr. Mikulis stands to profit from this device if it is successfully commercialized. The University Health Network similarly stands to gain financially from the commercialization of the device.

Questions

If you have any questions, concerns or would like to speak to the study team for any reason, please call the study coordinator at 416-603-5800 extension 6586 or Dr. David Mikulis at 416-603-5800 extension 5612.

If you have any questions about your rights as a research participant or have concerns about this study, call the Chair of the University Health Network Research Ethics Board (REB) or the Research Ethics office at 416-581-7849. The REB is a group of people who oversee the ethical conduct of research studies. These people are not part of the study team. Everything that you discuss with the REB will be kept confidential.

Consent

This study has been explained to me and any questions I had have been answered.
I know that I may leave the study at any time. I agree to take part in this study.

_____	_____	_____
Print Study Participant's Name	Signature	Date

(You will be given a signed copy of this consent form)

My signature means that I have explained the study to the participant named above. I have answered all questions.

_____	_____	_____
Print Name of Person Obtaining Consent	Signature	Date

Appendix 2. Neuropsychological Testing – Behavioural Neurology Assessment (Revised)

Subscales	HC (N=10)	MCI (N=10)	AD (N=4)	All Subjects
TOTAL Orientation	11.6 (0.50)	11.3 (0.79)	11.3 (0.50)	11.4 (0.64)
TOTAL Memory Immediate	22.5 (3.47)	16.2 (3.49)	17.3 (2.87)	19.0 (4.46)
TOTAL Memory Delayed	18.0 (4.00)	10.9 (6.07)	3.5 (2.89)	12.8 (7.03)
TOTAL Memory Recognition	20.4 (0.81)	18.7 (2.10)	16.8 (2.75)	19.1 (2.14)
TOTAL Visuospatial[1]	30.5 (0.69)	29.9 (1.17)	24.5 (5.51)	29.3 (3.07)
TOTAL Executive/Attention[2,3]	111.1 (5.05)	103.8 (11.91)	100.0 (11.27)	106.7 (9.81)
TOTAL Language	80.8 (6.26)	75.1 (7.18)	73.5 (2.38)	77.3 (6.84)
BNA-R TOTAL	294.8 (12.46)	268.8 (22.54)	244.3 (13.05)	278.0 (24.53)

Specific Subtests	HC (N=10)	MCI (N=10)	AD (N=4)	All Subjects
Orientation	11.6 (0.50)	11.3 (0.79)	11.3 (0.50)	11.4 (0.64)
Serial 7s	11.3 (1.68)	10.2 (4.96)	10.8 (4.50)	10.7 (3.69)
Serial 3s	13.0 (0)	12.1 (1.81)	10.0 (6.0)	12.2 (2.59)
CERAD Trial 1	6.1 (1.58)	4.0 (1.18)	3.5 (1.29)	4.8 (1.74)
CERAD Trial 2	7.7 (1.49)	5.7 (1.56)	6.8 (0.50)	6.7 (1.66)
CERAD Trial 3	8.6 (1.12)	6.5 (1.21)	7.0 (1.63)	7.5 (1.58)
Benson Figure Copy	15.7 (0.65)	16.0 (0.77)	13.8 (2.06)	15.5 (1.24)
Digit Span Forward	6.7 (0.79)	6.0 (1.67)	7.5 (0.58)	6.5 (1.30)
Digit Span Backwards	4.5 (1.04)	4.3 (1.10)	4.5 (1.0)	4.4 (1.03)
Clock Drawing[1]	14.7 (0.47)	13.4 (1.51)	10.8 (3.77)	13.6 (2.16)
Trails Numbers	23.8 (0.4)	23.8 (0.4)	24.0 (0)	23.8 (0.37)
Trails Number-letter	23.6 (0.67)	23.1 (0.7)	23.0 (1.41)	23.3 (0.84)
CERAD Delayed Recall	6.4 (2.29)	2.7 (1.68)	1.8 (2.06)	4.1 (2.78)
CERAD Recognition Recall	19.5 (0.69)	18.0 (2.1)	16.0 (2.45)	18.3 (2.06)
Benson Delayed Recall	11.6 (2.8)	8.2 (4.83)	1.8 (3.5)	8.7 (5.06)
Benson Recognition Recall	0.8 (0.4)	0.7 (0.47)	0.8 (0.5)	0.8 (0.43)
Alternating Sequences[2]	1.8 (0.6)	2 (0.47)	1 (1.15)	1.8 (0.72)
Similarities[3]	9.9 (0.3)	8.9 (2.02)	9.3 (1.15)	9.4 (1.44)
Verbal Fluency - F Words[3]	16.4 (3.72)	13.4 (4.54)	12.3 (4.04)	14.6 (4.3)
Verbal Fluency - Animals	18.8 (2.04)	14.1 (4.66)	12 (2.45)	15.8 (4.32)
MiNT Naming	13.8 (2.68)	13.1 (1.76)	14.3 (0.96)	13.6 (2.1)
Repetition	9.6 (0.81)	9.6 (0.67)	8.3 (0.5)	9.4 (0.86)
Single Word Comprehension	8 (0)	7.7 (0.65)	8 (0)	7.9 (0.43)
Single Word Reading Comprehension	2 (0)	2 (0)	2 (0)	2 (0)
Sentence Comprehension	7.2 (1.25)	7.2 (1.08)	7 (1.15)	7.2 (1.12)
Single Word Reading	11.5 (1.29)	12 (0)	12 (0)	11.8 (0.86)
Semantic Knowledge	9.9 (0.3)	9.4 (0.92)	10 (0)	9.7 (0.68)

[1]HC (N=9); [2]MCI (N=9), [3]AD (N=3)

Copyright Acknowledgements